CHEMICAL REVIEWS

Review

pubs.acs.org/CR

Born–Oppenheimer and Non-Born–Oppenheimer, Atomic and Molecular Calculations with Explicitly Correlated Gaussians

This paper is part of the 2012 Quantum Chemistry thematic issue.

Sergiy Bubin,*[,†] Michele Pavanello,*[,‡] Wei-Cheng Tung,[§] Keeper L. Sharkey,[§] and Ludwik Adamowicz*[,§,∥]

[†]Department of Physics and Astronomy, Vanderbilt University, Nashville, Tennessee 37235, United States

[‡]Department of Chemistry, Rutgers University Newark, Newark, New Jersey 07102, United States

[§]Department of Chemistry and Biochemistry and [∥]Department of Physics, University of Arizona, Tucson, Arizona 85721, United States

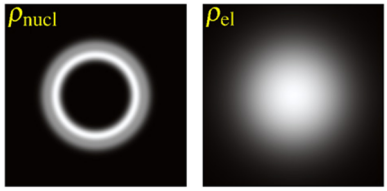

CONTENTS

Received: April 13, 2011
Published: October 1, 2012

   dx.doi.org/10.1021/cr200419d | *Chem. Rev.* 2013, 113, 36–79

1. INTRODUCTION

Since the early work of Hylleraas on the helium atom,[1] it has been common knowledge that, to accurately account for the interaction between the electrons in an atom or a molecule, wave functions that explicitly depend on interelectronic distances must be employed. To overcome the algebraic and computational difficulties associated with the use of the Hylleraas functions for systems with more than two to three electrons, in 1960 Boys[2] and Singer[3] introduced a simpler format of basis functions that explicitly depend on the interelectronic distances, the so-called explicitly correlated (or exponentially correlated) Gaussian functions (ECGs). ECGs, due to the simplicity of calculating the Hamiltonian matrix elements with those functions, have become popular in very accurate quantum-mechanical calculations of small atoms, molecules, and other quantum systems in the past 30 years.[4−7] They have been successfully applied in high-accuracy atomic and molecular calculations performed with and without the assumption of the Born−Oppenheimer (BO) approximation for systems with three to eight particles . Those include very accurate calculations of the BO potential energy surfaces (PESs) of two-, three-, and four-electron systems.

The problem of finding an effective and highly accurate approximation to the wave function that describes electrons and nuclei in an atom or a molecule, or more generally a system of particles interacting with attractive and/or repulsive Coulombic forces, is very complex and requires a careful physical analysis and insight. This particularly applies to the proper description of the interparticle correlation effects resulting from the repulsion of charged equivalent particles (e.g., electrons) subject to the Pauli exclusion principle. In calculations where the BO approximation is not assumed, the correlation effects also involve coupling of the motions of particles with opposite charges, such as nuclei and electrons in a molecule. In this case, the correlation effects include the electron−nucleus correlation resulting from the electrons, particularly the core electrons, following very closely the nuclei, as they are strongly attracted to them.

Another issue that arises in describing the correlation effects is related to whether the correlation is primarily radial, i.e., whether the shape of the Coulomb hole (in the case of two repelling particles) is symmetric or it has some angular anisotropy. The angular correlation anisotropy appears, for example, in excited states of atoms, where two electrons may occupy configurations where they are not only "radially" separated but they are also separated by having different angular wave functions. Such a situation occurs, for example, in excited Rydberg ^{2}D states of the lithium atom corresponding to electron configurations $1s^2nd$, n = 3, 4, 5, ..., where, in addition to the contribution to the wave function from the main $1s^2d$ configurations, there are contributions from configurations $1s^1p^2$. We will elaborate on this issue later in this review.

The goal of the present publication is to review recent works that have used all-particle ECGs in very accurate variational BO and non-BO quantum-mechanical calculations on atoms and molecules. In addition to providing a general overview, we will focus particular attention on the key issues related to the effective implementation of computational algorithms. We will also describe several representative examples of BO and non-BO calculations of some small atomic and molecular systems, with emphasis on how well the results of the calculations compare with the best available experimental measurements.

Even though the variational method combined with expanding the wave function in terms of all-particle ECGs is one of the most accurate methods available to solve for the ground and excited states of quantum systems, it suffers from unfavorable $N!$ dependency on the number of identical particles. This limits the applicability of the method at present to small atomic and molecular systems. It should also be mentioned that, even though orbital calculations are usually significantly less accurate and slower converging for small systems than the calculations with explicitly correlated functions, in some instances with proper extrapolations such calculations are quite competitive and capable of providing very accurate results as well.

In Table 1 we summarize the acronyms used in this review.

1.1. Need for High-Accuracy BO and Non-BO Calculations

From the very beginning of molecular quantum mechanics, the development of highly accurate theoretical models that produce results agreeing with the most up-to-date high-resolution spectroscopic measurements has been an important source of knowledge and information. It has allowed the validation of the theoretical foundations and provided better understanding of the electronic structures of atoms and molecules. As the experimental techniques advance and achieve higher levels of precision, refinements have to be made in theoretical models to describe effects and interactions neglected or treated more approximately in the previous models. In recent years the measurements of such quantities as molecular rovibrational transition energies, ionization potentials, and electron affinities have reached the precision of 0.01−0.001 cm^{-1} and even

dx.doi.org/10.1021/cr200419d | Chem. Rev. 2013, 113, 36−79

Table 1. Glossary of Acronyms and Abbreviations Used in This Review

abbreviation	description
BO	Born−Oppenheimer
non−BO	non-Born−Oppenheimer
BP	Breit−Pauli
CC	coupled cluster
CH	Coulomb Hamiltonian
CN	clamped nuclei
COM	center of mass
CPU	central processing unit
D	Dirac
DB	Dirac−Breit
DBOC	diagonal Born−Oppenheimer correction
DC	Dirac−Coulomb
ECG	explicitly correlated Gaussian
EFG	electric field gradient
FPO	frozen partial optimization
FICI	free iterative-complement interaction
FNM	finite nuclear mass
GPT	Gaussian product theorem
GSEP/GHEP	generalized symmetric/Hermitian eigenvalue problem
ICI	iterative-complement interaction
INM	infinite nuclear mass
JC	James−Coolidge
KG	Klein−Gordon
MDC	matrix differential calculus
MBPT	many-body perturbation theory
MV	mass-velocity
NRQED	nonrelativistic quantum electrodynamics
PEC	potential energy curve
PES	potential energy surface
QED	quantum electrodynamics
SE	Schrödinger equation
SVM	stochastic variational method

higher. Obtaining a similar precision in theoretical calculations (which usually means converging the energy to the relative accuracy of 10^{-6}−10^{-9} or higher) is a very challenging task. As recent works have shown,[8−21] achieving high accuracy in the calculations requires not only a very accurate description of the correlation effects, but also the inclusion of relativistic, quantum electrodynamics (QED) and, possibly, the effects due to the finite size of the nuclei. These types of effects have already been calculated for two- and three-electron atomic systems, leading to theoretical results which are very precise and accurate when compared to the experiments.[22−32] Now the challenge lies in extending these types of calculations to atoms with more than three electrons and to small molecular systems with three or more nuclei. High-accuracy theoretical results for such systems will provide new grounds for the verification of the theoretical models and for the assessment of their limitations. It should be noted that based on the comparison of the theoretical and experimental data it is in principle possible to accurately determine the values of fundamental constants, nuclear radii, nuclear quadrupole moments, and other quantities. Therefore, highly accurate calculations on small atoms and molecules may become a very valuable tool for the precision measurement science. As an example, we can mention the determination of the proton/electron mass ratio[33] and the nuclear charge radii.[24,31,34−36]

The development of high-level quantum-mechanical methods related to the use of ECGs in atomic and molecular calculations can also serve as an important source of ideas and technical solutions for the development of other approaches, which can be applied to larger systems. As ECGs will start to replace products of single-particle Gaussian orbitals as basis functions in expanding the wave function in high-level molecular BO calculations, these techniques may find new applications. For example, further development of such approaches as the R12 (F12) method[37−41] may benefit from utilizing the analytic gradient. Another example is the use of the ECGs with time-dependent nonlinear parameters (e.g., Gaussian centers) in studying the dynamics of chemical processes such as processes initiated by photoexcitations in clusters. Techniques employing ECGs can also provide useful tools for the development of methods that describe the dynamics of the coupled nucleus−electron motion in atomic and molecular systems which can now be studied with the femto- and attosecond spectroscopies.

Another important reason for performing accurate calculations on small atoms and molecules with very high accuracy is that such benchmark calculations can provide valuable reference data for testing of less accurate quantum-chemical methods. An example is the total nonrelativistic energy of the system, which is one of the most commonly computed quantities. The nonrelativistic energy is difficult to determine very precisely even if highly accurate experimental data for ionization potentials, electron affinities, dissociation energies, or transition frequencies are available. This is because the determination of the total nonrelativistic energy requires the knowledge of the binding energies of all subsystems and, more importantly, the exact contribution of relativistic and QED effects. The latter quantities cannot be directly obtained in the experiment.

There is also a predictive purpose for carrying out very accurate atomic and molecular calculations. Several recent non-BO and BO ECG calculations have produced quantities that either have not yet been measured experimentally or have been measured, but with significant error bars exceeding the uncertainty of the calculations. The existence of very precise theoretical predictions may inspire the development of more precise experimental tools and stimulate remeasurement of those quantities. The breadth and accuracy of the experimental data have been increasing rapidly, and further major improvements are expected due to the development of new experimental methods for UV laser generation and frequency metrology with phase-locked femtosecond combs.[42] The data collected using those new techniques are beginning to reveal deviations that suggest that the accuracy of the existing calculations is no longer adequate. For example, extensive studies of the spectrum of H_3^+, by Oka's group at the University of Chicago,[43,44] have gone considerably beyond the limits of the existing theoretical work. More accurate laboratory and field (including interstellar) observations and measurements of spectra of atoms and molecules require more accurate theoretical calculations for interpretation and assignment.

1.2. Challenges in High-Accuracy Calculations

Very accurate BO calculations of ground and excited states of atomic and molecular systems are rare in quantum-chemical studies because they usually require in-house software development and substantial computational resources. Even more scarce are atomic and molecular calculations where the BO

dx.doi.org/10.1021/cr200419d | Chem. Rev. 2013, 113, 36−79

approximation is not assumed. High accuracy also requires that the calculations include relativistic and QED corrections. Those are usually calculated with the perturbation theory. A few groups have developed capabilities to carry out such calculations for systems with one and two electrons. The actual applications, however, in most cases have been limited to one- or two-electron systems only. This is particularly true for molecular systems computed without using the BO approximation. While the development of methods describing the coupled motion of the electrons and the nuclei has received some attention,[45−51] none of the works has reached a level of accuracy similar to that achievable in the calculations with ECGs. Non-BO calculations of the ground and excited states of molecular systems are difficult for the following reasons:

(i) Treating nuclei and electrons of a molecular system on equal footing adds complexity to the problem due to the increased number of the degrees of freedom one needs to accurately represent in the wave function. Additional degrees of freedom require additional computational effort.

(ii) The non-BO wave function needs to very accurately represent the correlated motion of the nuclei and the electrons, and it has to be constructed using basis functions that can effectively describe the electron−electron, nucleus−electron, and nucleus−nucleus correlation effects. It may sound somewhat unusual to talk about the nucleus−nucleus correlation, as the term "correlation" is usually used to described the effects pertaining to electrons, but if nuclei and electrons are treated on equal footing, as happens in non−BO calculations, the nucleus−nucleus correlated motion also needs to be represented in the wave functions in a similar way as the electron−electron correlated motion is. In addition, the masses of the nuclei being much larger than that of the electron may lead to rapid variation of the relative internuclear wave function, which is hard to represent with the usual basis functions. Moreover, the nucleus−nucleus correlation is much stronger than the electron−electron correlation in the sense that the nuclei are heavy and they stay separated (i.e., their motion is more correlated) with the separation distance varying much less than the separation distance between much lighter and, thus, more delocalized electrons. The nucleus−nucleus correlation can only be described in the wave function by including correlation factors.

(iii) After separating the translational degrees of freedom, the internal Hamiltonian of an atomic or a molecular system in isolation is "isotropic" (i.e., rotationally invariant) and its eigenfunctions belong to the irreducible representations of the group of three-dimensional (3D) rotations. It is necessary that the basis functions used in the wave function expansion reflect this symmetry.

(iv) As the vibrational and electronic degrees of freedom are coupled, the manifold of the excited states for a non-BO molecular system corresponding to a particular value of the total rotational quantum number includes a mixture of vibrational and electronic states. While the mixture for the lower lying states is usually strongly dominated by a single component, being a product of the electronic wave function times a vibrational wave function, for states lying close to the dissociation limit, two or more components may provide more significant contributions. Those components may have electronic wave functions representing different electronic states and vibrational wave functions corresponding to different vibrational quantum numbers. Some of those states may have multiple nodes (e.g., high vibrational states) and require flexible basis functions to be described.

(v) Including angular dependency in the wave function (to determine higher rotational states) requires addition of angular factors to the basis functions. For such functions, the multiparticle Hamiltonian integrals are more complicated than those for basis functions describing states with zero angular momenta. More complicated are also the expressions for the derivatives of the Hamiltonian matrix elements that need to be calculated to determine the analytic energy gradient whose use is crucial in the minimization of the variational energy functional.

(vi) If accuracy similar to that of high-resolution experiments is the aim of the calculation, the lowest-order relativistic and QED effects need to be accounted for. Matrix elements involving operators representing those effects are more complicated than the Hamiltonian matrix elements.

1.3. Very Accurate BO Calculations of Molecular Potential Energy Surfaces (PESs)

The first success of very accurate molecular calculations that utilized explicitly correlated basis functions was the work of Kołos and Wolniewicz concerning the H_2 molecule. In their work published in 1975[52] they presented calculations of the H_2 spectra that agreed with the experimental data of Herzberg within 1 cm^{-1}. Their work also led to some revisions of Herzberg's original line assignment. In spite of the enormous advances in computer hardware, it took the next 30 years to achieve a comparable level of accuracy in the calculations of rovibrational spectra of a three-proton, two-electron system, H_3^+. However, even at present the H_3^+ rovibrational spectrum is well understood only for states lying below the barrier to linearity of this system, which is located 10 000 cm^{-1} above the ground state level. Precise assignment of the spectral lines above this barrier still remains a great challenge for both theory and experiment. Once the assignment is made, the H_3^+ ion will be the best understood three-nucleus system ever studied experimentally and theoretically.

The ECGs were introduced to quantum-chemical calculations by Boys and Singer.[2,3] In 1964 an important paper by Lester and Krauss on the Hamiltonian integrals with ECGs for two-electron molecular systems appeared[53] that had given momentum to several works concerning implementation of these functions in the molecular calculations. In the 1970s, Adamowicz and Sadlej had extended the Lester and Krauss approach to calculate the electron correlation energy for some small diatomics in the framework of the perturbation theory.[54−60] About the same time Jeziorski and Szalewicz employed ECGs in very accurate calculations of the interaction energies using the symmetry-adapted perturbation theory.[61,62]

The late 1970s and early 1980s witnessed development of nonvariational methods for calculating electronic structures of atoms and molecules. Many-body perturbation theory (MBPT) and the coupled cluster (CC) methods had been implemented and started becoming routine tools for high-level ab initio calculations of small and medium-size molecules.[63,64] Motivated by this development, the team of Monkhorst, Jeziorski, Szalewicz, and Zabolitzky introduced ECGs to the CC method[65−68] and this was achieved by using the coupled cluster equations at the pair level reformulated as a system of integro-differential equations for spin-free pair functions. These equations were solved using two-electron ECGs (also called

dx.doi.org/10.1021/cr200419d | Chem. Rev. 2013, 113, 36−79

Gaussian geminals). The work resulted in a series of benchmark studies for small atomic and molecular systems.

Another important development concerning the use of ECGs in MBPT/CC calculations of medium-size molecular systems originated with the work of Kutzelnigg,[37,69] who suggested that linear r_{ij} correlation factors should be added to orbital products to improve the description of the electron correlation. In order to improve the computational efficiency in the calculations, he suggested using the resolution of identity to avoid explicit calculation of integrals involving more than two electrons. The approach was termed the "R12 method" and quickly became a mainstream technique in computational chemistry to perform high-accuracy atomic and molecular calculations.[70,71] Recently the R12 method has evolved to an array of methods, most notably the F12 method where the linear r_{12} correlation factor is replaced by a Slater-type geminal,[72,73] $\exp[-\alpha r_{12}]$, and the G12 method where the explicit correlation is given by a Gaussian geminal, i.e., $\exp[-\alpha {r_{12}}^2]$.

The works on the implementation of ECGs in the MBPT/CC methods have been paralleled by progress in the ECG variational calculations. For example, variational ECG calculations were able to reach a nanohartree (subwavenumber) precision level for nonrelativistic adiabatic calculations of the helium dimer[74] and below picohartree level for the hydrogen molecule[75] using ECG calculations.

Following the important works of Kołos and Wolniewicz, there have been several other works on very accurate calculations of small molecular systems.[76−80] As this review primarily deals with the calculations performed with the use of ECGs, we should particularly mention the works of the group of Rychlewski.[4,74,81−87]

In recent years several methods have been developed and implemented for more efficient generation of PESs of small molecular systems employing ECGs.[7] The key element of this development has been the use of the analytical gradient determined with respect to the Gaussian nonlinear parameters in the variational energy minimization.[88−91] One can compare the increase of the efficiency associated with the use of the gradient in this case with the efficiency increase in the molecular-structure optimization after the energy gradient determined with respect to molecular geometrical parameters was introduced to the field. As computational resources become increasingly more accessible and affordable, such calculations become more feasible. However, as the size of the molecules increases, the complexity and the cost of the ECG PES calculations also increase. Let us consider two-electron systems with different numbers of nuclei as an example. For a system with one nucleus, e.g., the helium atom, one can reach 1×10^{-9} hartree accuracy of the energy with only 200 Gaussians.[92] In the case of two and three nuclei, H_2 and H_3^+, 500 and 1000 Gaussians are needed, respectively, to achieve similar accuracy.[93,94] Also, for a four-electron, four-nuclear system, $(H_2)_2$, even 7000 Gaussians only yield 1×10^{-6} hartree accuracy.[95] In the ECG calculations of larger molecular systems, besides the need for larger basis sets, a problem which one can encounter and has to deal with more often is the occurrence of the linear dependency between the basis functions. Effectively dealing with this problem requires rather sophisticated approaches. Also, better techniques for handling the usage of memory, for guessing new basis functions when the size of the basis set is being extended, and for the basis set optimization have to be developed. These measures will be elaborated on in this review.

The main purpose of the BO molecular calculations employing ECGs is to generate PESs of ground and excited states that can be used to perform rovibrational calculations. The ECG PESs of small systems are usually capable of delivering a subwavenumber accuracy for the full range of the vibrational transitions provided that at least the adiabatic correction is included in the energy of each PES point. We will show examples of such calculations in this review. If the calculations also provide the corresponding surface of the molecular dipole moment, the rovibrational transition moments, and thus the band intensities, can be calculated. PESs can also be used to perform reaction dynamics calculations using either the classical trajectory approach or a wave packet quantum approach. In both approaches nonadiabaticity, or hopping between PESs of several electronic states, can be simulated. Such simulations involve calculating adiabatic and nonadiabatic coupling matrix elements, which can be relatively easily done (though it has never been reported so far) for energy points determined using wave functions expanded in terms of ECGs.

The ECG PES calculations performed so far have been limited to states described with wave functions with no nodes at the nuclei. If such nodes exist, the Gaussians in the basis functions need to be multiplied by a coordinate or a product of coordinates.[96] Such coordinate premultipliers to ECGs are also used in other applications (see section 3).

Finally, the development and implementation of new algorithms and procedures always involves solving numerous technical problems at both the algebraic and computational levels. A part of this review is devoted to this. We particularly emphasize those issues that have broader implications and applications in the areas that are not limited to the development of methods for very accurate BO and non-BO calculations of small atomic and molecular systems.

2. FORMALISM

2.1. Nonrelativistic Hamiltonian in the Laboratory Frame and Separation of the Center of Mass Motion

Let us consider a system comprised of N nonrelativistic particles interacting via Coulomb forces. If $\mathbf{R}_i$ is the position vector of the ith particle in the laboratory Cartesian coordinate frame, M_i is its mass, and Q_i is its charge, then the Hamiltonian of the system has the following form:

$$\hat{H}_{\mathrm{lab}} = -\sum_{i=1}^{N} \frac{1}{2M_i} {\nabla_{\mathbf{R}_i}}^2 + \sum_{i=1}^{N} \sum_{j>i}^{N} \frac{Q_i Q_j}{R_{ij}} \tag{1}$$

Here $\nabla_{\mathbf{R}_i}$ denotes the gradient with respect to $\mathbf{R}_i$ and $R_{ij} = |\mathbf{R}_j - \mathbf{R}_i|$ is the distance between the ith and jth particles. We will call $\hat{H}_{\mathrm{lab}}$ the laboratory frame Hamiltonian.

As the primary goal is solving for the bound states, the first step will be to separate out the translational motion of the system as a whole; i.e., we will eliminate the motion of the center of mass from further consideration. There are several possible ways to do that. Perhaps the most natural way is to use the interparticle coordinates. Let us place some particle at the origin of the new, internal, Cartesian coordinate system. This particle is called the reference particle. Then we can refer the other particles to the reference particle using relative coordinates $\mathbf{r}_i = \mathbf{R}_{i+1} - \mathbf{R}_1$. These coordinates, along with the three coordinates describing the position of the center of mass, $\mathbf{r}_0$, are our new coordinates. If we denote the total mass of the

dx.doi.org/10.1021/cr200419d | Chem. Rev. 2013, 113, 36−79

system as $M_{tot} = \sum_{i=1}^{N} M_i$ then the coordinate transform looks as follows:

$$\begin{aligned}
\mathbf{r}_0 &= \frac{M_1}{M_{tot}}\mathbf{R}_1 + \frac{M_2}{M_{tot}}\mathbf{R}_2 + ... + \frac{M_N}{M_{tot}}\mathbf{R}_N \\
\mathbf{r}_1 &= -\mathbf{R}_1 + \mathbf{R}_2 \\
\mathbf{r}_2 &= -\mathbf{R}_1 + \mathbf{R}_3 \\
&\vdots \\
\mathbf{r}_n &= -\mathbf{R}_1 + \mathbf{R}_N
\end{aligned} \tag{2}$$

while the inverse coordinate transformation is given by

$$\begin{aligned}
\mathbf{R}_1 &= \mathbf{r}_0 - \frac{M_2}{M_{tot}}\mathbf{r}_1 - \frac{M_3}{M_{tot}}\mathbf{r}_2 - ... - \frac{M_N}{M_{tot}}\mathbf{r}_n \\
\mathbf{R}_2 &= \mathbf{r}_0 + \left(1 - \frac{M_2}{M_{tot}}\right)\mathbf{r}_1 - \frac{M_3}{M_{tot}}\mathbf{r}_2 - ... - \frac{M_N}{M_{tot}}\mathbf{r}_n \\
\mathbf{R}_3 &= \mathbf{r}_0 - \frac{M_2}{M_{tot}}\mathbf{r}_1 + \left(1 - \frac{M_3}{M_{tot}}\right)\mathbf{r}_2 - ... - \frac{M_N}{M_{tot}}\mathbf{r}_n \\
&\vdots \\
\mathbf{R}_N &= \mathbf{r}_0 - \frac{M_2}{M_{tot}}\mathbf{r}_1 - \frac{M_3}{M_{tot}}\mathbf{r}_2 - ... + \left(1 - \frac{M_N}{M_{tot}}\right)\mathbf{r}_n
\end{aligned} \tag{3}$$

Upon the transformation of the laboratory frame, the Hamiltonian $\hat{H}_{lab}$ in eq 1 separates into two operators, i.e., the Hamiltonian describing the motion of the center of mass (COM) of the system

$$\hat{H}_{CM} = -\frac{1}{2M_{tot}}\nabla_{\mathbf{r}_0}^2 \tag{4}$$

and the following "internal" Hamiltonian that represents the relative motion of the particles:

$$\hat{H} = -\frac{1}{2}\left(\sum_{i=1}^{n}\frac{1}{\mu_i}\nabla_{\mathbf{r}_i}^2 + \sum_{i\neq j}^{n}\frac{1}{m_0}\nabla'_{\mathbf{r}_i}\nabla_{\mathbf{r}_j}\right) + \sum_{i=1}^{n}\frac{q_0 q_i}{r_i} + \sum_{i<j}^{n}\frac{q_i q_j}{r_{ij}} \tag{5}$$

where $n = N - 1$, the prime symbol denotes the matrix/vector transposition, $r_{ij} = |\mathbf{r}_j - \mathbf{r}_i|$, $m_i = M_{i+1}$, $q_i = Q_{i+1}$, and $\mu_i = m_0 m_i/(m_0 + m_i)$. The Hamiltonian in eq 5 describes the motion of n pseudoparticles with masses m_i and charges q_i in the central field of the reference particle. The motions of the pseudoparticles are coupled through the mass polarization terms $\sum_{i\neq j}^{n}(1m_0)\nabla'_{\mathbf{r}_i}\nabla_{\mathbf{r}j}$ and through the Coulombic interactions dependent on the distances between the pseudoparticles and the origin of the internal coordinate system, r_i, and on the relative distances between the pseudoparticles, r_{ij}.

Due to the separability of the internal motion and the motion of the center of mass, the solution of the Schrödinger equation (SE) with the laboratory Hamiltonian can be presented as the product

$$\psi_{lab} = \exp[\mathbf{i}\mathbf{k}'_0\mathbf{r}_0]\,\psi(\mathbf{r}_1, ..., \mathbf{r}_n) \tag{6}$$

where $\mathbf{k}_0$ is the momentum of the system as a whole and $\psi(\mathbf{r}_1,...,\mathbf{r}_n)$ is the solution of the SE with the internal Hamiltonian.

The Hamiltonian in eq 5 can be conveniently written in the matrix form. To do that we combine the coordinates of the pseudoparticle positions and the corresponding gradients into two $3n$-component column vectors:

$$\mathbf{r} = \begin{pmatrix}\mathbf{r}_1\\ \mathbf{r}_2\\ \vdots\\ \mathbf{r}_n\end{pmatrix}, \qquad \nabla_{\mathbf{r}} = \begin{pmatrix}\nabla_{\mathbf{r}_1}\\ \nabla_{\mathbf{r}_2}\\ \vdots\\ \nabla_{\mathbf{r}_n}\end{pmatrix} \tag{7}$$

With that we have

$$\hat{H} = -\nabla'_{\mathbf{r}}\mathbf{M}\nabla_{\mathbf{r}} + \sum_{i=1}^{n}\frac{q_0 q_i}{r_i} + \sum_{i<j}^{n}\frac{q_i q_j}{r_{ij}} \tag{8}$$

Here $\mathbf{M} = M \otimes I_3$ is the Kronecker product of the $n \times n$ matrix M and the 3×3 identity matrix, I_3. The diagonal elements of matrix M are $1/(2\mu_1)$, $1/(2\mu_2)$, ..., $1/(2\mu_n)$, while all off-diagonal elements are equal to $1/(2m_0)$.

2.2. Clamped-Nuclei Hamiltonian

Finding the eigenfunctions of the Coulomb Hamiltonian (CH) in eq 1 expressed in the laboratory frame would involve describing translational states of the COM and therefore the use of plane waves in the trial wave functions. The resulting states would be completely delocalized in space, having little practical use from a chemical prospective. As pointed out in section 2.1, the separation of the COM motion from the internal motion generates a Hamiltonian of the type in eq 5. Such a Hamiltonian in the mass polarization terms mixes derivatives of the electronic and nuclear coordinates. The direct use of the Hamiltonian in eq 5 is far from being trivial and is

dx.doi.org/10.1021/cr200419d | Chem. Rev. 2013, 113, 36–79

the subject of the sections devoted to the non-BO approach. To simplify the problem, first Heitler and London[97] and then Born and Oppenheimer[98] decided to consider the nuclei as being particles with infinite masses. This led to a formalism, partly used also by Handy and Lee,[99] involving the splitting of the CH into two contributions:

$$\hat{H}_{\mathrm{lab}} = \hat{H}_{\mathrm{el}} + \hat{T}_{\mathrm{n}} \tag{9}$$

$\hat{H}_{el}$ is defined as

$$\hat{H}_{\mathrm{el}} = -\frac{1}{2m_{\mathrm{e}}}\sum_{i=1}^{N_{\mathrm{e}}} \nabla_{\mathbf{r}_i^{\mathrm{e}}}{}^2 + V(\{\mathbf{r}^{\mathrm{e}}\};\{\mathbf{r}^{\mathrm{n}}\}) \tag{10}$$

where $\{\mathbf{r}^{\mathrm{e}}\}$ and $\{\mathbf{r}^{\mathrm{n}}\}$ are labels of electronic and nuclear coordinates, respectively, and $\nabla_{\mathbf{r}_i^{\mathrm{e}}}{}^2$ is a Laplacian operator that acts only on the three Cartesian coordinates of the ith electron, N_{e} represents the total number of electrons in the system. $\hat{T}_{\mathrm{n}}$ is the kinetic energy of the nuclei and is defined as

$$\hat{T}_{\mathrm{n}} = -\sum_{\alpha=1}^{N_{\mathrm{n}}} \frac{1}{2M_\alpha}\nabla_{\mathbf{r}_\alpha^{\mathrm{n}}}{}^2 \tag{11}$$

where M_α is the mass of nucleus α. From eq 11 it follows that if the nuclear masses are allowed to reach very large values (at the limit of infinite masses) the only term to survive in eq 9 is $\hat{H}_{\mathrm{el}}$, also known as the clamped-nuclei (CN) Hamiltonian. In this review, we refer to BO calculations as those that approximate the eigenfunctions of the CN Hamiltonian, where the nuclei are kept at fixed positions in space and the only variables the wave function depends on are the positions of the electrons.

2.3. The Adiabatic Approximation

The SE involving the CN Hamiltonian has the following form:

$$\hat{H}_{\mathrm{el}}\Phi_\mu(\mathbf{r}^{\mathrm{e}};\mathbf{r}^{\mathrm{n}}) = E^\mu(\mathbf{r}^{\mathrm{n}})\,\Phi_\mu(\mathbf{r}^{\mathrm{e}};\mathbf{r}^{\mathrm{n}}) \tag{12}$$

The solutions $\Phi_\mu(\mathbf{r}^{\mathrm{e}};\mathbf{r}^{\mathrm{n}})$ are also called electronic wave functions, and sometimes the CN Hamiltonian is called the electronic Hamiltonian. In this section we assume that the solutions of eq 12 are nondegenerate. The semicolon separating the electronic and nuclear coordinates in eq 12 denotes the fact that the nuclear coordinates are treated as parameters in both the Hamiltonian and the wave function. This means that the nuclear coordinates take part in neither the derivative operations nor the integrals.

In the calculation of the ground state wave function, once $\Phi_0(\mathbf{r}^{\mathrm{e}};\mathbf{r}^{\mathrm{n}})$ is available, or approximated to a sufficient degree of accuracy, a trial solution to the CH can be attempted as a product of a purely nuclear function, denoted as $\chi(\mathbf{r}^{\mathrm{n}})$, with $\Phi_0(\mathbf{r}^{\mathrm{e}};\mathbf{r}^{\mathrm{n}})$, namely

$$\Psi_{\mathrm{a}}^0(\mathbf{r}^{\mathrm{e}},\mathbf{r}^{\mathrm{n}}) = \chi(\mathbf{r}^{\mathrm{n}})\,\Phi_0(\mathbf{r}^{\mathrm{e}};\mathbf{r}^{\mathrm{n}}) \tag{13}$$

where the subscript "a" stands for *adiabatic* to indicate that the electronic part of the wave function is calculated assuming that the electrons follow the motions of the nuclei adiabatically, i.e., without transferring any part of their energy to the nuclei, and vice versa.

Because the electronic wave function $\Phi_0(\mathbf{r}^{\mathrm{e}};\mathbf{r}^{\mathrm{n}})$ must be independent of the COM motion, the nuclear coordinates in the trial wave function above are a redundant set. In mathematical terms we can impose the independence of the electronic wave function from the COM motion by having $\Phi_0(\mathbf{r}^{\mathrm{e}};\mathbf{r}^{\mathrm{n}})$ being a constant upon any displacement of the COM coordinates, namely

$$\hat{H}_{\mathrm{CM}}\Psi_{\mathrm{a}}^0(\mathbf{r}^{\mathrm{e}},\mathbf{r}^{\mathrm{n}}) = -\frac{1}{2M}\nabla_{\mathbf{r}_0}{}^2\Psi_{\mathrm{a}}^0(\mathbf{r}^{\mathrm{e}},\mathbf{r}^{\mathrm{n}}) = 0 \tag{14}$$

With the above properties of $\Psi_{\mathrm{a}}(\mathbf{r}^{\mathrm{e}},\mathbf{r}^{\mathrm{n}})$, it can be used as a trial wave function in the SE involving the CH with the assumption that the electronic part needs no further improvement and can be integrated out. The function $\chi(\mathbf{r}^{\mathrm{n}})$ is then obtained by first integrating over the electronic coordinates with the $\Phi_0(\mathbf{r}^{\mathrm{e}};\mathbf{r}^{\mathrm{n}})$ being replaced by $\Phi_0(\mathbf{r}^{\mathrm{e}},\mathbf{r}^{\mathrm{n}})$, where now the nuclear coordinates are promoted from parameter to variable status. Carrying out such a procedure, one obtains the following SE for the nuclear functions $\chi_k(\mathbf{r}^{\mathrm{n}})$:[99]

$$\left(-\sum_{\alpha=1}^{N_{\mathrm{n}}}\frac{1}{2\mu_\alpha}\nabla_\alpha{}^2 + U^\mu(\mathbf{r}^{\mathrm{n}}) - \lambda_k\right)\chi_k(\mathbf{r}^{\mathrm{n}}) = 0 \tag{15}$$

where λ_k represents the eigenvalue corresponding to $\chi_k(\mathbf{r}^{\mathrm{n}})$ and the potential, in which the nuclei move, is generally specific to the electronic state (μ), namely

$$U^\mu(\mathbf{r}^{\mathrm{n}}) = E^\mu(\mathbf{r}^{\mathrm{n}}) + \langle\Phi_\mu(\mathbf{r}^{\mathrm{e}},\mathbf{r}^{\mathrm{n}})|\hat{T}_{\mathrm{n}}|\Phi_\mu(\mathbf{r}^{\mathrm{e}},\mathbf{r}^{\mathrm{n}})\rangle_{\mathbf{r}^{\mathrm{e}}} \tag{16}$$

The $\langle\,\rangle_{\mathrm{re}}$ stands for integration over the electronic coordinates. In the right-hand side of eq 15 terms that involve other solutions to the CN Hamiltonian, or electronic excited states, do not appear because they have not been introduced in the ansatz in eq 13.

Equation 11 shows that the potential in which the nuclei move is not just the corresponding eigenvalue of the electronic wave function. An additional term needs to be added, called the *adiabatic correction*, or the diagonal Born−Oppenheimer correction (DBOC hereafter). Generally, the DBOC is specific to the particular electronic state described by the wave function $\Phi_\mu(\mathbf{r}^{\mathrm{e}},\mathbf{r}^{\mathrm{n}})$, and has the following form:

$$E_{\mathrm{a}}^\mu(\mathbf{r}^{\mathrm{n}}) = -\sum_\alpha \frac{1}{2M_\alpha}\langle\Phi_\mu(\mathbf{r}^{\mathrm{e}},\mathbf{r}^{\mathrm{n}})|\nabla_\alpha{}^2|\Phi_\mu(\mathbf{r}^{\mathrm{e}},\mathbf{r}^{\mathrm{n}})\rangle_{\mathbf{r}^{\mathrm{e}}} \tag{17}$$

The inclusion of the DBOC of eq 17 corrects the CN energy by a term of the order of $O(m_{\mathrm{e}}/M)$. In section 11.3 the methodology of calculating the DBOC with floating ECG is presented.

The above procedure to obtain the adiabatic corrections should be taken by the reader with a grain of salt. Here, we aim to approximate the solutions of the CH starting from the solutions of the CN Hamiltonian. We are not trying to justify whether the form of the trial wave function in eq 13 is appropriate, such as having proper permutational and rotational symmetry. For a more in-depth discussion of the links between the CH and the CN Hamiltonian, we refer the interested reader elsewhere.[100,101]

2.4. Including the Nonadiabatic Effects by Means of Perturbation Theory

The correction derived in section 2.3 refines the CN energy by a term having the $O(m_{\mathrm{e}}/M)$ magnitude. This correction modifies the BO PES by the addition of a term. The corrected PES is then

$$U^\mu(\mathbf{r}^{\mathrm{n}}) = E^\mu(\mathbf{r}^{\mathrm{n}}) + E_{\mathrm{a}}^\mu(\mathbf{r}^{\mathrm{n}}) \tag{18}$$

A nonadiabatic correction to the ground state energy cannot be included in the same way as the adiabatic correction. That is because any nonadiabaticity will mix ground and excited electronic states, as well as ground and excited rovibrational states. It is impossible to disentangle these two contributions.

dx.doi.org/10.1021/cr200419d | Chem. Rev. 2013, 113, 36–79

Therefore, the correction to the adiabatic energy must depend on both nuclear and electronic coordinates, namely $E^0_{na}(\mathbf{r}^e,\mathbf{r}^n)$, and it is specific to the rovibrational adiabatic state considered. The nonadiabatic correction is derived by considering wave function corrections orthogonal to the adiabatic wave function of eq 13, e.g., orthogonal to $\Phi^0(\mathbf{r}^e;\mathbf{r}^n)$ in the electronic coordinates, and/or orthogonal to $\chi(\mathbf{r}^n)$ in the nuclear coordinates. An ansatz of the wave function that goes beyond the adiabatic approximation is commonly written as

$$\Psi(\mathbf{r}^e, \mathbf{r}^n) = \sum_{\mu,k} c_{\mu,k}\chi_k(\mathbf{r}^n)\,\Phi_\mu(\mathbf{r}^e; \mathbf{r}^n) \tag{19}$$

$$= \Psi_a(\mathbf{r}^e, \mathbf{r}^n) + \Psi_{na}(\mathbf{r}^e, \mathbf{r}^n) \tag{20}$$

where Φ_μ are the wave functions of electronic excited states obtained by solving the CN SE in eq 12, the χ_k are approximate nuclear wave functions, and the $c_{\mu,k}$ are some real-valued expansion coefficients. For the sake of clarity, the label denoting the electronic state has been omitted by the total wave functions in eqs 19 and 20, as well as in the equations that follow. In an intermediate normalization framework, the first term of the series in eq 20 would be identical to the wave function in eq 13.

The nonadiabatic correction can be derived using the perturbative formalism with the CH represented as a sum of adiabatic Hamiltonian, $\hat{H}_a$, and a perturbation, $\hat{H}'$. The adiabatic Hamiltonian can be written in a spectral form in terms of its eigenvalues and the CN electronic eigenfunctions as

$$\hat{H}_a = \sum_\mu |\Phi_\mu\rangle U^\mu \langle\Phi_\mu| \tag{21}$$

and the perturbation is defined as what is left to make up the CH:

$$\hat{H}' = \hat{H}_{lab} - \hat{H}_a \tag{22}$$

In order to numerically solve the problem, it is not possible to consider matrix elements of the $\hat{H}'$ perturbation, as they are not well-defined.[102] A better approach[103,104] is to start by splitting the wave function into adiabatic and nonadiabatic contributions, as in eq 19, and derive perturbative-like solutions to the nonadiabatic part.

By applying eqs 12 and 16, and by noticing that the first-order nonadiabatic correction to the adiabatic energy is zero, the first result can be derived right away, namely

$$\langle\Phi_0|\hat{H}'|\Phi_0\rangle_{\mathbf{r}^e} = 0 \tag{23}$$

Thus, the leading correction is a second-order quantity. The first step in computing this correction is by finding an expression for the first-order correction to the wave function, that is, the Ψ_{na} term in eq 20. In doing so, Pachucki and Komasa[103,104] derived the following equation:

$$\Psi_{na} = \Phi_0\delta\chi + \frac{1}{(E^0(\mathbf{r}^n) - \hat{H}_{el})'}\hat{T}_n\Psi_a \tag{24}$$

where the operators have the same meaning as in eq 9; the prime indicates that the reference state, Φ_0, is excluded from the inversion. The $\delta\chi$ function indicates the nonadiabatic correction to the nuclear wave function. The Pachucki–Komasa[103,104] nonadiabatic correction to the electronic energy takes the form

$$E_{na} = \langle\Psi_a|\hat{H}'|\Psi_{na}\rangle = \langle\Psi_a|\hat{T}_n|\Psi_{na}\rangle = \left\langle \Psi_a \middle| \hat{T}_n \frac{1}{(E^0(\mathbf{r}^n) - \hat{H}_{el})'}\hat{T}_n \middle| \Psi_a \right\rangle \tag{25}$$

which is of second order in terms of the perturbation eq 22. We should note that the adiabatic ansatz involved in eq 25 could be labeled with a rotational and a vibrational quantum number, thus showing that the nonadiabatic corrections are specific to each rovibrational state.

2.5. The Variational Method

Most of the calculations considered in this review are performed within the framework of the Ritz variational method. The main idea of the variational method in nonrelativistic quantum mechanics is based on the fact that the expectation value of the Hamiltonian of the system computed with an arbitrary wave function, $\psi(\mathbf{r})$ (here $\mathbf{r}$ denotes the coordinates of all active particles), which satisfies the proper symmetry constraints, is always an upper bound to the exact ground state energy, $\langle\psi|\hat{H}|\psi\rangle/\langle\psi|\psi\rangle \geq E_0$. This general property of the energy functional facilitates a way to obtain very accurate approximations to the exact wave function by the optimization of the parameters, both linear and nonlinear, which the function comprises. This optimization is accomplished by the energy minimization. If the wave function is expanded in terms of some basis functions

$$\psi(\mathbf{r}) = \sum_{k=1}^{K} c_k\phi_k(\mathbf{r}) \tag{26}$$

and only the linear coefficients are optimized, then the energy minimization procedure reduces to solving the generalized eigenvalue problem

$$\mathrm{Hc} = \varepsilon\mathrm{Sc} \tag{27}$$

where H and S are $K \times K$ symmetric (or Hermitian if the basis functions are complex) matrices of the Hamiltonian and overlap $H_{kl} = \langle\phi_k|\hat{H}|\phi_l\rangle$ and $S_{kl} = \langle\phi_k|\phi_l\rangle$, while c is a K-component vector of the linear coefficients. Equation 27 has K solutions, i.e., K energy values and K corresponding wave functions. According to the mini–max theorem, if the energy values are set in an increasing order, the first one provides an upper bound to the exact nonrelativistic ground state energy of the system and the kth one provides an upper bound to the exact energy of the $(k-1)$th excited state (details of the proof can be found in ref 5).

In addition to varying the linear coefficients in the wave function expansion, one can also vary nonlinear parameters involved in the basis functions. The accuracy of atomic and molecular quantum mechanical calculations, particularly those involving explicitly correlated basis functions, is primarily achieved by performing extensive optimization of the basis function nonlinear parameters.

2.6. Choices of Basis Functions for Highly Accurate Variational BO and Non-BO Calculations

In atomic calculations the possible choices of the basis functions are limited. The most crucial limitation is related to the need for accurate and expeditious calculation of the Hamiltonian matrix elements. Also, the basis set has to accurately describe the state of the system under consideration

dx.doi.org/10.1021/cr200419d | Chem. Rev. 2013, 113, 36–79

Table 2. BO Energies (in hartrees) of Hydrogen Molecule at R_{H-H} = 1.4011 bohr[a]

K	energy	ΔE	type	year	authors
22 363	−1.174 475 931 400 215 99	0.000 000 217 179 772 54	JC	2010	Pachucki[80]
4800	−1.174 475 931 400 135	0.000 000 217 179 772	ECG	2008	Cencek and Szalewicz[75]
2400	−1.174 475 931 399 860	0.000 000 217 179 772	ECG	2008	Cencek and Szalewicz[75]
1200	−1.174 475 931 395	0.000 000 217 180	ECG	2008	Cencek and Szalewicz[75]
600	−1.174 475 931 326	0.000 000 217 180	ECG	2008	Cencek and Szalewicz[75]
300	−1.174 475 929 976	0.000 000 217 179	ECG	2008	Cencek and Szalewicz[75]
6776	−1.174 475 931 400 027		ICI	2007	Nakatsuji et al.[122]
7034	−1.174 475 931 399 84	0.000 000 217 179 76	JC	2006	Sims and Hagstrom[123]
883	−1.174 475 930 742	0.000 000 217 177	KW	1995	Wolniewicz[120]

[a] ΔE is the energy difference between calculations at R_{H-H} = 1.4011 bohr and R_{H-H} = 1.4 bohr.

and, in particular, the electron correlation effects in the state. As these effects concern electrons avoiding each other in their motions around the nucleus, the most effective basis functions for describing the correlation phenomenon are functions explicitly dependent on the interelectron distances. The most efficient explicitly correlated functions are those that simultaneously depend on distances of all electrons in the system.

The most serious problem in the development of methods employing explicitly correlated functions is the difficulty that may arise in accurately calculating the integrals which appear in the Hamiltonian matrix elements. As the complexity of these integrals grows with the increasing number of electrons and with the electrons occupying higher angular momentum states, more complicated expressions for these integrals appear. This may create difficulties in extending the calculations to systems with more electrons.

Among the basis functions most often used in quantum calculations of small atoms with less than four electrons, there are the Hylleraas-type functions[31,105−109] and the exponential functions (also known as the Slater-type functions).[110−113] For a three-electron atomic system the Hylleraas function has the following form (here we consider the states with zero total angular momentum):

$$\phi(\mathbf{r}_1, \mathbf{r}_2, \mathbf{r}_3) = r_{23}^{n_1} r_{31}^{n_2} r_{12}^{n_3} r_1^{n_4} r_2^{n_5} r_3^{n_6} \exp(-\alpha_1 r_1 - \alpha_2 r_2 - \alpha_3 r_3) \quad (28)$$

where r_i are electron−nucleus distances, r_{ij} are interelectron distances, and α's are parameters which are subject to optimization in the variational calculation. One notices that the Hylleraas functions are only correlated through the preexponential polynomials and there is no r_{ij} presence in the exponent. In the exponential functions

$$\phi(\mathbf{r}_1, \mathbf{r}_2, \mathbf{r}_3) = \exp(-\alpha_1 r_1 - \alpha_2 r_2 - \alpha_3 r_3 - \beta_1 r_{23} - \beta_2 r_{31} - \beta r_{12}) \quad (29)$$

the opposite happens: the r_{ij} factors are only present in the exponent. Recently, it was demonstrated that the exponential functions in eq 29 are very effective in calculations of atoms with three electrons[113] and other four-body Coulomb systems.[114] Clearly, they are capable of describing both the short-range cusp behavior of the wave function as defined by the Kato conditions[115] and the long-range behavior. However, neither the Hylleraas functions nor the exponential functions have been applied to study atomic systems with more than three electrons. This limitation is due to the lack of algorithms for accurate and efficient calculation of Hamiltonian matrix elements with those functions for systems with more than three electrons. However, such algorithms exist for ECGs, which will be discussed later in this review.

Explicitly correlated functions have also been employed in molecular BO calculations. The most thoroughly investigated system has been the H_2 molecule, whose first study dates back to James and Coolidge.[116] Some of the most impressive calculations performed for this system have been those of Kołos and Wolniewicz. The wave functions in their approach were inspired by the work of James and Coolidge and were expanded in terms of the following functions (denoted by G_k below) expressed in terms of elliptic coordinates of the two electrons denoted by the labels 1 and 2:[117−120]

$$G_k(1, 2) = (x_1 + iy_1)^{\Lambda} g_k(1, 2) \pm (x_2 + iy_2)^{\Lambda} g_k(2, 1) \quad (30)$$

$$g_{\nu,r,s,\bar{r},\bar{s}}(1, 2) = \exp(-\alpha\xi_1 - \bar{\alpha}\xi_2)\rho^{\nu}\xi_1^{r}\eta_1^{s}\xi_2^{\bar{r}} \eta_2^{\bar{s}}\{\exp(\beta\eta_1 + \bar{\beta}\eta_2) + (-1)^{s+\bar{s}+\Lambda+p} \exp(-\beta\eta_1 - \bar{\beta}\eta_2)\} \quad (31)$$

The "±" in eq 31 refers to singlet and triplet states, respectively, Λ is the angular momentum projection quantum number, and p = 0, 1 for g and u symmetries, respectively. $\xi_j = (r_{ja} + r_{jb})/R$ and $\eta_j = (r_{ja} - r_{jb})/R$ are the elliptic, and x_j and y_j the Cartesian coordinates for the two electrons with the z axis coinciding with the internuclear axis ("a" and "b" denote nuclei). $\rho = 2r_{12}/R$, r_{12} is the interelectronic distance, and c_i, α, $\bar{\alpha}$, β, and $\bar{\beta}$ are variational parameters. Thus the basis set is defined by the set of exponents ν_i, r_i, s_i, $\bar{r}_i$, and $\bar{s}_1$. The calculations reported in 1995 by Wolniewicz[120] with the basis functions in eq 31 still remain some of the most accurate ever performed with the BO approach involving the calculation of the potential energy surface first and then calculating the rovibrational energy levels by solving the Schrödinger equation for the nuclear motion. The drawback of the basis functions in eq 31 is that they cannot be extended to study molecules with more than two nuclei. Even an extension of the approach to diatomics with more than two electrons has not been accomplished. Thus, at present, the only basis set of explicitly correlated functions that can be extended to systems with more than two electrons and/or more than two nuclei are Gaussians. We will describe the various types of molecular Gaussian functions used in the BO and non-BO, atomic and molecular calculations in section 3.

2.7. Competition between ECG and JC Functions

Very recently, Pachucki[80] employed another type of explicitly correlated functions, the James−Coolidge (JC) functions,[116] in BO variational calculations of the hydrogen molecule. In those calculations he obtained a lower energy at the equilibrium

dx.doi.org/10.1021/cr200419d | Chem. Rev. 2013, 113, 36−79

internuclear distance than the previous best result by Cencek and Szalewicz obtained with 4800 ECGs.[75] The advantage of using the JC basis set in H_2 calculations lies in the fact that this set comprises many fewer nonlinear parameters that need to be optimized than the ECG basis set. However, the JC basis is again restricted to two-electron, two-nucleus molecules and cannot be extended to larger systems.

A comparison of the variationally lowest energies ever obtained in calculations for the hydrogen molecule at the equilibrium distance is shown in Table 2. Among those energies, there is the result of Kołos and Wolniewicz (KW)[121] obtained with generalized JC functions defined in eq 31, which include more nonlinear parameters than the original JC functions to better describe the long-range asymptotic behavior of the wave function. There is also the result obtained by Nakatsuji et al.[122] with the iterative-complement-interaction (ICI) method which essentially generated a set of basis functions (exponents times prefactors) depending on elliptic coordinates. This result was the best energy value at the time it was published.

In Table 2 we also show the H_2 BO energies of Cencek and Szalewicz[75] calculated at R_{H-H} = 1.4 bohr with different numbers of ECGs. The results are not quite comparable with the other literature values because most of those values have been calculated at R_{H-H} = 1.4011 bohr. Based on the ECG basis set Cencek and Szalewicz obtained for H_2 at R_{H-H} = 1.4 bohr, they generated basis sets for several other internuclear distances using a procedure that automatically shifts the Gaussian centers to adjust them for the changing internuclear distance. This allowed them to calculate an H_2 PEC without reoptimization of the Gaussians at each PEC point, which would be very time-consuming. Only the linear expansion coefficients in the wave function were reoptimized by solving the secular equation problem. They showed that the shifting procedure allows maintaining the accuracy of the whole PEC at an almost constant level. This demonstrates that the computational time for ECG calculations can be significantly reduced if an effective approach for guessing new Gaussians to be added to the basis set and for optimizing them is developed.

Another example where an effective approach of this kind was impelmented is the ECG calculations of Cencek et al.[124] concerning the molecular hydrogen dimer, $(H_2)_2$. The approach involved contracting two large H_2 ECG basis sets to form a basis set for the dimer with tens of thousands of ECGs. The nonlinear parameters in this basis set were not optimized, but instead some additional ECGs were included to better account for the interaction between the hydrogen molecules. The nonlinear parameters of these added ECGs were variationally optimized in the calculations.

We should stress that, even though the variational calculations involving all-electron ECGs scale as the factorial of the number of the electrons, they can be extended to larger numbers of electrons than two, as the algorithms for calculating the Hamiltonian and overlap matrix elements are general. This is not the case for the JC functions, where the integrals need to be rederived (they have not been yet) to calculate molecular systems with more than two electrons.

3. EXPLICITLY CORRELATED GAUSSIAN BASIS SETS

As mentioned, the main advantage of using ECGs in atomic and molecular calculations is due to the simplicity in evaluating the overlap and Hamiltonian matrix elements and easy generalization to atoms and molecules with an arbitrary number of electrons. While ECGs have been shown to form a complete basis set,[125−127] they have improper short-distance behavior (unable to satisfy Kato cusp conditions[115]) and too-fast decaying long-range behavior. Even though these deficiencies can be effectively remedied by using longer expansions, they may cause a significant increase in the amount of computational effort needed for a well-converged calculation. Certain issues may also arise in the calculations of relativistic corrections and other properties, where proper short-range behavior is important.

3.1. Basis Sets for Atomic Calculations with Infinite and Finite Nuclear Mass

We will first discuss the basis sets we have used in atomic and molecular calculations performed without assuming the BO approximation. For atoms, the non-BO calculations are more often called finite-nuclear-mass (FNM) calculations. Even though such atomic calculations are only marginally more difficult (the Hamiltonian includes the mass polarization term, which is absent when the nuclear mass is set to zero) and essentially equally as time-consuming as the infinite-nuclear-mass (INM) calculations, most very accurate atomic calculations published in the literature have been performed with the INM approach. However, there have been also atomic calculations which employed the FNM approach.[15−17,128−131] This method not only allows for directly calculating energies of ground and exited states of different isotopes, thus enabling determination of isotopic energy shifts, but it also, by setting the nuclear mass to infinity, allows generation of INM results. When different isotopes of a particular element are calculated, one may consider reoptimizing the nonlinear parameters of the Gaussians in the basis set for each of them. However, as the numerical experiments show, the change in the mass of the nucleus can be effectively accounted for by readjusting the linear coefficients of the basis functions, i.e., by recomputing the Hamiltonian matrix and solving the eigenvalue problem with the same basis set. Since the change of the wave function remains small when the mass of the nucleus is varied (true as long as the nuclear mass stays much larger than the mass of electrons), such a simplification has virtually no effect on the accuracy of the calculations.

In the calculations of atoms with only s electrons the r_{ij} dependency in the Gaussian functions can be limited to the exponential factor. For an n-electron system these functions have the following form:

$$\phi_k(\mathbf{r}_1, \mathbf{r}_2, ..., \mathbf{r}_n) = \exp[-\mathbf{r}'(A_k \otimes I_3)\mathbf{r}] \tag{32}$$

where $\mathbf{r}$ is a $3n$-component vector formed by stacking $\mathbf{r}_1$, $\mathbf{r}_2$, ..., $\mathbf{r}_n$ on top of each other (r_i is the distance between electron i and the nucleus), A_k is a $n \times n$ symmetric matrix, I_3 is a 3×3 identity matrix, "$\otimes$" is the Kronecker product symbol, and the prime indicates vector (matrix) transpose. In some of the expressions in this review we will use a shorter notation for the Kronecker product of a matrix and I_3: $\mathbf{A}_k \equiv A_k \otimes I_3$. In general, A_k does not have to be a symmetric matrix. However, one can always rearrange its elements in such a way that it becomes symmetric without changing the quadratic form $\mathbf{r}'\mathbf{A}_k\mathbf{r}$. Since dealing with symmetric matrices has certain practical advantages in further considerations, we will always assume the symmetry of A_k.

As the basis functions used in describing bound states must be square integrable, some restrictions must be imposed on the elements of A_k matrices. Each A_k matrix must be positive

dx.doi.org/10.1021/cr200419d | Chem. Rev. 2013, 113, 36−79

definite. Rather than enforcing the positive definiteness of A_k, which usually leads to cumbersome constraints, we use the following Cholesky factored form of A_k: $A_k = L_k L_k'$, where L_k is a lower triangular matrix. With this representation, A_k is automatically positive definite for any values of L_k ranging from ∞ to $-\infty$. Thus, the variational energy minimization with respect to the L_k parameters can be carried out without any restrictions. It should be noted that the $L_k L_k'$ representation of A_k matrix does not limit the flexibility of basis functions, because any symmetric positive definite matrix can be represented in a Cholesky factored form.

In order to improve the quality of the atomic *s*-type ECGs (eq 32), particularly in terms of providing a better description of the short- or long-range behavior, one can include in those functions preexponential factors similar to those present in the Hylleraas functions defined in eq 28:

$$\phi_k(\mathbf{r}_1, \mathbf{r}_2, ..., \mathbf{r}_n) = \left(\prod_{i>j}^{n} r_{ij}^{n_{ij}}\right) \exp[-\mathbf{r}'(A_k \otimes I_3)\mathbf{r}] \tag{33}$$

From a practical point of view, it is easier to use even powers of the interelectron distances in such factors (n_{ij} even), or just their squares ($n_{ij} = 2$), because the evaluation of the Hamiltonian integrals is then more straightforward. By including the r_{ij}^2 prefactors in Gaussians,[32] one obtains the following exponentially and preexponentially, explicitly correlated Gaussian functions:

$$\phi_k(\mathbf{r}_1, \mathbf{r}_2, ..., \mathbf{r}_n) = \left(\prod_{i>j}^{n} r_{ij}^{2}\right) \exp[-\mathbf{r}'(A_k \otimes I_3)\mathbf{r}] \tag{34}$$

Even though, in principle, all interelectron distances should be included in $\prod_{i>j}^{n} r_{ij}^2$, a simpler approach with only a limited number of those distances can also be considered. In such an approach the Gaussian basis set would comprise the following subsets of functions:

$$\{\{\exp[-\mathbf{r}'(A_k \otimes I_3)\mathbf{r}]\}, \quad \{r_{ij}^2 \exp[-\mathbf{r}'(A_k \otimes I_3)\mathbf{r}]\}, \quad \{r_{ij}^2 r_{kl}^2 \exp[-\mathbf{r}'(A_k \otimes I_3)\mathbf{r}]\}, \quad ...\} \tag{35}$$

In particular, one can consider a basis set that only includes the two first subsets:

$$\{\{\exp[-\mathbf{r}'(A_k \otimes I_3)\mathbf{r}]\}, \quad \{r_{ij}^2 \exp(-\mathbf{r}'(A_k \otimes I_3)\mathbf{r})\}\} \tag{36}$$

Such a basis set was recently tested,[132] and it was shown that placing r_{ij}^2 factors in front of the Gaussian exponents leads to a noticeable improvement of the energy convergence.

There is another issue that arises in atomic calculations, particularly in those concerning excited states. It is related to describing radial nodes and angular nodes in the wave functions. In dealing with the radial nodes, for example, in the calculations of ^{1}S excited states of the beryllium atom, the radial flexibility of the Gaussians is a key factor. For lower lying states, the standard correlated Gaussians, eq 32, provide a sufficiently flexible basis set to describe the few radial nodes. However, for higher lying states with more radial nodes the standard Gaussians may need to be modified to facilitate more radial flexibility. This can be accomplished using the following complex Gaussians:[128,133,134]

$$\phi_k = \exp[-\mathbf{r}'\mathbf{C}_k\mathbf{r}] \equiv \exp[-\mathbf{r}'((A_k + iB_k) \otimes I_3)\mathbf{r}] \tag{37}$$

where A_k and B_k are $n \times n$ symmetric matrices that represent the real and imaginary parts of $\mathbf{C}_k$, respectively.

Considering ground states of atoms with more than four electrons (for example, the boron atom) or some excited states of even smaller atomic systems requires that angular factors are placed in front of the exponents of the Gaussian basis functions (more details on the rotational symmetry of the basis functions will be given in section 4.3). For the states corresponding to a dominant configuration with just one p electron, the following form of Gaussians can be used:

$$\phi_k = z_{m_k} \exp[-\mathbf{r}'(A_k \otimes I_3)\mathbf{r}] \tag{38}$$

Here m_k is an integer that depends on k and may take values from 1 to n. It is convenient to represent functions 38 as

$$\phi_k = (\mathbf{v}^k)'\mathbf{r} \exp[-\mathbf{r}'\mathbf{A}_k\mathbf{r}] \tag{39}$$

where $\mathbf{v}^k$ is a vector whose components are all 0, except the $3m_k$th component, which is set to 1.

For the case of states with two p electrons (for example, the ground $1s^2 2s^2 2p^2$ state of the carbon atom) or one d electron, one can use Gaussians with two electron coordinates placed in front of the exponent:[135−139]

$$\phi_k = \xi_{i_k}\xi_{j_k} \exp[-\mathbf{r}'(A_k \otimes I_3)\mathbf{r}] \tag{40}$$

where ξ_{i_k} and ξ_{j_k} can either be x, y, or z coordinates of electron i_k and j_k, respectively, with i_k and j_k either equal or not equal to each other.

In particular, in describing states with two p electrons (for example, in the calculations of the ^{3}P^o ground and first excited states of the carbon atom) the following Gaussian basis functions[135]

$$\phi_k = (x_{i_k}y_{j_k} - x_{j_k}y_{i_k}) \exp[-\mathbf{r}'(A_k \otimes I_3)\mathbf{r}] \tag{41}$$

were used. In calculating D states involving one d electron, the Gaussians had the form[138,139]

$$\phi_k = (x_{i_k}x_{j_k} + y_{j_k}y_{i_k} - 2z_{i_k}z_{j_k}) \exp[-\mathbf{r}'(A_k \otimes I_3)\mathbf{r}] \tag{42}$$

where electron indices i_k and j_k are either equal or not equal to each other.

It is convenient to use an alternative form of the angular preexponential multiplier. It involves the general quadratic form, $\mathbf{r}'\mathbf{W}_k\mathbf{r}$, that represents the preexponential factor. This form allows for a more generalized approach in deriving the matrix elements. For example, the Gaussians with the factor $x_{i_k}x_{j_k} + y_{i_k}y_{j_k} - 2z_{i_k}z_{j_k}$) can be written as

$$\phi_k = (\mathbf{r}'\mathbf{W}_k\mathbf{r}) \exp[-\mathbf{r}'(A_k \otimes I_3)\mathbf{r}] \tag{43}$$

where $\mathbf{W}_k$ is a sparse $3n \times 3n$ symmetric matrix that for $i_k = j_k$ comprises only three nonzero elements: $W_{3(i_k-1)+1,3(i_k-1)+1} = 1$, $W_{3(i_k-1)+2,3(i_k-1)+2} = 1$, and $W_{3(i_k-1)+3,3(i_k-1)+3} = -2$, and for $i_k \neq j_k$ it comprises six nonzero elements: $W_{3(i_k-1)+1,3(j_k-1)+1} = W_{3(j_k-1)+1,3(i_k-1)+1} = 1/2$, $W_{3(i_k-1)+2,3(j_k-1)+2} = W_{3(j_k-1)+2,3(i_k-1)+2} = 1/2$, and $W_{3(i_k-1)+3,3(j_k-1)+3} = W_{3(j_k-1)+3,3(i_k-1)+3} = 1$. It should be noted that, in general, we could have used a nonsymmetric matrix $\mathbf{W}_k$ (for $i_k \neq j_k$) with only three nonzero elements (yielding the same quadratic form) since there are only three terms in eq 42. However, as already mentioned, it is much more convenient to deal with symmetric matrices in practice. The main reason for this is that the derivation of matrix elements

dx.doi.org/10.1021/cr200419d | Chem. Rev. 2013, 113, 36−79

becomes considerably simpler. In a similar manner, one can devise forms of Gaussians even for states with higher total orbital angular momenta (or higher than 2 number of non-s electrons). These forms, however, become progressively more complex.

3.2. Basis Sets for Non-BO Calculations on Diatomic Molecules

After separating the center-of-mass motion from the laboratory-frame Hamiltonian of a molecule, the Hamiltonian that describes the intrinsic motion of the system, the internal Hamiltonian, is isotropic (i.e., spherically symmetric). Eigenfunctions of such a Hamiltonian form an irreducible representation of the fully symmetric group of rotations. Thus, those functions are atom-like functions, which, besides being eigenfunctions of the Hamiltonian, are also eigenfunctions of the square of the total orbital angular momentum operator and the operator representing its projection on a selected axis. As such, the Hamiltonian matrix calculated with eigenfunctions of the square of the total orbital angular momentum is a block-diagonal matrix. This allows for separating the calculations of states corresponding to different total orbital angular momentum quantum numbers. In particular, when spherically symmetric basis functions are used in the calculations, the so-called rotationless states are obtained. Those states correspond to the ground and excited "vibrational" states of the system. We put "vibrational" in quotation marks because, if the BO approximation is not assumed in the calculation, the electronic and vibrational degrees of freedom mix and the wave function for a particular "vibrational" state may contain contributions from products of different electronic wave functions and different vibrational wave functions. Due to this coupling of the vibrational and electronic motions the vibrational quantum number is no longer a good quantum number. It should be, perhaps more correctly, regarded as a number which numbers consecutive states in the manifold corresponding to the particular total orbital angular momentum quantum number.

In the fully non-BO ECG calculations for diatomic molecules performed so far only rotationless states, i.e., states represented by spherically symmetric wave functions, have been considered.[7,140,141] In the calculations of those states the following explicitly correlated Gaussians multiplied by even powers of the internuclear distance, r_1 (the powers usually range from 0 to 250), have been used:

$$\phi_k = {r_1}^{p_k} \exp[-\mathbf{r}'\mathbf{A}_k\mathbf{r}] \tag{44}$$

where it is assumed that the center of the internal coordinate system is placed on the first nucleus (usually the heaviest one), the first pseudoparticle represents the second nucleus, and the remaining pseudoparticles represent the electrons.

As one notices, function 44 is spherically symmetric with respect to the center of the coordinate system. All particles are explicitly correlated in the Gaussian exponent (i.e., the exponent explicitly depends on all interparticle distances). There is also an additional correlation factor for the two nuclei that depends on powers of the internuclear distance, ${r_1}^{p_k}$. The purpose of this factor is to effectively separate the nuclei from each other and to describe the oscillations of the wave function resulting from vibrational excitation. In the vibrational ground state the wave function should have a maximum for r_1 around the vibrationally averaged ground state internuclear distance. The combination of the ${r_1}^{p_k}$ factors with different p_k powers and the Gaussian exponent can very effectively generate such a maximum. In the first vibrational excited state the wave function has a single node and it can also be very well described by Gaussians (44). Moreover, as the calculations of the complete vibrational spectra for such systems as H_2^+ and its isotopologues,[142−144] H_2 and its isotopologues,[145−149] HeH^+,[150,151] and larger systems[21,152,153] have demonstrated, the Gaussians can very effectively describe even the highest vibrational excitations with multiple nodes.

The Hamiltonian integrals involving function 44 are more complicated than integrals with functions without premultipliers. With that the integrals take considerably longer to compute. Also, we should note that the powers of the internuclear distance in the basis functions used to calculate the ground state are smaller than those needed to calculate excited states.

In order to describe the vibrational states corresponding to the first rotational excited states, one needs to use the following Gaussians in expanding the wave functions of those states:

$$\phi_k = z_1 {r_1}^{p_k} \exp[-\mathbf{r}'\mathbf{A}_k\mathbf{r}] \tag{45}$$

Here we assume that the contribution of basis functions where z_1 is replaced by x_i, where $i \sim 1$, is unimportant. This assumption may be not be strictly correct for higher states near the dissociation threshold, for which z_1 in eq 45 should be replaced with z_{m_k}, where m_k ranges from 1 to n.

3.3. Basis Sets for Non-BO Calculations on Systems with More Than Two Nuclei

Let us first consider a molecule with three nuclei (the simplest such molecule is the H_3^+ ion). Applying the same arguments as used to justify the use of Gaussians eq 44 in non-BO diatomic calculations, the appropriate basis set of correlated spherically symmetric (one-center) Gaussians to describe rotationless states of a triatomic molecule, such as H_3^+, should consist of the following functions:

$$\phi_k = {r_1}^{p_k} {r_2}^{q_k} {r_{12}}^{t_k} \exp[-\mathbf{r}'\mathbf{A}_k\mathbf{r}] \tag{46}$$

As one notices, the preexponential multipier of the functions in eq 46 includes not one, as in eq 44, but three factors. The factors are powers of all three internuclear distances in the molecule. The presence of the powers allows for effectively separating the nuclei and placing them at relative distances which are on average equal to the equilibrium distances for the state which is being calculated. The powers are also important in generating radial nodes in the wave function in excited vibrational states. Unfortunately, the Hamiltonian and overlap matrix elements with the basis functions given in eq 46 become more complicated. While the expressions for them were derived in a closed algebraic form,[154] an efficient numerical implementation is problematic due to a large number of summation loops in the integral formulas which results from the powers of the internuclear distance in the preexponential factor.

A Gaussian basis set which, in principle, can be used for rotationless states of triatomic molecules and even of molecules with more than three nuclei is the basis of complex Gaussians in eq 37. An appropriate linear combinations of these Gaussians should generate sine/cosine type oscillations in the wave function which are needed in describing vibrational excited states. Future tests will show how effective Gaussians (37) are in describing those oscillations.

dx.doi.org/10.1021/cr200419d | Chem. Rev. 2013, 113, 36−79

3.4. Basis Sets for Non-BO Molecular Calculations in the Presence of External Electric Field

Let us consider an isolated diatomic molecule without the BO approximation. Such a consideration has many fundamental aspects and also provides a procedure for describing asymmetry in the charge distribution in molecular systems due to isotopic substitution (such an effect takes place, for example, in the HD molecule). As mentioned, the ground state ($L = 0$) wave function of the molecule is a spherically symmetric function. Let us now expose the molecule to a static electric field. If a calculation performed with the BO approximation shows that the molecule has a nonzero dipole moment or an anisotropy of the polarizability, the interaction with the field will result in the molecule orienting itself in space to minimize the interaction energy. When the field is small this orientation is only partial, but as the field increases the dipole moment axis of the molecule or the axis of its highest polarizability essentially becomes fully aligned with the direction of the field. It usually takes a very small field to achieve this full alignment. One can call this effect the orientational polarizability. When this happens, the non-BO wave function of the molecule loses its spherical symmetry and acquires an axial symmetry.

In addition to affecting the rotational state of the molecule (in a way one can say that the field excites the molecule to a high rotational state when the molecular dipole aligns with the direction of the field), the field also affects the vibrational and electronic motions. The field essentially polarizes the molecule vibrationally and electronically. To describe the field-induced deformation of a molecule in its ground state, the following correlated Gaussians with shifted centers were used:[155,156]

$$\phi_k = \exp[-(\mathbf{r} - \mathbf{s}_k)'\mathbf{A}_k(\mathbf{r} - \mathbf{s}_k)] \tag{47}$$

where $\mathbf{s}_k$ are the shifts of the Gaussian centers. Functions in eq 47 are also called explicitly correlated shifted Gaussians or floating ECGs. The shifts allow for deforming the molecular wave function to a cylindrical (oval) shape in the presence of the field. ECG basis eq 47 is, in principle, also capable of describing the ground state of the molecule in the absence of the field. It is not the most optimal basis for such a case, but with all the Gaussian centers being located at the origin of the coordinate system, it has the right symmetry of the system without the field. In refs 155 and 156 the non-BO dipole moments of isotopologues of H_2 and LiH were also evaluated using an approximate procedure employing the finite-field approach. Good agreement with the experimental values was achieved. The reader may also review the recent paper by Fernandez,[157] where the procedure used in refs 155 and 156 and the results obtained there were put into question.

3.5. Basis Sets for Molecular BO Calculations

In molecular BO calculations, there is no need to transform the coordinate system into an internal coordinate system representation. That is because the nuclei are fixed in space and therefore the center of mass does not move. A consequence is that the coordinates can be represented in the laboratory frame without any effect on the outcome of the calculation. In BO calculations ECGs become functions of the electronic coordinates only, expressed in the laboratory frame. The simplest Gaussians used in the BO calculations are those given in eq 47, with $\mathbf{L}_k$, I_3, and $\mathbf{s}_k$ having the same meaning as in eq 47, but with $\mathbf{r}$ containing only the electronic coordinates in the laboratory frame stacked similarly to the definition in eq 7. Gaussians 47 can only be used to describe states whose wave functions do not have nodes on the nuclei.

Equations in sections 2.2 and 2.3 show how in BO calculations the nuclear positions are formally present in the wave functions as parameters. In most of the available quantum chemistry software packages this parametrical dependence is explicitly accounted for by centering the atomic orbitals to the positions of the nuclei in a molecule. Deformations of the wave function needed to describe the directionality of chemical bonds are then obtained by employing Gaussian orbitals containing premultipliers (usually powers of Cartesian coordinates). Angular momentum functions with up to $l = 5$ are typically used.

The ECG-type functions defined in eq 47 do not include any angular momentum factors. Employing such angular momentum factors would be impractical as the formulas for calculating matrix elements of the clamped-nuclei Hamiltonian sandwiched by functions of the type in eq 47 quickly become complicated when $L \geq 2$. The problem is readily circumvented by avoiding the use of angular momentum functions and making up for that by allowing the centers of the ECGs to float. Technically, that is achieved by not equating the $\mathbf{s}_k$ vectors with the nuclear positions. Using floating ECGs means that the basis functions do not display any explicit parametrical dependence on the nuclear positions. Instead their Gaussian centers, $\mathbf{s}_k$, are considered to be adjustable parameters in the variational optimization. It is important to note that employing a floating centers basis set maintains an implicit parametrical dependence with respect to the nuclear positions. This can be understood if one realizes that the variationally optimized wave function is found using a Hamiltonian that is explicitly dependent on the nuclear positions, such as the CN Hamiltonian (11) used in the BO calculations.

To summarize, the use of floating ECGs allows the description of chemical bonds through the deformations of the electron density that are described by basis functions that float away from a nucleus. This choice of basis functions enables employing numerically sound overlap and Hamiltonian matrix elements at the expense of having to optimize $3N_e \times K$ nonlinear parameters, in addition to the Gaussian exponents (L_k) and the linear expansion coefficients (c_k) in eq 26, where N_e and K are the number of electrons and the number of basis functions employed.

3.5.1. Use of Premultipliers in ECG Basis Sets for Molecular BO Calculations. ECGs with floating centers defined in eq 47 perform best when used in the calculations of states with nodeless wave functions at the nuclei. A node in the wave function can only be described with floating ECGs by a superposition of Gaussians that have opposite signs. Depending on the nature of the node, such an "arithmetical" generation of the node can lead to numerical instabilities. This does not happen when the node lies, for example, on the imaginary line interconnecting two nuclei, which is the case of Σ_u^+ excited states in He_2[92,158] and H_2.[159] In this situation the node occurs in a region away from where the electron density peaks (at the nuclei); therefore, the arithmetic node generation is less likely to incur into a numerical instability. Different is the case of nodes occurring at the position of an nucleus. Such cases take place in many excited states of small molecules and atoms, and in some cases also in the ground state, as in the CH^+ molecular ion. To effectively describe a node at a nucleus, it is sufficient to append a proper angular function as a premultiplier to the ECG basis functions, namely

dx.doi.org/10.1021/cr200419d | Chem. Rev. 2013, 113, 36–79

$$\phi_k = Y(\mathbf{r}_i - \mathbf{r}^{\mathrm{nucl}}) \exp[-(\mathbf{r} - \mathbf{s}_k)'\mathbf{A}_k(\mathbf{r} - \mathbf{s}_k)] \quad (48)$$

where $Y(\mathbf{r}_i - \mathbf{r}^{\mathrm{nucl}})$ is some angular momentum function such as a spherical harmonic multiplied by the $(\mathbf{r}_i - \mathbf{r}^{\mathrm{nucl}})^l$ factor.

3.5.2. Ionic and Covalent Basis Functions. When atom-centered atomic orbitals (AOs) are used in molecular BO calculations, the wave function is expressed as an antisymmetrized product of molecular orbitals (MOs) and spin functions. The MOs are linear combination of AOs having proper spatial symmetry. The wave function obtained with the outlined procedure can then be decomposed into several antisymmetrized products of atomic orbitals and spin functions. As an example, consider the ground state of the hydrogen molecule in the minimal AO basis constituted by two 1s orbitals centered on either hydrogen atom, $1s_A$ or $1s_B$, respectively. The spatial electronic wave function becomes a product of doubly occupied MOs denoted as σ_g:

$$\Psi_{H_2} = \sigma_g^{\,2} \quad (49)$$

The above product expanded in terms of the (unnormalized) AOs ($\sigma_g = 1s_A + 1s_B$, where "A" and "B" refer to the atoms), after some rearrangement, takes the form

$$\begin{aligned}\Psi_{H_2} = {} & 1s_A(\mathbf{r}_1)\,1s_A(\mathbf{r}_2) \quad \text{ionic} \\ & + 1s_A(\mathbf{r}_1)\,1s_B(\mathbf{r}_2) \quad \text{covalent} \\ & + 1s_B(\mathbf{r}_1)\,1s_A(\mathbf{r}_2) \quad \text{covalent} \\ & + 1s_B(\mathbf{r}_1)\,1s_B(\mathbf{r}_2) \quad \text{ionic}\end{aligned} \quad (50)$$

where the electronic coordinates in the laboratory frame of the two electrons are included explicitly. In eq 50, labeling of "ionic" and "covalent" products has been assigned to those products of AOs that involve AOs centered on the same atom or on different atoms, respectively. Similarly to the above case, the application of ECGs to the calculation of the electronic wave function of the hydrogen molecule involves basis functions of the type

$$\exp\left[(\mathbf{r}_1 - \mathbf{s}_k^1, \mathbf{r}_2 - \mathbf{s}_k^2)\begin{pmatrix} A_k^{11} & A_k^{12} \\ A_k^{21} & A_k^{22} \end{pmatrix}\begin{pmatrix} \mathbf{r}_1 - \mathbf{s}_k^1 \\ \mathbf{r}_2 - \mathbf{s}_k^2 \end{pmatrix}\right] \quad (51)$$

which also can be labeled as "ionic" and "covalent" depending on whether the centers $\mathbf{s}_k^1$ and $\mathbf{s}_k^2$ are in the neighborhood of the same or different atoms. In the simplified case of eq 50 the minimal AO basis set for the H_2 molecule generated a wave function having 50% ionic and 50% covalent products. This hints that when using ECGs the ratio of ionic/covalent functions must be optimized to achieve a better energy convergence with respect to the number of basis functions employed.

The simple example of eq 50 also shows how the ratio of ionic/covalent basis functions must change as the internuclear distances of a molecule are varied. Consider the spatial wave function of the H_2 molecule in its minimal AO basis when the molecule is completely dissociated. Because the dissociation limit consists of two noninteracting hydrogen atoms, the spatial wave function becomes

$$\Psi_{H_2} = \frac{1}{\sqrt{2}}(1s_A(\mathbf{r}_1)\,1s_B(\mathbf{r}_2) + 1s_A(\mathbf{r}_2)\,1s_B(\mathbf{r}_1)) \quad (52)$$

which consists of a 100% covalent AO product and has no ionic components. Therefore, when the H_2 molecule is calculated with ECGs, as the internuclear distance stretches, some basis functions must convert from ionic to covalent. Such a conversion may require migration of some Gaussian centers by several atomic units and usually overcoming an energy barrier, which is unlikely to occur during the variational energy minimization. This problem will be tackled later in this review when the details of the optimization of the nonlinear parameters in BO calculations are discussed in sections 7.1.1 and 7.2.

4. SYMMETRY OF THE WAVE FUNCTION

The Hamiltonian of a few-particle Coulombic system always possesses certain symmetries, or in other words, it commutes with the wave function transformations that belong to certain groups. Among these groups there may be continuous groups such as the group of 3D rotations, or point groups, such as the symmetric group S_p. In this section we briefly consider what the possible implications of these symmetries are and how to perform calculations that take them into account.

4.1. Permutational Symmetry

Practically any atomic or molecular system consisting of more than two particles contains some subsets of identical particles in it. Most commonly, we think of electrons in this regard. However, the identical particles could also be nuclei and even such exotic particles as positrons and muons. According to the Pauli principle, the total wave function (including the spin degrees of freedom) of such quantum systems must either be symmetric or antisymmetric with respect to permutations of identical particles. Any approximation to the exact wave function, which aspires to be accurate, should take this requirement into account. In variational calculations this puts a constraint on the symmetry of the basis functions that can be used. It should be said that in some cases, such as when we are interested in the ground state of a bosonic system, we might in principle use a basis that does not possess any symmetry. If the state of interest is the lowest (or one of the very lowest) in energy among the states of any symmetry, the total trial wave function will eventually converge to the form corresponding to the proper permutational symmetry as the basis size goes to infinity. For any finite basis set, however, there is a big likelihood of the presence of some symmetry contamination. More importantly, such calculations are usually far less efficient in terms of CPU time and memory requirements as the number of basis functions necessary to achieve the same accuracy as in the case of properly symmetrized basis is significantly larger. Thus, even in those few special cases it is a good idea to use basis functions of the proper symmetry. When we deal with systems consisting of fermions (i.e., electrons), enforcing the proper permutational symmetry on the basis functions is not only a matter of the computational efficiency, it is essentially a strict requirement. Even the ground state variational calculations of fermionic systems are not possible without a properly antisymmetrized basis.

In general, in order to build properly (anti)symmetric wave functions, one has to deal with both the spatial and spin coordinates. Due to the fact that the Hamiltonian of a nonrelativistic Coulomb system does not depend on the spin of particles, it is possible to completely eliminate the spin variables from consideration. The corresponding mathematical formalism has been well developed (see, for example, monographs of Hamermesh[160] and Pauncz[161]). In this formalism projection operators for irreducible representations of the symmetric

dx.doi.org/10.1021/cr200419d | Chem. Rev. 2013, 113, 36–79

group (called Young operators) are obtained in a straightforward manner from their corresponding Young tableaux. A Young tableau is created from a Young diagram (sometimes called Young frame), which, for a system of p particles is a series of p connected boxes, such as

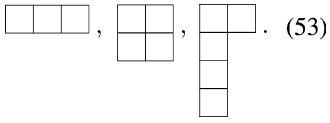 (53)

The shape of the Young diagram corresponding to the desired irreducible representation of the symmetric group is determined by the nature of the particles in the system (bosons or fermions, and their spin). For a set of fermions with spin 1/2 (i.e., electrons) the Young diagram for the spatial wave function must contain no more than two columns. For fermions with spin 3/2 the maximum number of columns would be four. The number of columns for bosons is not limited.

A Young tableau is created by filling a Young diagram with numbers from 1 to p so that they increase when going from left to right and from top to bottom, such as

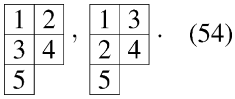 (54)

Generally, there is more than one way to write a Young tableau. The number of ways determines the dimension of the representation. In the actual calculations we may restrict ourselves with the use of basis functions corresponding to any of the equivalent diagrams (the equivalent ones are those that have the same shape). The shape of the diagram also determines the multiplicity of the state. The tableaux in eq 54 would correspond to a doublet (a single unpaired electron), while the following ones

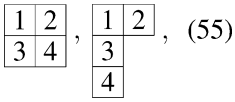 (55)

correspond to a singlet and triplet, respectively.

Once we have an appropriate Young tableaux, the Young operator can be written as $\hat{Y} = \hat{S}\hat{A}$, where

$$\hat{A} = \prod_c \hat{A}_c, \qquad \hat{S} = \prod_r \hat{S}_r \tag{56}$$

are the product of antisymmetrizers over each column and the product of symmetrizers over each row, respectively.

The symmetrizers and antisymmetrizers can be conveniently represented by compact expressions that involve transpositions (pair permutations of particles), which we will denote $\hat{P}_{kl}$. For example, if we have two particles whose numbers are 1 and 2, then the symmetrizer is

$$\hat{S}_{12} = 1 + \hat{P}_{12} \tag{57}$$

The antisymmetrizer over particles 1 and 2 also has a simple form:

$$\hat{A}_{12} = 1 - \hat{P}_{12} \tag{58}$$

For the sake of simplicity we dropped the normalization factor in both expressions 57 and 58 as it not essential here. In the case of larger than 2 number of particles over which the symmetrization or antisymmetrization needs to be done, the corresponding expressions can be given in a factorized form. Let us assume that the number of particles in a subset is k and their numbers range from 1 to k. Then the symmetrizer and antisymmetrizer would look as follows:

$$\hat{S}_{1,\ldots,k} = (1 + \hat{P}_{12})(1 + \hat{P}_{13} + \hat{P}_{23})\cdots(1 + \hat{P}_{1k} + \ldots + \hat{P}_{k-1,k}) \tag{59}$$

$$\hat{A}_{1,\ldots,k} = (1 - \hat{P}_{12})(1 - \hat{P}_{13} - \hat{P}_{23})\cdots(1 - \hat{P}_{1k} - \ldots - \hat{P}_{k-1,k}) \tag{60}$$

Again, the normalization factors $(1/\sqrt{k!})$ were dropped for convenience. As an illustration, let us write the Young operator for a doublet state of five identical particles with spin 1/2 (corresponds to the first Young tableau in eq 54). We symmetrize over rows 1 and 2 by applying $1 + \hat{P}_{12}$ and $1 + \hat{P}_{34}$. Then we antisymmetrize over columns 1 and 2 by means of operators $(1 - \hat{P}_{13})(1 - \hat{P}_{15} - \hat{P}_{35})$ and $1 - \hat{P}_{24}$. The final expression for the Young operator is then

$$\hat{Y} = (1 - \hat{P}_{24})(1 - \hat{P}_{13})(1 - \hat{P}_{15} - \hat{P}_{35})(1 + \hat{P}_{12})(1 + \hat{P}_{34}) \tag{61}$$

The operators whose matrix elements are needed in the variational calculation (such as the Hamiltonian, etc.) usually commute with all the permutation operators involved in the projector $\hat{Y}$, and thus, they commute with $\hat{Y}$ itself. Moreover, we can restrict ourselves to the implementation of only those cases where the permutational operators are applied to the *ket*, because

$$\langle \hat{Y}\phi_k | \hat{O} | \hat{Y}\phi_l \rangle = \langle \phi_k | \hat{O} | \hat{Y}^\dagger \hat{Y} \phi_l \rangle \tag{62}$$

Here $\hat{O}$ denotes an operator representing the quantity of interest. Operator $Y^\dagger\hat{Y}$ can be simplified so that it contains only $p!$ elemental terms (permutations), where p is the number of identical particles.

Now let us consider how each of those permutations of particles act on primitive ECG basis functions. A permutation of the real particles (i.e., not the pseudoparticles) involved in a permutational operator, $\hat{P}$, can be represented as a linear transformation of the laboratory-frame coordinates, $\mathbf{R}$, of the particles. Since the relation between the laboratory coordinates, $\mathbf{R}$, and the internal coordinates, $\mathbf{r}$, is linear, the transformation of the internal coordinates under the permutation of the particles is also linear. Therefore, it can be described by a permutation matrix, $\mathbf{P} = P \otimes I_3$. The application of $\hat{P}$ to the simplest basis functions in eq 32 gives

$$\begin{aligned} \hat{P}\phi_l &= \hat{P} \exp[-\mathbf{r}'\mathbf{A}_l\mathbf{r}] \\ &= \exp[-(\mathbf{P}\mathbf{r})'\mathbf{A}_l(\mathbf{P}\mathbf{r})] \\ &= \exp[-\mathbf{r}'(\mathbf{P}'\mathbf{A}_l\mathbf{P})\mathbf{r}] \end{aligned}$$

As can be seen from the above expression, the symmetry transformation of ϕ_l is equivalent to a similarity transformation of the matrix of the nonlinear parameters for that basis function ($\mathbf{A}_l \rightarrow \mathbf{P}'\mathbf{A}_l\mathbf{P}$). Based on this, a procedure that implements the permutational symmetry in calculating matrix elements with symmetry-projected basis functions can be developed. Evaluating these matrix elements involves a summation of integrals, whose actual numerical values depend on transformed matrices $\mathbf{A}_k$ and $\mathbf{A}_l$.

dx.doi.org/10.1021/cr200419d | Chem. Rev. 2013, 113, 36–79

4.2. Permutational and Spatial Symmetry in BO Calculations

When employing all-electron basis functions, spatial symmetry and permutational symmetry in BO wave functions are treated on a similar footing. Generally, the basis functions in eq 47 do not possess the proper permutational or spatial symmetry. As mentioned above, in the general case, the approach usually chosen is to project away the part of the basis functions that does not have the proper symmetry. This is achieved by using tensor products of Wigner-type projectors. The total symmetry operator, $\hat{P}$, acts on an ECG function as follows:

$$\begin{aligned}\hat{P}\phi_l &= \hat{P}\exp[-(\mathbf{r}-\mathbf{s}_l)'\mathbf{A}_l(\mathbf{r}-\mathbf{s}_l)]\\ &= \exp[-(\mathbf{Pr}-\mathbf{PP}'\mathbf{s}_l)'\mathbf{A}_l(\mathbf{P}(\mathbf{r}-\mathbf{PP}'\mathbf{s}_l))]\\ &= \exp[-(\mathbf{r}-\mathbf{P}'\mathbf{s}_l)'(\mathbf{P}'\mathbf{A}_l\mathbf{P})(\mathbf{r}-\mathbf{P}'\mathbf{s}_l)]\end{aligned} \tag{63}$$

The symmetry operator contains a product of operations belonging to the group of permutations of n particles, if n are the electrons in the studied molecule, and elements of the point symmetry group the molecule belongs to. The general form of the $\hat{P}$ operator is

$$\hat{P} = \hat{P}_{S_n} \otimes \hat{P}^{\Gamma}_{\mathbf{G}} = \frac{1}{n!g}\sum_{i=1}^{n!}\sum_{\alpha\in\mathbf{G}} D_i^{S_n} D_\alpha^{\mathbf{G}} \hat{O}_i\hat{O}_\alpha \tag{64}$$

where "⊗" stands for tensor product operation, **G** is the label of a point group, Γ a specific irreducible representation of that point group, and g is the number of elements in the point group **G**. The coefficients $D_i^{S_n}$ and D_α^{G} can be the characters of a specific irreducible representation of either the symmetric group or the point group, or an element of the matrices that constitute the irreducible representation. When calculating the molecular electronic ground state, the irreducible representation to use is fully symmetric with every $D_\alpha^{\mathrm{G}} = 1$. Excited states, instead, may have negative values of D_α^{G}, or values in magnitude different from unity. As an example, consider the H_3^+ molecular ion. The point group symmetry for this ion in its ground state equilibrium geometry is D_{3h}. This point group contains six elements, and for the A_1 and E states, the projection operators onto the respective point group symmetry irreducible representation can be written as

$$\hat{P}^{\mathrm{A_1}}_{D_{3h}} = 1 + \hat{C}_3 + \hat{C}_3^{\,2} + \hat{\sigma}_1 + \hat{\sigma}_2 + \hat{\sigma}_3 \tag{65}$$

$$\hat{P}^{\mathrm{E}}_{D_{3h}} = 2 - \hat{C}_3 - \hat{C}_3^{\,2} + 2\hat{\sigma}_1 - \hat{\sigma}_2 - \hat{\sigma}_3 \tag{66}$$

respectively. The operator in eq 66 was obtained after noticing that C_{3v} is isomorphic with the permutation group of three particles, S_3, and by employing the $\begin{array}{|c|c|}\hline 1 & 2 \\ \hline 3 \\ \cline{1-1}\end{array}$ Young tableau. It is interesting to notice that at the ground state equilibrium geometry of H_3^+ there is a conical intersection of two degenerate E states (the E representation is two-dimensional). For the second of the two states the symmetry projector can be generated using the $\begin{array}{|c|c|}\hline 1 & 3 \\ \hline 2 \\ \cline{1-1}\end{array}$ Young tableau.

4.3. Spatial Symmetry in Non-BO Calculations

In the case when there are no clamped particles in the system and no external fields are present, the Hamiltonian commutes with the total orbital angular momentum operator, $\hat{L}^2$. Therefore, the exact solutions of the corresponding Schrödinger equation must also be the eigenfunctions of $\hat{L}^2$. For this reason, basis functions for a variational calculation of a given system/state need to possess certain rotational symmetry properties. It should be said that in some cases the proper rotational symmetry of basis functions is not strictly *required*. For example, when one deals with the ground state of the system and does not impose any rotational symmetry of the wave function in the calculation, the total non-BO trial wave function should converge to the ground state provided the basis functions have sufficient flexibility and one performs a thorough optimization of the linear and nonlinear parameters involved in the trial function. The trial wave function will eventually approach the right rotational symmetry of the ground state in the limit of a complete basis set. Nonetheless, even in such a case it is a good idea to use basis functions of the correct symmetry as this yields a much faster convergence rate. For consideration of excited states, the use of correct rotational symmetry is usually not optional. If the symmetry is not imposed, the trial wave function will simply converge to a wrong state when the linear coefficients and nonlinear parameters are optimized. To remedy this, one may include some penalty terms in the variational energy functional which, even without strictly imposing the right rotational symmetry, would force the wave function to effectively assume this right symmetry in the process of the basis set optimization.

In addition to the Hamiltonian commuting with $\hat{L}^2$, it also commutes with the projection of the total orbital angular momentum operator on a selected axis, $\hat{L}_z$ (again, assuming no clamped nuclei are involved in the system). Due to the degeneracy of the energy levels corresponding to different quantum numbers M (eigenvalues of $\hat{L}_z$), it is not required that basis functions must correspond to a particular M value. In principle, one can use any linear combination of basis states with different M's (and the same L and other quantum numbers). However, for efficient numerical implementation, it is desirable that the basis functions be real. This is automatically satisfied when $M = 0$.

For states with $L = 0$ (even those that arise from the coupling of the nonzero angular momenta of separate particles) the wave function of the system is rotationally invariant. Thus, any spherically symmetric Gaussian $\exp[-\mathbf{r}'(A_k \otimes I_3)\mathbf{r}]$ multiplied by an arbitrary function of the absolute values of $\mathbf{r}_i$, $\mathbf{r}_{ij}$, or their dot products, is a suitable basis function. The actual choice of the premultiplier is dictated by the structural peculiarities of the considered system and its state, so that the convergence of the variational expansion is sufficiently fast. For example, for the ground state of an atom with s electrons only, it is usually sufficient to use the premultipliers that are equal to unity. For excited Rydberg states of atoms the calculation may benefit from using in some of the basis functions factors of the form r_i^2 or even higher even powers of the electron−nucleus distances to better describe the radial nodes in the wave functions of these states. For a diatomic molecule, where particles 1 and 2 are nuclei, premultipliers need to be introduced to describe the spatial separation of these particles. As mentioned before, these premultipliers can have the form of powers of the internuclear distance, $r_i^{2m} = R_{12}^{2m}$, where m is an integer which in typical non-BO calculations may range from 0 to 100.

To obtain a proper functional form of the basis functions suitable for the calculations of states with a given L and corresponding to a given coupling scheme (i.e., a certain set of intermediate total angular momenta) of the orbital angular momenta of the constituent particles, one can use the well-known rules of the addition of the angular momenta. The case

dx.doi.org/10.1021/cr200419d | Chem. Rev. 2013, 113, 36−79

of an $L = 1$ state, in which all particles but one have zero angular momentum (i.e., $l_i = 1$, $l_k = 0$, $k \neq i$; here l_j is the orbital angular momentum quantum number of particle j), is trivial and leads to a prefactor in the form $r_i Y_{10}(\mathbf{r}_i)$, where $Y_{lm}(\mathbf{r}_i)$ denotes spherical harmonics. Since $Y_{10}(\mathbf{r}_i)$ is proportional to z_i/r_i, the following basis functions are generated:

$$\phi_k = z_i \exp[-\mathbf{r}'(A_k \otimes I_3)\mathbf{r}] \tag{67}$$

In a slightly more sophisticated case of two particles with nonzero angular momenta (l_i, l_j) the expression for the premultiplier is evaluated as the following sum:

$$r_i^{l_i} r_j^{l_j} |L\,M\rangle = r_i^{l_i} r_j^{l_j} \sum_{\substack{m_i, m_j \\ m_i + m_j = M}} (L\,M|l_i\,m_i\,l_j\,m_j)|l_i\,m_i\rangle|l_j\,m_j\rangle \tag{68}$$

where $(L\ M|l_i\,m_i\ l_j\ m_j)$ are the Clebsch−Gordan coefficients, and $|l_i m_i\rangle$ are shorthand for spherical harmonics $Y_{l_i m_i}(\mathbf{r}_i)$. The mathematical functions given by eq 68 without the $r_i^{l_i} r_j^{l_j}$ factor are often called the bipolar harmonics.[162]

When many or all particles in the system have nonzero orbital angular momenta, their coupling into multipolar harmonics, which may symbolically be represented as

$$r_1^{l_1} \cdots r_n^{l_n} [[[|l_1,\ m_1\rangle|l_2,\ m_2\rangle]_{L_{12}, M_{12}}|l_3,\ m_3\rangle]_{L_{123}, M_{123}} \cdots |l_n,\ m_n\rangle]_{L,M} \tag{69}$$

becomes progressively more complicated as the number of particles increases. Nonetheless, for any relatively small number of particles, the exact form of the proper Gaussian premultiplier can be easily determined with the use of modern computer algebra packages. For very complicated cases one may also employ the approach proposed by Varga, Suzuki, and Usukura,[5,163] which avoids the coupling of orbital angular momenta completely. This approach can be particularly useful in calculations of states with very high L. The spatial basis functions in this approach have the following form:

$$\phi_k = \exp[-\mathbf{r}'\mathbf{A}_k\mathbf{r}](v^k)^{2p_k} Y_{LM}(\mathbf{v}^k) \tag{70}$$

where $\mathbf{v}^k = u^{k\prime}\mathbf{r} \equiv \sum_{i=1}^{n} u_i^k \mathbf{r}_i$, p_k is a nonnegative integer parameter, and u_i^k are a set of additional nonlinear parameters. Both p_k and u^k are subject to optimization. Only the total angular momentum L appears in eq 70, while the coupling scheme of the individual angular momenta of the particles is not strictly defined. In general, it is a linear combination of different coupling schemes corresponding to the same final L value and this linear combination (or the weights of the different coupling schemes) may change continuously during the energy minimization. The energy minimization performed with respect to u^k amounts to finding the most suitable angle or a linear combination of angles defined by the $\mathbf{v}^k/v^k$ unit vector, in terms of which the wave function is expanded.

5. EVALUATION OF MATRIX ELEMENTS

The derivations of the Hamiltonian and overlap matrix elements with ECGs can be conveniently carried out with the use of the formalism of matrix differential calculus (MDC). While this formalism is often employed in the field of econometrics and statistics, it has not been well-known in chemistry and physics. It has proven to be a very suitable tool to work with all types of ECGs. A detailed introduction to the subject of MDC can be found in ref 164. In this section we will supply the reader with most important definitions and briefly describe the general procedures for evaluating the Hamiltonian and energy gradient matrix elements. For a complete description and explanation of all technical details, we refer the reader to refs 7, 91, 128, 134−137, and 166.

5.1. vech Operation

In some situations, such as when computing derivatives of matrix elements, it is handy to make use of the operator vech. It transforms a matrix into a vector by stacking the columns of a matrix, one underneath the other, but for each column only the elements located on and below the diagonal of the matrix are used in the stacking. Hence, vech transforms an $n \times n$ matrix into a $n(n+1)/2$-component vector. For example, if X is a 3×3 matrix with elements X_{ij}, then

$$\text{vech } X = \begin{pmatrix} X_{11} \\ X_{21} \\ X_{31} \\ X_{22} \\ X_{32} \\ X_{33} \end{pmatrix} \tag{71}$$

The vech operator is particularly useful in the case of symmetric matrices; then vech X contains only independent elements of X.

5.2. Gaussian Integral in p Dimensions

In the evaluation of the Hamiltonian and overlap matrix elements the following p-dimensional Gaussian integral is used most often:

$$\int_{-\infty}^{+\infty} \exp[-x'Ax + y'x]\,dx = \frac{\pi^{p/2}}{|A|^{1/2}} \exp[y'A^{-1}y] \tag{72}$$

where x is a p-component vector of variables, A is a symmetric $p \times p$ positive definite matrix, and y is a p-component constant vector.

5.3. Evaluation of Integrals Involving Gaussians with Angular Preexponential Factors

Let us start with the simplest n-particle ECG basis function that is used to construct the basis for calculating bound states of atoms with only s electrons:

$$\phi_k = \exp[-\mathbf{r}'\mathbf{A}_k\mathbf{r}] \tag{73}$$

By directly applying eq 72, we obtain the expression for the overlap integral between two basis functions given by eq 73:

$$\langle\phi_k|\phi_l\rangle = \frac{\pi^{3n/2}}{|A_{kl}|^{3/2}} \tag{74}$$

where $A_{kl} = A_k + A_l$. In deriving integrals over Gaussian basis functions representing atomic states with higher angular momenta, the so-called "generator" functions are used. Let us consider angular Gaussians generated by multiplying eq 73 by one or two single particle Cartesian coordinates. For the former case the generator Gaussian function is

$$\phi_k = \exp[-\mathbf{r}'\mathbf{A}_k\mathbf{r} + \alpha_k(\mathbf{v}^k)'\mathbf{r}] \tag{75}$$

where α_k is a parameter and $\mathbf{v}^k$ is a vector whose components are all 0, except the $3m_k$ component, which is set to 1. For the latter case one can choose the generator Gaussian to be

$$\phi_k = \exp[-\mathbf{r}'\mathbf{A}_k\mathbf{r} + \alpha_k\mathbf{r}'\mathbf{W}_k\mathbf{r}] \tag{76}$$

dx.doi.org/10.1021/cr200419d | Chem. Rev. 2013, 113, 36−79

where $\mathbf{W}_k$ (which will define the preexponential factor $x_{i_k}y_{j_k} - x_{j_k}y_{i_k}$ or a similar one) is a sparse $3n \times 3n$ symmetric matrix comprising only four nonzero elements, two of which have values of 1/2 and the other two have values of −1/2. The 1/2 elements are placed in the $(3i_k - 2, 3j_k - 1)$ and $(3j_k - 1, 3i_k - 2)$ positions, while the −1/2 elements are placed in $(3j_k - 2, 3i_k - 1)$ and $(3i_k - 1, 3j_k - 2)$ positions.

The generator Gaussians are used to generate Gaussian basis sets for expanding wave functions with different angular momenta. For example, the basis function $z_i \exp[-\mathbf{r}'A_k\mathbf{r}]$ is generated from eq 75 by differentiating with respect to α_k and setting α_k to 0. In this case the elements of the $\mathbf{v}^k$ vector are all 0 except for the 3ith element, which is set to 1. In the same manner, in order to generate the basis function $(x_{i_k}y_{j_k} - x_{j_k}y_{i_k}) \exp[-\mathbf{r}'A_k\mathbf{r}]$, one needs to differentiate the generator in eq 76 with respect to α_k and set α_k to 0. This approach, in principle, can be extended to generate any angular preexponential factor for a Gaussian basis function.

As an example, let us consider the overlap integral between functions of the following type:

$$\phi_k = (x_{i_k}y_{j_k} - x_{j_k}y_{i_k}) \exp[-\mathbf{r}'A_k\mathbf{r}]$$

It can be obtained as

$$\begin{aligned}\langle\phi_k|\phi_l\rangle &= \frac{\partial}{\partial\alpha_k}\frac{\partial}{\partial\alpha_l}\langle\varphi_k|\varphi_l\rangle\Big|_{\alpha_k=\alpha_l=0} \\ &= \frac{\partial}{\partial\alpha_k} \\ &\frac{\partial}{\partial\alpha_l}\int_{-\infty}^{+\infty}\exp[-\mathbf{r}'(\mathbf{A}_{kl} + \alpha_k\mathbf{W}_k + \alpha_l\mathbf{W}_l)\mathbf{r}]\,\mathrm{d}\mathbf{r}\Big|_{\alpha_k=\alpha_l=0}\end{aligned} \tag{77}$$

This approach can be used to evaluate all other types of integrals that appear in the calculations with ECGs containing Cartesian prefactors.

In non-BO calculations of diatomic molecules a suitable basis set consists of ECGs multiplied by powers of the internuclear distance. Even in a simpler case of atomic calculations one needs to deal with powers of the internuclear distance when evaluating the matrix elements of the potential energy. To obtain these matrix elements it is convenient to use an approach employing the Dirac delta functions.The expression for the matrix element of the Dirac delta function, $\delta(\mathbf{r}_{ij}-\boldsymbol{\xi})$, where $\boldsymbol{\xi}$ is some three-dimensional vector (parameter), allows one to evaluate the matrix element of an arbitrary function $f(\mathbf{r}_{ij})$, which depends on a single pseudoparticle coordinate or a linear combination of the coordinates. For the case of a simple (no premultipliers) spherical Gaussians we have:

$$\begin{aligned}\langle\phi_k|f(\mathbf{r}_{ij})|\phi_l\rangle &= \int f(\mathbf{r}_{ij})\langle\phi_k|\delta(\mathbf{r}_{ij} - \boldsymbol{\xi})|\phi_l\rangle\,\mathrm{d}\boldsymbol{\xi} \\ &= \langle\phi_k|\phi_l\rangle\frac{1}{\pi^{3/2}}\int f\left(\frac{\boldsymbol{\xi}}{\mathrm{tr}[A_{kl}{}^{-1}J_{ij}]^{1/2}}\right)\mathrm{e}^{-\xi^2}\,\mathrm{d}\boldsymbol{\xi}\end{aligned} \tag{78}$$

with J_{ij} being a symmetric matrix with 1 in the ii and jj diagonal elements and −1 in the ij and ji off-diagonal elements. When f depends only on the absolute value of the interpseudoparticle distance, this formula becomes

$$\langle\phi_k|f(r_{ij})|\phi_l\rangle = \langle\phi_k|\phi_l\rangle\frac{4}{\sqrt{\pi}}\int_0^\infty f(\mathrm{tr}[A_{kl}{}^{-1}J_{ij}]^{1/2}\xi)\xi^2\mathrm{e}^{-\xi^2}\,\mathrm{d}\xi \tag{79}$$

The above integral is easily evaluated analytically for many common forms of $f(\mathbf{r}_{ij})$ (including $1/\mathbf{r}_{ij}$). In the worst case scenario it can always be computed with quadrature formulas.

5.4. Analytic Gradient of the Energy

A very important aspect of the atomic (and molecular) calculations with ECGs is that achieving high accuracy is possible only when the nonlinear exponential parameters of Gaussians are extensively optimized based on the minimization of the energy. This process usually takes large amounts of computer time. To accelerate the basis set optimization in the ECG calculations, one can derive and implement the analytic gradient of the energy with respect to the nonlinear parameters of the Gaussian basis functions. The term "analytic" here means that the components of the gradient are not evaluated using finite differences of the energy (which is a very costly procedure since the number of those components may reach many thousands for large basis sets). Instead, they are evaluated numerically using analytic expressions. The use of the analytic gradient has enabled the performance of very accurate BO and non-BO calculations of various atomic and molecular systems with accuracy unmatched by previous calculations.

Below we outline the approach used in calculating the gradient. We start with the differential of the secular equation (eq 27):

$$\mathrm{d}(\mathrm{H} - \varepsilon\mathrm{S})\mathrm{c} = (\mathrm{dH})\mathrm{c} - (\mathrm{d}\varepsilon)\mathrm{Sc} - \varepsilon(\mathrm{dS})\mathrm{c} + (\mathrm{H} - \varepsilon\mathrm{S})\,\mathrm{dc} \tag{80}$$

Multiplying this equation by $\mathrm{c}^\dagger$ from the left, we obtain:

$$\mathrm{d}\varepsilon = \mathrm{c}^\dagger(\mathrm{dH} - \varepsilon\,\mathrm{dS})\mathrm{c} \tag{81}$$

To get eq 81, we utilize eq 27 and assume that the wave function is normalized, i.e., $\mathrm{c}^\dagger\mathrm{Sc} = 1$. For generality we also assume that the basis functions and their linear coefficients may be complex. The relation in eq 81 constitutes the well-known Hellmann−Feynman theorem.

Now let α_t be a nonlinear parameter, which basis function φ_t depends on. As the tth row and tth column of matrices H and S depend on α_t, the derivative of any arbitrary element belonging to that row or that column of either of the two matrices can be written as

$$\frac{\partial\mathrm{H}_{kl}}{\partial\alpha_t} = \frac{\partial\mathrm{H}_{kl}}{\partial\alpha_t}(\delta_{kt} + \delta_{lt} - \delta_{kt}\delta_{lt}), \qquad k, l = 1, ..., K \tag{82}$$

and

$$\frac{\partial\mathrm{S}_{kl}}{\partial\alpha_t} = \frac{\partial\mathrm{S}_{kl}}{\partial\alpha_t}(\delta_{kt} + \delta_{lt} - \delta_{kt}\delta_{lt}), \qquad k, l = 1, ..., K \tag{83}$$

Next, applying relations 81−83, the derivative of the total energy, ε, with respect to parameter α_t is

dx.doi.org/10.1021/cr200419d | Chem. Rev. 2013, 113, 36−79

$$\frac{\partial \varepsilon}{\partial \alpha_t} = c_t^* \sum_{l=1}^{K} c_l \left(\frac{\partial H_{tl}}{\partial \alpha_t} - \varepsilon \frac{\partial S_{tl}}{\partial \alpha_t} \right) + c_t \sum_{l=1}^{K} c_l^* \left(\frac{\partial H_{lt}}{\partial \alpha_t} - \varepsilon \frac{\partial S_{lt}}{\partial \alpha_t} \right) - c_t c_t^* \left(\frac{\partial H_{tt}}{\partial \alpha_t} - \varepsilon \frac{\partial S_{tt}}{\partial \alpha_t} \right)$$
$$= 2\Re \left[c_t^* \sum_{l=1}^{K} c_l \left(\frac{\partial H_{tl}}{\partial \alpha_t} - \varepsilon \frac{\partial S_{tl}}{\partial \alpha_t} \right) \right] - c_t c_t^* \left(\frac{\partial H_{tt}}{\partial \alpha_t} - \varepsilon \frac{\partial S_{tt}}{\partial \alpha_t} \right) \quad (84)$$

By calculating all such derivatives for each α_t, the complete energy gradient is obtained. The total number of the gradient components is equal to the product of the basis size and the number of nonlinear parameters contained in each basis function.

To make the calculations efficient, it is best to evaluate all derivatives of ε with respect to the entire vech L_k vector (and other nonlinear parameters if any) in a single step rather than performing separate differentiations for individual parameters $(L_k)_{11}$, $(L_k)_{21}$, ..., $(L_k)_{nn}$ because many of the operations in calculating the derivatives are identical. With that, the calculation of expression 84 requires knowledge of the following derivatives of the H and S matrix elements:

$$\frac{\partial H_{kl}}{\partial (\text{vech } L_k)}, \quad \frac{\partial H_{kl}}{\partial (\text{vech } L_l)}, \quad \frac{\partial S_{kl}}{\partial (\text{vech } L_k)}, \quad \frac{\partial S_{kl}}{\partial (\text{vech } L_l)} \quad (85)$$

The explicit expressions for these derivatives for different types of ECGs were derived and presented in several papers.[90,91,128,132,135−137,165−168]

5.5. Evaluation of Matrix Elements for Molecular BO Calculations

There are many similarities in the derivation of the integrals used in BO calculations and the ones used in the non-BO calculations. This is particularly the case in the derivation of the overlap and the kinetic energy integrals. In the derivation of the potential energy integrals, i.e., the electron repulsion and the nuclear attraction integral, the following transformation and identity can be employed.[7]

$$\frac{1}{r_{ij}} = \frac{2}{\pi^{1/2}} \int_0^\infty \exp[-\mu^2 r_{ij}^2] \, d\mu \quad (86)$$

$$\int_0^\infty (1 + \alpha\mu^2)^{-3/2} \exp\left[-\frac{\beta\mu^2}{1 + \alpha\mu^2} \right] d\mu = \frac{\pi^{1/2}}{2\beta^{1/2}} \text{erf}\left[\left(\frac{\beta}{\alpha} \right)^{1/2} \right] \quad (87)$$

Here the square of the interelectron distance can be represented as a quadratic form:

$$r_{ij}^2 = \mathbf{r}' \mathbf{J}_{ij} \mathbf{r} \quad (88)$$

Following Kinghorn,[165] the gradient of the molecular integrals with respect to the nonlinear variational parameters (i.e., the exponential parameters A_k and the Gaussian centers $\mathbf{s}_k$) are also derived using the methods of MDC. The gradient of ε now involves the derivatives of the overlap and Hamiltonian matrix elements with respect to not only vech L_k, but also with respect to the coordinates of shift vectors $\mathbf{s}_k$:

$$\frac{\partial H_{kl}}{\partial (\text{vech } L_k)}, \quad \frac{\partial S_{kl}}{\partial (\text{vech } L_k)}, \quad \frac{\partial H_{kl}}{\partial \mathbf{s}_k}, \quad \frac{\partial S_{kl}}{\partial \mathbf{s}_k} \quad (89)$$

Details concerning the derivation of the gradient matrix elements and the corresponding algorithms can be found in refs 7 and 91.

6. VARIATIONAL OPTIMIZATION OF THE GAUSSIAN NONLINEAR PARAMETERS IN ATOMIC AND MOLECULAR NON-BO CALCULATIONS

6.1. Solution of the Generalized Eigenvalue Problem

Using quick and stable algorithms for solving the generalized symmetric/Hermitian eigenvalue problem (GSEP/GHEP) given by eq 27 is very crucial for the overall efficiency of the variational calculations with ECGs. This is particularly important when the size of the ECG expansion of the wave function is large (thousands of terms). It is worthwhile to note that, in principle, one can vary the linear coefficients of the basis function without resorting to the solution of the generalized secular equation at all. It is possible to simply minimize the Rayleigh quotient based on some nonlinear optimization algorithm (with appropriate orthogonality constraints imposed on the wave function in excited state calculations). In practice, however, using numerical algorithms of linear algebra is much more convenient and computationally efficient.

The most straightforward approach to solving for all or some of the eigenvalues in eq 27 is based on the reduction of the GSEP/GHEP to the standard (i.e., nongeneralized) eigenvalue problem. Due to positive-definite nature of S, it can be factorized in the Cholesky form, S = LL′. Then, after applying the inverse of L on the left and the inverse of L′ on the right, one obtains the standard eigenvalue problem. This scheme is implemented in many numerical linear algebra packages, such as LAPACK. However, this general algorithm has several drawbacks, one of which is a relatively low speed. For large matrix dimensions, K, the solution of eq 27 becomes quite expensive, and for smaller atoms and molecules, it may even take more computer time than the evaluation of the S and H matrix elements. This happens because the solution of the GSEP/GHEP with dense matrices requires $\propto K^3$ arithmetic operations, while the evaluation of matrix elements requires only $\propto K^2$ operations. Although the proportionality constant is much larger in the latter K^2 term than in the K^3 term, as K increases the time required to solve eq 27 may start to exceed the time needed for the evaluation of matrix elements. For this reason it is very important to use an eigensolver which is efficient for large dimensions of the basis.

It should also be noted that in the calculations that involve optimization of nonlinear parameters, eq 27 usually needs to be solved a very large number of times (thousands, if not millions). In addition to that, high relative accuracy of the eigenvalues/eigenvectors is desirable in the calculations.

dx.doi.org/10.1021/cr200419d | Chem. Rev. 2013, 113, 36−79

Perhaps the most important factor in choosing the most suitable algorithm is its ability to obtain the solution by performing a quick update of the previous solution in the case when just one or a few basis functions have been changed, i.e. when only one or few rows/columns of matrices S and H have been modified. One such computationally cheap scheme is given by Varga and Suzuki.[169] In their works they perform the Gram−Schmidt orthogonalization, which reduces the generalized eigenvalue problem with already diagonalized $(K-1)\times(K-1)$ submatrices (this diagonalization needs to be carried out only once if the first $K-1$ basis functions are kept unchanged) to the conventional form. Another option is to use the inverse iteration method.[170] In the vast majority of cases one is usually interested in determining only a single eigenvalue/eigenvector and a good approximation, $\varepsilon_{\mathrm{appr}}$, to the eigenvalue in usually known. The idea of the method is simple and consists in performing the following iterations:

$$(\mathrm{H}-\varepsilon_{\mathrm{appr}}\mathrm{S})\mathrm{c}^{(j+1)}=\mathrm{S}\mathrm{c}^{(j)} \tag{90}$$

The initial vector to start the iteration process, $\mathrm{c}^{(0)}$, can be chosen randomly if no better guess is available. Another option is to take the solution obtained in the previous step of the optimization procedure and update it for the changed matrices S and H. Such an approach works particularly well if the changes in matrices S and H are small and limited to only a few rows/columns of these matrices. The iteration process (90) converges as long as the desired eigenvalue is closer to $\varepsilon_{\mathrm{appr}}$ than any other eigenvalue. The rate of convergence depends on the ratio $(\varepsilon_{\mathrm{appr}}-\varepsilon_{\mathrm{nc}})/(\varepsilon_{\mathrm{appr}}-\varepsilon_i)$, where ε_i is the desired eigenvalue and $\varepsilon_{\mathrm{nc}}$ is the next closest (after ε_i) eigenvalue. Typically, just a few iterations are needed to obtain the desired eigenvalue and the corresponding eigenvector with sufficiently high accuracy. In each iteration one has to perform a matrix−vector multiplication and solve a system of linear equations with a symmetric (Hermitian) matrix $\mathrm{H}-\varepsilon_{\mathrm{appr}}\mathrm{S}$. In the case when the calculated state is the ground state of the system and $\varepsilon_{\mathrm{appr}}$ is chosen to be below the actual eigenvalue, one can use the Cholesky method (note that the matrix factorization requiring $\propto K^3$ operations needs to be performed only once regardless of the number of iterations). In the general case, however, the matrix $\mathrm{H}-\varepsilon_{\mathrm{appr}}\mathrm{S}$ is not positive definite and instead of the Cholesky factorization one should use another type of factorization, such as LU, QR, or LDL^T (LDL^H is used for complex matrices). The LDL^T factorization is probably the best choice as it takes advantage of the symmetry of the matrix and requires the least amount of computational work.

The above-described algorithm of solving the generalized eigenvalue problem is rather robust and accurate despite an apparent problem with the matrix $(\mathrm{H}-\varepsilon_{\mathrm{appr}}\mathrm{S})$, which may become ill-conditioned when $\varepsilon_{\mathrm{appr}}$ lies close to the actual eigenvalue. As discussed by Partlett,[170] the error which may occur when solving the system of linear equations with a nearly singular matrix is concentrated in the direction of the eigenvector and therefore does not lead to a failure of the algorithm.

A very important feature of the algorithm with LDL^T (LDL^H) factorization is the fact that, upon changing the last row and column (or a few last rows and columns) of matrices S and H, the updated solution can be obtained by performing only $\propto K^2$ operations. Even in the case when one must obtain the solution of GSEP/GHEP from scratch, the inverse iteration scheme given by eq 90 is several times faster than the usual reduction of GSEP/GHEP to the standard eigenvalue problem. Besides that, the inverse iteration scheme generally exhibits better numerical stability.

6.2. Generating the Initial Guess for Nonlinear Parameters

The convergence of the wave function expansion in terms of correlated Gaussians strongly depends on how one selects the nonlinear parameters in the Gaussian exponentials, as well as other parameters present in the basis functions (including integer parameters, such as the values of powers in preexponential polynomials and the indices referring to the coordinates of particles involved in those polynomials). In order to reach high accuracy in the calculations, it is necessary to perform optimization of those parameters. The key component here, as was discussed before, is the use of the analytic gradient. Another possible method, which can also be very capable, is based on the stochastic selection of the nonlinear parameters. The idea and the potential of this conceptually simple yet very powerful approach (often called SVM, stochastic variational method) was first demonstrated by Kukulin and Krasnopol'sky[171] and then further developed by Varga and Suzuki.[5,169,172] Some calculations based on stochastic generation of the nonlinear parameters were also performed by Alexander et al.,[173,174] and others. It should be noted that even if one heavily relies on the direct optimization with the use of the analytical gradient, it is still very important to be able to generate a good initial guess, where the optimization can start from. As the numerical experience shows, a totally random guess may lead to a convergence to a very shallow local minimum and/or result in very slow progress of the optimization. Unfortunately, the hypersurface of the objective function (which is the total energy in our case) becomes extremely complicated when the number of basis functions exceeds a few tens. For this reason, generating a good initial guess of the nonlinear parameters for a basis consisting of thousands of functions is a nontrivial task. Usually the following strategy works quite well. The basis set is grown incrementally and the initial values of the nonlinear parameters of new basis functions are selected using an approach similar to SVM. That is, the selection procedure is based on the distribution of the nonlinear parameters in the basis functions already included the basis set. In its simplest version, the generation of each nonlinear parameter of new random candidates can be done using a linear combination of normal distributions centered at the values defined by the nonlinear parameters of those already included basis functions. For example, if each basis function, ϕ_k, contains m continuous nonlinear parameters $\alpha_1^k,\ldots,\alpha_m^k$, and the current basis size is K, then the ith nonlinear parameter of the candidates for the next basis function, ϕ_{K+1}, is obtained from the following distribution:

$$\rho(x)=\frac{1}{K}\sum_{k=1}^{K}\frac{1}{\sqrt{2\pi(\sigma_i^k)^2}}\exp\left\{-\frac{(x-\alpha_i^k)^2}{2(\sigma_i^k)^2}\right\} \tag{91}$$

In the above equation σ_i^k are some constants whose magnitude is comparable to the magnitude of α_i^k. Usually a large number of basis function candidates (hundreds if not thousands) is generated and then tested against the total energy lowering. The candidate which lowers the energy the most is then included in the basis as ϕ_{K+1}. After that (or after including several more basis functions), the nonlinear parameters of the new basis function(s) are further optimized using the gradient-

dx.doi.org/10.1021/cr200419d | Chem. Rev. 2013, 113, 36−79

based approach. This procedure is repeated until the size of the basis reaches the desired value. At the end of the procedure one gets relatively good initial values of the nonlinear parameters. Using these initial values, it is then possible to use algorithms for direct minimization of the energy functional to continue the optimization of the nonlinear parameters of basis functions until the desired level of convergence is achieved.

6.3. Dealing with Linear Dependencies of the Gaussians during the Variational Energy Minimization

In some cases thorough optimization of the nonlinear parameters may lead to linear dependencies between basis functions. The reason for the appearance of linear dependencies varies from case to case. Often the linear dependencies arise as a result of poor ability of the basis functions to effectively describe certain features of the wave function of the system under study. In any case, the linear dependencies between basis functions may cause numerical instabilities in the calculation, particularly when solving the secular equation. It should be noted, however, that the presence of linearly dependent functions as such does not automatically lead to numerical instabilities in the computed eigenvalues. Some linear dependencies, such as those randomly generated, might not cause any harm at all, provided a proper algorithm for solving the generalized eigenvalue problem is chosen. On the other hand, the linear dependencies that arise during optimization of the nonlinear variational parameters may cause problems in the calculation. This happens, for example, when the linear coefficients of two (or more) basis functions are large, close in magnitude, but have opposite signs. Let us assume that basis functions ϕ_i and ϕ_j are almost identical (i.e., almost linearly dependent). Remembering that each eigenvalue of eq 27 can be represented as a simple Rayleigh quotient, it is not difficult to realize that a cancellation of leading digits will occur in the course of subtraction $\langle\phi_i|\hat{O}|\phi_i\rangle + \langle\phi_j|\hat{O}|\phi_j\rangle - \langle\phi_i|\hat{O}|\phi_j\rangle - \langle\phi_j|\hat{O}|\phi_i\rangle$, where $\hat{O}$ is either the Hamiltonian or the identity (overlap) operator. Therefore, the "contributions" to the final eigenvalue due to the linearly dependent basis functions will be of reduced accuracy and, depending on the overall importance of those basis functions, the last several digits of the computed energy eigenvalue may be inaccurate. In the case of severe linear dependencies the associated numerical inaccuracy may not only affect the quality of the optimization of the nonlinear parameters (which is sensitive to the accuracy of the computed eigenvalues), but may even lead to completely unreliable results. Therefore, it is generally a good practice to avoid severe linear dependencies in the variational calculations.

There are several ways to keep the linear dependency problem under control. The most straightforward approach is to remove linearly dependent functions from the basis set. This may be of particular use when new basis functions are generated during the process of growing the basis set. The criterion of linear dependency can be adopted from the Gram–Schmidt orthogonalization process. Our experience has shown that by far most often linear dependencies occur as pair linear dependencies; i.e., one basis function becomes very close to another one. When this happens, the magnitude of their normalized overlap, S_{ij}, becomes very close to unity. In this case, testing for linear dependency amounts to checking all current overlap matrix elements. When a new basis function is added to the basis, the test is reduced to checking a single row of the overlap matrix, which takes very little computational time.

Rejecting a new basis function whose overlap matrix elements exceed a certain threshold can be easily implemented and works very well when a stochastic selection of new basis function candidates is performed. The situation becomes somewhat more complicated when one needs to optimize the nonlinear parameters of the existing basis functions. One possible way to proceed here is to simply discard any changes of the nonlinear parameters that result in the basis function becoming too linearly dependent with another function in the basis set. However, this strategy cannot be easily adopted in actual calculations, as it is the optimization procedure/software that picks the values of the nonlinear parameters in each given optimization step. A better approach is to use a penalty function, which adds a certain positive value to the minimized function (the total energy) whenever the overlap of two or more basis functions is larger than the assumed threshold. Since one wants to keep the objective function smooth, it narrows the choice of possible expressions for the penalty function. One can, for example, use the following form of it:

$$\mathcal{P} = \sum \mathcal{P}_{ij} \tag{92}$$

where the sum is over all monitored basis function pairs and

$$\mathcal{P}_{ij} = \begin{cases} \beta\dfrac{|S_{ij}|^2 - t^2}{1 - t^2}, & |S_{ij}| > t \\ 0, & |S_{ij}| \le t \end{cases} \tag{93}$$

In eq 93, t is the value of the overlap threshold and β controls the magnitude (i.e., maximum) of the penalty for each pair overlap. The choice of t and β is usually based on experience and may differ depending on the system and the size of the basis. The value $t = 0.99$ can be a reasonable choice in most cases, while β should normally be taken as a small fraction of the total energy of the system. Excessively large values of β tend to cause failures in the optimization, because then the objective function exhibits very sharp "jumps", which are inconsistent with the assumption of a smooth, differentiable function. On the other hand, too tiny values of β may not result in efficient elimination of pair linear dependencies.

7. VARIATIONAL OPTIMIZATION OF THE GAUSSIAN NONLINEAR PARAMETERS IN ATOMIC AND MOLECULAR BO CALCULATIONS

7.1. Optimization Approach Used in the BO Molecular Variational Calculations

A practical BO PES calculation involves (at least) two steps: building the basis set for the wave function expansion at the equilibrium structure of the molecule and generating the PES for different geometrical structures. Both steps usually require a significant computational effort. The computational resources needed for the calculation increase rapidly with the number of electrons ($n!$ dependency). In general, three factors determine the amount of the computational time needed for the calculation. The first factor is the number of exponential parameters involved in each ECG has, which is $[(n(n + 1))/2] + 3n$, where n is the number of electrons. The second factor is the number of ECGs needed to reach the adequate level of the energy convergence.[95] This number increases with the increase of the number of electrons in the system. The time needed for the calculation of the Hamiltonian and overlap matrices scales as K^2 with the number of ECGs, K. Also, the calculation time

dx.doi.org/10.1021/cr200419d | Chem. Rev. 2013, 113, 36–79

for each primitive matrix element (before symmetrization) increases as n^3 with the number of electrons. The third factor is related to satisfying the Pauli principle and implementing the correct permutational symmetry of the wave function. It involves acting with an appropriate symmetry operator either on the *ket* or *bra* basis function in calculating each Hamiltonian or overlap matrix element. As the symmetry operator includes $n!$ terms, the computational time of each matrix element scales as $n!$. This is the factor which makes the calculation time increase most rapidly when a larger system is considered.

There are also other factors that influence the calculation time. One of them is the efficiency of the optimization of the ECG exponential parameters. This efficiency usually decreases as the number of electrons and the number of ECGs increase, because more parameters have to be optimized. Therefore, the development of more effective optimization strategies has become particularly important as the molecules considered in the calculations become larger. One of the goals of making the optimization more effective has been the reduction of the number of ECGs by better optimizing them. Optimization approaches are discussed in sections 7.1.1 and 7.1.2.

7.1.1. Building the Basis Set. In building a larger basis set, new ECGs need to be guessed. At the beginning of the basis building process, an initial small set of functions is usually randomly chosen using Gaussian exponents taken from a standard orbital basis set. After this initial set is optimized, the calculation proceeds to grow the basis set larger. One way to guess new Gaussians is to employ the free iterative-complement-interaction (FICI) preoptimization procedure.[175] More details of the procedure are described in section 7.2. We should note that the procedure adjusts the positions of the Gaussian centers more efficiently than the procedure based on the energy minimization where such center adjustment has to often overcome significant energy barriers. After the basis set is enlarged in this manner to a certain target number of functions, a variational, gradient-based reoptimization can be applied to the whole basis set.

In the optimization of the whole basis set, either one can choose to optimize all nonlinear parameters simultaneously, i.e., perform the full optimization, or one can choose to optimize only a part of the nonlinear parameters at a time. We call the latter approach "partial optimization". Usually the energy converges significantly faster (in terms of the basis size) in the full optimization than in the one-function-at-a-time optimization.

In Table 3 we show the energy convergence with the number of ECGs in BO calculations of the LiH molecule performed at the equilibrium internuclear distance with the optimization procedure employing the analytical energy gradient and the full optimization approach.[95] The results are compared with the results of Cencek and Rychlewski[81] obtained in the optimizations performed without the gradient and employing the one-function-at-a-time optimization approach. The comparison shows the advantage of using the gradient-based full optimization in this case. At the same basis sizes the energies obtained by Tung et al.[95] are considerably lower than those of Cencek and Rychlewski. However, to be fair, it needs to be mentioned that the calculations of Cencek and Rychlewski were done 10 years before Tung et al.'s and certainly the improved computer hardware has also contributed to the increased accuracy of the results obtained in ref 95. Full optimization does have certain drawbacks. They are the frequent appearance of linear dependencies between the optimized basis functions

Table 3. Comparison of the Convergence of the BO Energy with the Number of Basis Functions, in hartrees, for the Ground State of the LiH Molecule at R = 3.015 bohr

basis size	Tung et al.[95]	Cencek and Rychlewski[81]
75	−8.068 104 2	−8.066 975
150	−8.069 654 1	−8.069 481
300	−8.070 336 2	−8.070 221
600	−8.070 494 9	−8.070 452
1200	−8.070 529 4	−8.070 512
2400	−8.070 547 3	−8.070 538
estd		−8.070 548[a]

[a]The estimated nonrelativistic BO energy at R = 3.015 bohr made by Cencek and Rychlewski[81] using the BO energy of atoms, adiabatic corrections, and the experimental equilibrium dissociation energy.

and, possibly, large memory demands. These limit the usefulness of the approach.

As linear dependencies frequently appear in the basis set optimization, particularly at earlier stages of the basis set building (when K is small), they need to be continuously eliminated in the course of the procedure in order to maintain the numerical stability of the calculation. The progress made by the basis set enlargement could be significantly hampered or even put on hold by this phenomenon. As for the memory demands, they occur because of the use of the analytical energy gradient in the optimization. The gradient comprised the derivatives of the Hamiltonian (and overlap) matrix elements, eq 89. The size of the Hamiltonian matrix derivative is equal to the number of nonlinear parameters in a single function times the square of the size of the Hamiltonian matrix, $K^2([(n(n+1))/2] + 3n)$. When thousands of ECGs are generated in the calculation, the size of the Hamiltonian matrix derivative may exceed the amount of random access memory available. It should be mentioned that in principle it is possible to organize calculations without storing the entire matrix derivative. However, this comes at a cost of additional complexity and somewhat increased computational time.

Though the linear-dependency problem can be easily handled by switching to the one-function-at-a-time partial optimization approach (called "partial optimization"), the use of the full optimization is more desirable in the calculations. Besides the better energy convergence (as shown in Table 3), there are two other reasons. First, to build a molecular PES, the basis sets at different geometries of the molecule have to be reoptimized to ensure a similar accuracy level at all PES points. This can be accomplished in the full optimization by monitoring the norm of the analytical gradient vector and always converging the calculation to a value of the norm below a certain assumed threshold. This is not possible in the partial optimization, because a small value of the gradient norm for individual ECGs does not guarantee that at the end of the optimization the norm of the total gradient is also small. Second, as the molecular geometry is deformed from the equilibrium in the PES calculation, the nonlinear parameters require less adjustment. In such a case, it only takes a few iterations for the full optimization approach to converge.

The procedure for handling linear dependencies between basis functions in the BO calculations performed by Pavanello et al.[176] comprise four steps. They are called *to identify*, *to replace*, *to avoid*, and *to bypass*. At different stages of the calculation (i.e., different sizes of the basis set) different procedures are usually used to achieve the best overall

dx.doi.org/10.1021/cr200419d | Chem. Rev. 2013, 113, 36–79

computational performance. The four steps involve the following:

1. *To identify*.[176] At various stages of the calculation the overlap for each pair of basis functions is checked. Two functions, ϕ_k and ϕ_l, are considered linearly dependent if the following criterion is met:

$$\frac{|\langle\phi_k|\phi_l\rangle|}{\sqrt{\langle\phi_k|\phi_k\rangle\langle\phi_l|\phi_l\rangle}} \geq t \tag{94}$$

If the absolute value of the overlap is close to 1 and higher than a certain assumed threshold, t (typically 0.99 is used for t), this pair of functions is marked as linearly dependent and further treatment is applied to resolve the problem.

2. *To replace*.[94] It is sufficient to replace one of the functions in the linearly dependent pair to remove the linear dependency. Nonlinear parameters of the replacement function, ϕ, are generated by maximizing the overlap between the function and the linear combination of the functions, ϕ_k and ϕ_l, of the linearly dependent pair taken with the linear coefficients with which the pair enters the wave function,

$$\frac{c_k\langle\phi_k|\phi\rangle + c_l\langle\phi_l|\phi\rangle}{\sqrt{(c_k^2\langle\phi_k|\phi_k\rangle + c_l^2\langle\phi_l|\phi_l\rangle + 2c_kc_l\langle\phi_k|\phi_l\rangle)\langle\phi|\phi\rangle}} \tag{95}$$

After the optimization, the linearly dependent pair is replaced by a pair comprising the newly generated function and one of the old functions of the pair. After the replacement, the optimization of the basis set is restarted.

3. *To avoid*.[7,95] The *replace* procedure was proven to be effective in the PES calculations of two-electron systems, (i.e., H_3^+). However, the efficiency drops for four-electron systems. Furthermore, any basis function replacement requires restarting the optimization. Also, it usually results in some increase of the total energy. The additional time needed for the energy to return to the value before the replacement considerably slows down the optimization process. This causes the function replacement to be computationally expensive and impractical when the size of the basis set becomes large. Thus, for larger basis sets, instead of replacing functions in linearly dependent pairs, a method that prevents the formation of linear dependencies altogether in the optimization process was developed.[7,95] It involves adding the penalty term given by eq 93 to the variational energy functional. When the value of the overlap between a pair of basis functions reaches threshold t, the penalty term for that pair, which was zero (below the threshold), becomes positive and its value increases if the pair becomes more linearly dependent. In the minimization of the energy functional, which includes the penalty term eq 93 for each pair of basis functions, the functions automatically stay linearly independent.

4. *To bypass*.[95] In the case when linear dependency occurs too frequently, and none of the above procedures is able to correct the problem, a decoupled approach (partial optimization) is applied in the optimization. In this approach, the basis set is partitioned into subsets and each subset is optimized separately. This lowers the probability of the linear dependency occurrence. In extreme cases, each function is optimized separately. This actually may improve the scalability of parallel calculations as each processor in this case can carry out the optimization of a different function and the amount of interprocessor communication is significantly reduced. Usually, after enlarging the basis set to a certain size using the partial optimization, the approach is switched back to the full optimization to finish the calculation.

As shown by Tung et al.,[95] the linear dependency problem becomes much less severe or even vanishes entirely when the basis set grows to a large size. At that point, the basis set is extended enough to describe certain missing features of the wave function and the appearance of linearly dependent functions (which would otherwise describe those features) in the course of optimization is no longer favorable. This explanation is based on an observation that certain features of the wave function can be represented either by pairs of almost linearly dependent functions or, alternatively, by functions which are not linearly dependent but whose centers are shifted to the right places. It is unpredictable which representation is "used" in the basis set optimization. If, however, the representation with a linearly dependent pair of functions is selected by the optimization procedure, it can be always converted to the other representation. This is what the *replace* procedure does.

7.1.2. Generating the BO PES. The question in the PES calculation is how to effectively generate basis sets for different PES points. It is clear that, instead of regenerating a new basis set for each PES point from the beginning, a more effective way would be to generate the basis from the basis set of a nearby PES point, where the optimization of the basis function parameters was already performed, and then reoptimize it for the next point. The high quality of the basis set at each PES point is crucial for an effective and accurate PES calculation. In generating the basis set for a PES point from the basis of a nearby point, it is assumed that the two points are close enough that the exponential parameters, $\mathbf{L}_k$, for the two points are very similar. The only parameters that need some adjustment are the Gaussian shifts, $\mathbf{s}_k$. Two methods have been developed to handle this problem: the spring model[94] and the Gaussian product theorem model.[95] Both methods adjust the Gaussian centers when the PES calculation moves from one PES point to another.

In the spring model each Gaussian center is assumed to be attached to every nuclei of the molecule with springlike connections. If the position of nucleus α changes from $\mathbf{R}_\alpha$ to $\mathbf{R}_\alpha + \Delta\mathbf{R}_\alpha$, the Gaussian center, $\mathbf{s}_k^i$, where i is the index of the Gaussian, follow the nuclear movement and changes to $\mathbf{s}_k^i + \Delta\mathbf{s}_k^i$, where

$$\Delta\mathbf{s}_k^i = d\left(\sum_{\alpha=1}^{N}\frac{\Delta\mathbf{R}_\alpha}{R_{i\alpha}}\right)$$
$$d = \left(\sum_{\alpha=1}^{N}\frac{1}{R_{i\alpha}}\right)^{-1} \tag{96}$$

and $R_{i\alpha}$ are the distances from a Gaussian center $\mathbf{s}_k^i$ to the nuclei.

The other method for adjusting the Gaussian centers is a reformulation of the procedure by Cencek and Kutzelnigg.[159] In brief, the procedure involves transforming each ECG to a product of ECGs with centers coinciding with the positions of the nuclei, $\phi_k = \prod_{i=1}^{N}\varphi_i$. A more detailed description of this method can be found in section 12, where it is used for the calculation of adiabatic corrections to the BO energy. By shifting these centers along with shifting the nuclei in the point-by-point PES calculation and then retransforming the ECG from the product form back to its original form, the new basis

dx.doi.org/10.1021/cr200419d | Chem. Rev. 2013, 113, 36–79

set is obtained. These approaches work best if the PES points are close to each other.

Though only the Gaussian centers are adjusted from one PES point to a neighboring point, in the calculations performed by Pavanello et al.[94] and Tung et al.,[95] the exponential parameters, $\mathbf{L}_k$, are tuned during reoptimization of the basis. It is worth noting that there are as many as $[(n(n+1))/2] + 3n$ nonlinear parameters, where n is the number of electrons, in each Gaussian and $K([(n(n+1))/2] + 3n)$ is the number of parameters in the basis set of K basis functions. Only the use of the analytical gradient allows for an efficient optimization with such a large number of variables.

Though the linear dependency is not a concern at this stage, in the variational energy minimization one can either optimize all the above-mentioned parameters simultaneously or optimize them separately to achieve a better computational performance. Also decoupling the optimization of the Gaussian centers from the optimization of the $\mathbf{L}_k$ exponential parameters can be a helpful approach. The advantage of decoupling is based on the fact that the formulas for the first derivatives of the total energy with respect to the Gaussian centers are much simpler than the formulas for the derivatives with respect to the $\mathbf{L}_k$ exponential parameters. In the decoupling approach, one usually performs the optimization of the Gaussian centers first (total of $K(3n)$ parameters). This is followed by the optimization of $\mathbf{L}_k$.

7.2. FICI Method and the Multistep Procedure Used in Growing the Basis Set

Reaching spectroscopic accuracy with BO energy calculations of molecules containing more than two electrons with floating ECGs is a challenge.[92] An important issue in the variational optimization of floating ECGs is how to grow the basis set to achieve a faster convergence of the calculation. In this section some ideas concerning this topic are discussed. In particular we describe how to tackle this problem with an approach based on the free FICI method developed by Nakatsuji and co-workers.[177−179] The method described here has been applied in calculations of three- and four-electron molecules.[95,175,180] For two-electron molecules, such as H_3^+, optimization of the basis set based solely on the principle of minimum energy leads to excellent results.[94,176]

The exact BO wave function, Ψ, satisfies the Schrödinger equation involving the CN or the electronic Hamiltonian defined in eq 10:

$$(\hat{H}_{el} - E_{el})|\Psi\rangle = 0 \tag{97}$$

A trial wave function, Φ, is not exact and does not satisfy eq 97. Instead, it gives

$$(\hat{H} - E_\Phi)|\Phi\rangle \neq 0 \tag{98}$$

where, for the sake of clarity, we dropped the subscript "el" and introduced the subscript Φ to denote $E_\Phi = \langle\Phi|H|\Phi\rangle/\langle\Phi|\Phi\rangle$. It is easy to notice that the result of $(\hat{H} - E_\Phi)$ acting on Φ is a function orthogonal to Φ:

$$\langle\Phi|(\hat{H} - E_\Phi)|\Phi\rangle = 0 \tag{99}$$

Let us call function $\chi = (\hat{H} - E_\Phi)\Phi$ the Nakatsuji function associated with Φ. If such an orthogonal function is added to the wave function expansion, the energy would be lowered. This is because χ has a nonzero off-diagonal matrix element with the Hamiltonian and Φ, namely

$$\begin{aligned}\langle\Phi|H|\chi\rangle &= \langle\Phi|H(\hat{H} - E_\Phi)|\Phi\rangle \\ &= \langle\Phi|H^2|\Phi\rangle - {E_\Phi}^2 \neq 0\end{aligned} \tag{100}$$

Thus, the $\hat{H} - E_\Phi$ operator may be used to generate a correction to the approximate wave function to bring it closer to the exact wave function Ψ. Following this idea, Nakatsuji[177] used the following series to construct Ψ:

$$\Psi = \sum_k a_k(\hat{H} - E_k)^k\Phi \tag{101}$$

where E_k is the energy associated with the kth truncation of eq 101 and a_k are determined variationally. Provided that Φ satisfies certain conditions,[177] eq 97 should monotonically converge to the exact wave function as k increases. Even though it is not yet clear whether the FICI method should lead to an improvement of the convergence of the variational calculation, it provides a systematic way of improving the variational energy. In several applications of the FICI model to atomic and molecular systems, Nakatsuji and co-workers[177] showed how expansions eq 101 obtained with just few iterations (usually $k \leq 6$) produce nonrelativistic BO energies with a sub-cm^{-1} absolute accuracy.

Utilizing the orthogonality of the Nakatsuji function generated in eq 98 and the property in eq 100, Pavanello et al.[175] devised an approach where the floating ECG basis set in the variational molecular calculation is enlarged by guessing new Gaussians to best resemble the Nakatsuji function. In the approach the following procedure based on the first-order term in eq 101 was used. Let us assume that an approximate wave function expanded in terms of K_0 floating ECGs, Φ_{K_0}, has already been fully optimized. The procedure for growing the basis set to $K_0 + K_1$ functions comprises the following five steps:

1. A set of K_1 new floating ECGs is constructed. The $\mathbf{A}_i$ matrices of these functions are generated randomly and the Gaussian centers, $\mathbf{s}_i$, are placed at the nuclei. With the addition of the new functions, the basis set now has $K_0 + K_1$ functions.
2. The linear expansion parameters of the wave function are found by a simultaneous diagonalization of the Hamiltonian and the overlap matrices.
3. Only the nonlinear parameters of the newly added floating ECGs are optimized (recall that this step was termed *partial optimization* before) using a functional that makes the newly guessed functions to best approximate the Nakatsuji function for Φ_{K_0}.
4. The whole $K_0 + K_1$ basis set is fully optimized, i.e., the nonlinear parameters of *all* $K_0 + K_1$ basis functions are subject to variational optimization (recall that this step was termed *full optimization* before). In every optimization cycle the linear parameters are updated.
5. The incremental enlargement routine relabels the $K_0 + K_1$ set as the new K_0 set, and the procedure returns to step 1.

The functional for the partial optimization of step 3 is designed to best approximate the $k = 1$ term in eq 101 by K_1 floating ECGs. It involves maximizing of the following functional:

$$F[K_1] = \frac{\langle\sum_{i=1}^{K_1} c_i^1 g_i^1|\hat{H} - E_{K_0}|\Phi_{K_0}\rangle}{\langle\sum_{i=1}^{K_1} c_i^1 g_i^1|\sum_{i=1}^{K_1} c_i^1 g_i^1\rangle} \tag{102}$$

dx.doi.org/10.1021/cr200419d | Chem. Rev. 2013, 113, 36−79

The partial optimization in step 3 will be called the FICI refinement hereafter. In eq 102 the superscript 1 labels ECG functions, g_i^1, belonging to the K_1 set. It is straightforward to notice that the maximization of the $F[K_1]$ functional yields an approximation to the Nakatsuji function $(\hat{H} - E_{K_0})\Phi_{K_0}$. After the maximization of $F[K_1]$, the newly refined K_1 set of floating ECGs is added to the K_0 set and a partial variational optimization of the K_1 set is performed. Then steps 4 and 5 follow. The cycle of the five steps is repeated until satisfactory convergence of the energy is reached.

7.2.1. Implementation. In the actual implementation,[175] the maximization of the $F[K_1]$ functional is replaced by the minimization of the following functional:

$$G[K_1] = \frac{1}{1 + F[K_1]^2} \tag{103}$$

Having F^2 rather than F in the functional simplifies the calculation, because the functional becomes independent of the phase of the wave function. Using $1 + F^2$ instead of F^2 prevents the G functional from reaching a singularity at $F \simeq 0$, which can happen if the initial choice of the K_1 set is poor. In ref 175 the minimization of $G[K_1]$ was carried out using the truncated Newton optimization routine (TN) of Nash et al.[181] To speed up the convergence, it is also possible to supply the TN routine with the analytical gradient of $G[K_1]$ determined with respect to the nonlinear parameters of the functions in the K_1 set:[175]

$$\frac{\partial G[K_1]}{\partial K_1} = -\frac{2F[K_1]}{(1 + F[K_1]^2)^2} \frac{\partial F[K_1]}{\partial K_1} \tag{104}$$

where ∂K_1 represents the partial derivative with respect to the nonlinear parameters of the floating ECGs belonging to the K_1 set.

7.2.2. Improved Function Mobility and Barrier Tunneling. As pointed out in section 3.5, an important aspect of the floating ECG basis set is its flexibility in describing different features of the wave function including its ionic and covalent components. Usually the ratio of the number of ionic basis function with respect to the covalent functions is maintained at a certain level which varies depending on the specific molecular system.[94] If a certain ionic/covalent ratio is set for a basis set optimized using the variational method, it remains essentially unchanged during the calculation. This is because changing it and making some ionic floating ECGs become covalent or vice versa needs migration of centers of the floating ECGs between atomic centers, which requires overcoming energy barriers. This is unlikely to happen in the variational energy optimization.

An analysis of how the FICI refinement deals with adjusting the ionic/covalent ratio was carried out in ref 175. The numerical evidence presented there showed that FICI allows for a much improved function mobility in terms of a more pronounced variation of the positions of the Gaussian centers within each optimization cycle.

8. CALCULATION OF THE LEADING RELATIVISTIC AND QED CORRECTIONS

Recent theoretical studies of the helium atom that include the works performed by Morton et al.,[23] Korobov,[182,183] and Pachucki[26,29,184] have demonstrated that, by systematically including the finite mass corrections, as well as the relativistic and QED corrections, to the nonrelativistic energies of the ground and excited states of this system, one can achieve an accuracy of the predicted ionization and transition energies that in some cases exceed the accuracy of the present-day experiment. The recently published summary of the available theoretical and experimental results for the bound stationary states of He by Morton et al.[23] demonstrates very well the high level agreement between theory and experiment achieved in the calculations. It also shows that for a few states such as 2^1P_1 and 2^3P_J there is still some noticeable disagreement between the theoretical and the experimental values.

High-accuracy calculations on the H_2 molecule[118,185−187] also revealed that to achieve a high level of agreement between the experiment and the theory for electronic and vibrational transition energies the dominant α^2-dependent terms (where $\alpha = 1/c$ is the fine structure constant), relativistic corrections, and some higher order corrections have to be included in the calculations. The effective operators for higher order corrections are derived within the framework of nonrelativistic quantum electrodynamics (NRQED). For example, all terms up to α^3 were included in the calculations for the He atom by Morton et al.[23] Also QED terms of the order of α^4 were included for some lower states in the calculations performed by Korobov and Yelkhovsky,[182,188] by Pachucki,[29] and by Drake and Martin.[189] Moreover, there have been works where the terms of the order of α^6 for the He atom were calculated.[26,184] These make the He atom the most accurately described atomic system apart from the hydrogen atom. In addition to the relativistic and QED corrections, some He calculations also included corrections for finite values of the ^{3}He and ^{4}He nuclear charge radii of 1.9659 and 1.167 fm, respectively, which were derived from the isotope shift measured by Shiner et al. and from the measurements of the Lamb shift of the muonic hydrogen.[190,191]

Another system for which the theoretical calculations have been often used to make a comparison with highly accurate spectroscopic measurements is the lithium atom.[192,193] The most accurate calculations of this three-electron problem have been performed using Hylleraas-type functions that are capable of accurately describing the asymptotic behavior of the wave function at both the electron and nuclear cusps and at infinity. There have been several works devoted to very accurate Li calculations.[28,31,109,194−197] They have included the relativistic corrections of the order of α^2, as well as the QED corrections of the order of α^3 and estimates of the α^4 corrections.[27,198−200]

QED which describes the behavior of quantum particles in an electromagnetic field creates a general theoretical framework for the analysis of the relativistic and QED effects in bound states of atoms and molecules. However, even for small atomic and molecular systems with a few electrons, accurate relativistic calculations are very hard and too expensive to be carried out on present-day computers. Furthermore, the QED Dirac−Coulomb (DC) equation is only fully correct for a single electron in the Coulombic field and approximations are introduced when systems with more than one electron are considered. Also, an additional problem appears due to the lack of a lower bound for the negative energy spectrum in the DC equation. Faced with those difficulties, an effort has been made to develop an effective approach to account for the relativistic effects in light atomic and molecular systems in the framework of the perturbation theory. The zero-order level in such an approach is the nonrelativistic Schrödinger equation. The perturbation Hamiltonian representing the relativistic effects is then obtained based on the NRQED theory.[201,202] We should mention that the perturbation approach to account for the

dx.doi.org/10.1021/cr200419d | Chem. Rev. 2013, 113, 36−79

relativistic corrections can also be developed without using NRQED, as shown by Bethe and Salpeter.[203] The relativistic corrections can now be routinely computed by some quantum chemistry packages.

In the NRQED theory the relativistic corrections appear as quantities proportional to powers of the fine structure constant $\alpha \approx 1/137$ (in atomic units $\alpha = 1/c$, where c is the speed of light in a vacuum):

$$E(\alpha) = E_{NR} + \alpha^2 E_{REL} + \alpha^3 E_{QED} + \alpha^4 E_{HQED} + ... \quad (105)$$

This enables inclusion of increasingly higher order effects in a systematic way in the calculations. The leading terms of the expansion in eq 105, i.e., the nonrelativistic energy E_{NR}, the relativistic correction $\alpha^2 E_{REL}$, and the highest-order radiative correction $\alpha^3 E_{QED}$, have been well-known since early works of Bethe and Salpeter.[203] The relativistic and QED corrections are determined using the perturbation theory with the nonrelativistic wave function as the zero-order function. In addition to the NRQED corrections, one can also calculate corrections due to the structure of the nucleus and its polarizability. With those corrections NRQED is at present the most accurate theoretical framework for calculating bound state energies of light atoms and molecules.

In most of the very accurate atomic and molecular calculations the relativistic corrections are calculated as expectation values of the appropriate NRQED operators with the nonrelativistic wave function of the state of interest. If the BO (i.e., infinite-nuclear-mass) wave function is used, one can also include in the calculations the so-called recoil effects, which are finite-nuclear-mass corrections to the relativistic energy.

In the calculations performed by Stanke et al.[8−10,12−14,147,204] a somewhat different approach has been used. They started with the relativistic mass-velocity, Darwin, spin−spin, spin−orbit, and orbit−orbit operators for all particles involved in the system expressed in terms of laboratory coordinates and transformed them to an internal coordinate system. Then they determined the corrections as expectation values of those operators with the wave function obtained in a non-BO calculation that treats the nuclei (or nucleus for an atom) and the electrons on equal footing. In this way the recoil corrections were automatically included in the relativistic energy. Such a procedure allows, for example, direct calculation of how an isotopic substitution in the system affects the relativistic energy. The energy calculated this way includes the relativistic contributions due to the motion of the nuclei, as well as small relativistic contributions originating from the coupling of the electronic and nuclear motions. The transformation of the relativistic operators to an internal coordinate system is discussed in section 8.4.

8.1. The Relativistic Hamiltonian

A complete account of the interactions between elementary particles that include the electrostatic and magnetic forces described by the Lorentz-invariant interaction potential can be obtained from QED.[205,206] Within this model particles interact by emitting and absorbing virtual photons. Relativistic corrections have a simple form only for the hydrogen atom. For atoms and molecules with more electrons the relativistic problem is much more complicated. To account for the relativistic effects, a relativistic multiparticle Hamiltonian needs to be constructed. Such a Hamiltonian can be written for two interacting fermions described by a wave function consisting of 16 spinor components. However, for a more general case of N interacting fermions and/or bosons, the construction of the relativistic Hamiltonian cannot be done without making significant approximations. This can be best accomplished with the QED theory where a system of interacting particles in the relativistic limit is described by a sum of single-particle relativistic Hamiltonians ($H_{rel}(i)$) and two-particle interaction operators accounting for the Coulombic interactions ($V_{ij} = \sum_{i>j} 1/r_{ij}$) and the relativistic interactions (B_{ij}):

$$H = \sum_i H_{rel}(i) + \sum_{i>j} \frac{1}{r_{ij}} - \sum_{i>j} B_{ij} \quad (106)$$

The B_{ij} term originates from the application of the QED theory to two interacting particles and is derived by taking into account single-photon scattering amplitude in the calculation.

As in the non-BO approach one considers all particles on equal footing, one is forced to make a distinction between the fermions and bosons in the relativistic Hamiltonian. This distinction appears at the level of formulating the theory and at the level of the calculations. The case of the two interacting particles being fermions (f−f) is well described in the literature. Less discussed are cases where a fermion interacts with a boson (f−b) or a boson interacts with another boson. The distinction at the relativistic level between the fermions and the bosons seems, perhaps, somewhat artificial and arbitrary, as the difference in the relativistic treatment of the two types of particles is small. However, a rigorous, very accurate relativistic treatment of their interactions requires such a distinction. We will now discuss the α^2 relativistic contributions in two cases. The first case concerns a system where all particles are fermions and have spins equal to 1/2 (for example, the ^{3}He atom). In the second case the system consists of fermions (electrons and some of the nuclei) and bosons (the other nuclei).

States of a single fermion with spin $s = 1/2$ (an electron) and a single boson with spin $s = 0$ (for example, an α-particle) are described by the one-particle relativistic Dirac (D) and Klein−Gordon (KG) equations, respectively. The construction of a general N-particle quantum relativistic equation is, however, not as simple as in the case of the nonrelativistic Schrödinger equation. In the Schrödinger equation, it is sufficient to include the Coulomb operators to account for the interactions between the particles. In the relativistic case, apart from the Coulombic forces, there are interparticle interactions that are related to the magnetic properties of the particles. Those properties result from the orbital and spin motions of the particles. Furthermore, since all the interactions between particles are affected by the finite velocities of their motions, the so-called retardation effects appear.

8.2. A System of N Fermions

A system that consists of N fermions in the absence of an external field can be described using the Dirac−Breit (DB) Hamiltonian (H^{f-f}) extended to an N-fermion case. We consider only the Pauli approximation of this Hamiltonian. Using the generalized form of the DB Hamiltonian and expanding each term in powers of α, one gets H^{f-f}_{rel} (the Breit−Pauli (BP) operator) as a sum of the following terms of the order of α^2:

$$H^{f-f}_{MV} = -\frac{1}{8} \sum_{i=1}^{N} \frac{\mathbf{P}_i^4}{M_i^3} \quad (107)$$

dx.doi.org/10.1021/cr200419d | Chem. Rev. 2013, 113, 36−79

$$H_{\mathrm{D}}^{\mathrm{f-f}} = \frac{1}{8}\sum_{i=1}^{N}\sum_{i\neq j}^{N}\frac{Q_iQ_j}{M_i^2}\nabla_{\mathbf{R}_i}^2\frac{1}{R_{ij}} \tag{108}$$

$$H_{\mathrm{OO}}^{\mathrm{f-f}} = -\frac{1}{2}\sum_{j=1}^{N}\sum_{i>j}^{N}\frac{Q_iQ_j}{M_iM_j}\frac{1}{R_{ij}}\left(\mathbf{P}_i'\mathbf{P}_j + \frac{1}{R_{ij}^2}\mathbf{R}_{ij}'(\mathbf{R}_{ij}'\mathbf{P}_i)\mathbf{P}_j\right) \tag{109}$$

$$H_{\mathrm{SO}}^{\mathrm{f-f}} = -\frac{1}{2}\sum_{i=1}^{N}\sum_{j\neq i}^{N}\frac{Q_iQ_j}{M_j^2}\frac{1}{R_{ij}^3}(\mathbf{R}_{ij}\times\mathbf{P}_j)\mathbf{S}_j - \sum_{j=1}^{N}\sum_{i>j}^{N}\frac{Q_iQ_j}{M_iM_j}\frac{1}{R_{ij}^3}((\mathbf{R}_{ij}\times\mathbf{P}_j)\mathbf{S}_i - (\mathbf{R}_{ij}\times\mathbf{P}_i)\mathbf{S}_j) \tag{110}$$

$$H_{\mathrm{SS}}^{\mathrm{f-f}} = \sum_{j=1}^{N}\sum_{i>j}^{N}\frac{Q_iQ_j}{M_iM_j}\left[\frac{1}{R_{ij}^3}\left((\mathbf{S}_i'\mathbf{S}_j) - \frac{3}{R_{ij}^2}(\mathbf{S}_i'\mathbf{R}_{ij})(\mathbf{S}_i'\mathbf{R}_{ij})\right) - \frac{8\pi}{3}(\mathbf{S}_i'\mathbf{S}_j)\,\delta^3(\mathbf{R}_{ij})\right] \tag{111}$$

and

$$H_{\mathrm{rel}}^{\mathrm{f-f}} = H_{\mathrm{MV}}^{\mathrm{f-f}} + H_{\mathrm{D}}^{\mathrm{f-f}} + H_{\mathrm{OO}}^{\mathrm{f-f}} + H_{\mathrm{SO}}^{\mathrm{f-f}} + H_{\mathrm{SS}}^{\mathrm{f-f}}$$

where $H_{\mathrm{MV}}^{\mathrm{f-f}}$ is the mass−velocity Hamiltonian, $H_{\mathrm{D}}^{\mathrm{f-f}}$ is the Darwin Hamiltonian, $H_{\mathrm{OO}}^{\mathrm{f-f}}$ is the orbit−orbit interaction Hamiltonian, $H_{\mathrm{SO}}^{\mathrm{f-f}}$ is the spin−orbit Hamiltonian, and $H_{\mathrm{SS}}^{\mathrm{f-f}}$ is the spin−spin interaction Hamiltonian.

8.3. A Fermion−Boson System

As derived by Datta and Misra,[207] the fermion−boson Hamiltonian in the nonrelativistic limit ($H_{\mathrm{rel}}^{\mathrm{f-b}}$) has to include the interaction between the boson and the fermions. For a single electron and a boson these additional terms are the same as the nonrelativistic-limit Hamiltonian for two fermions with one small exception. The difference between the two Hamiltonians is the absence of the term in the Darwin operator describing the interaction of the boson with the field generated by the fermions. Let us explain this difference using a two-particle system. The Darwin operator in the BP equation for two fermions, 1 (M_1,Q_1) and 2 (M_2,Q_2), has the form

$$H_{\mathrm{D}}^{\mathrm{f-f}} = \frac{1}{8}\left(\frac{1}{M_1^2}\nabla_{\mathbf{R}_1}^2\frac{Q_1Q_2}{R_{12}} + \frac{1}{M_2^2}\nabla_{\mathbf{R}_2}^2\frac{Q_1Q_2}{R_{12}}\right)$$

The first term in the above operator

$$\frac{1}{8}\frac{1}{M_1^2}\nabla_{\mathbf{R}_1}^2\frac{Q_1Q_2}{R_{12}}$$

describes the interaction of fermion 1 with the field generated by fermion 2, and the second term

$$\frac{1}{8}\frac{1}{M_2^2}\nabla_{\mathbf{R}_2}^2\frac{Q_1Q_2}{R_{12}}$$

is due to the interaction of fermion 2 with the field generated by fermion 1. In the case of a fermion−boson pair (1 being the fermion and 2 being the boson), the term describing the interaction of the boson with the field generated by the fermion, the term

$$\frac{1}{8}\frac{1}{M_2^2}\nabla_{\mathbf{R}_2}^2\frac{Q_1Q_2}{R_{12}}$$

is absent in the order of α^2. However, it will appear in higher orders in α.[208]

8.4. Transformation of the Relativistic Operators to the Internal Coordinate System

The transformation of the nonrelativistic Hamiltonian to the internal coordinate system and the elimination of the COM motion was described in section 2.1. A similar transformation needs to be applied to the relativistic Hamiltonian. While a full separation of the laboratory Hamiltonian into the Hamiltonian describing the kinetic energy of the COM motion and the internal Hamiltonian can be exactly performed, the separation of the relativistic Hamiltonian into the internal and external parts is not exact. In general, the BP Hamiltonian in the new coordinate system can be written as a sum of three terms, $H_{\mathrm{rel}} = H_{\mathrm{rel}}^{\mathrm{CM}} + H_{\mathrm{rel}}^{\mathrm{int}} + H_{\mathrm{rel}}^{\mathrm{CM-int}}$, where $H_{\mathrm{rel}}^{\mathrm{CM}}$ is the term describing the relativistic effects of the motion of the center of mass, $H_{\mathrm{rel}}^{\mathrm{int}}$ describes the internal relativistic effects, and $H_{\mathrm{rel}}^{\mathrm{CM-int}}$ describes the relativistic coupling of the internal and external motions. The contributions to the energy of the system due to $H_{\mathrm{rel}}^{\mathrm{CM}}$ and $H_{\mathrm{rel}}^{\mathrm{CM-int}}$ vanish if the center of mass of the system is at rest. The relativistic corrections to the internal states of the system are calculated using $H_{\mathrm{rel}}^{\mathrm{int}}$. For states with the S symmetry, the transformation of the coordinate system leads to the relativistic operator in the following form:

$$H_{\mathrm{MV}}^{\mathrm{f-f}} = H_{\mathrm{MV}}^{\mathrm{f-b}} = -\frac{1}{8}\left[\frac{1}{m_0^3}\left(\sum_{i=1}^{n}\nabla_{\mathbf{r}_i}\right)^4 + \sum_{i=1}^{n}\frac{1}{m_i^3}\nabla_{\mathbf{r}_i}^4\right]$$

$$H_{\mathrm{D}}^{\mathrm{f-f}} = -\frac{\pi}{2}\left[\sum_{i=1}^{n}\left(\frac{1}{m_0^2} + \frac{1}{m_i^2}\right)q_0q_i\,\delta^3(\mathbf{r}_i) + \sum_{i=1}^{n}\sum_{j=1,j\neq i}^{n}\frac{1}{m_i^2}q_iq_j\,\delta^3(\mathbf{r}_{ij})\right]$$

$$H_{\mathrm{D}}^{\mathrm{f-b}} = -\frac{\pi}{2}\left[\sum_{i=1}^{n}\frac{1}{m_i^2}q_0q_i\,\delta^3(\mathbf{r}_i) + \sum_{i=1}^{n}\sum_{j=1,j\neq i}^{n}\frac{1}{m_i^2}q_iq_j\,\delta^3(\mathbf{r}_{ij})\right]$$

$$H_{\mathrm{OO}}^{\mathrm{f-f}} = H_{\mathrm{OO}}^{\mathrm{f-b}} = -\frac{1}{2}\sum_{i=1}^{n}\frac{q_0q_i}{m_0m_i}\left[\frac{1}{r_i}\nabla_{\mathbf{r}_i}'\nabla_{\mathbf{r}_i} + \frac{1}{r_i^3}\mathbf{r}_i'(\mathbf{r}_i'\nabla_{\mathbf{r}_i})\nabla_{\mathbf{r}_i}\right] - \frac{1}{2}\sum_{i=1}^{n}\sum_{j=1,j\neq i}^{n}\frac{q_0q_i}{m_0m_i}\left[\frac{1}{r_i}\nabla_{\mathbf{r}_i}'\nabla_{\mathbf{r}_j} + \frac{1}{r_i^3}\mathbf{r}_i'(\mathbf{r}_i'\nabla_{\mathbf{r}_i})\nabla_{\mathbf{r}_j}\right] + \frac{1}{2}\sum_{i=1}^{n-1}\sum_{j>i}^{n}\frac{q_iq_j}{m_im_j}\left[\frac{1}{r_{ij}}\nabla_{\mathbf{r}_i}'\nabla_{\mathbf{r}_j} + \frac{1}{r_{ij}^3}\mathbf{r}_{ij}'(\mathbf{r}_{ij}'\nabla_{\mathbf{r}_i})\nabla_{\mathbf{r}_j}\right]$$

dx.doi.org/10.1021/cr200419d | Chem. Rev. 2013, 113, 36−79

$$H_{SS}^{f-f} = -\frac{8\pi}{3}\sum_{i=1}^{n}\frac{q_0 q_i}{m_0 m_i}(\mathbf{S}_0'\mathbf{S}_i)\,\delta^3(\mathbf{r}_i) - \frac{8\pi}{3}\sum_{j=1}^{n}\sum_{i>j}^{n}\frac{q_i q_j}{m_i m_j}(\mathbf{S}_i'\mathbf{S}_j)\,\delta^3(\mathbf{r}_{ij})$$

$$H_{SS}^{f-b} = -\frac{8\pi}{3}\sum_{j=1}^{n}\sum_{i>j}^{n}\frac{q_i q_j}{m_i m_j}(\mathbf{S}_i'\mathbf{S}_j)\,\delta^3(\mathbf{r}_{ij})$$

where, for consistency of the notation, we used $m_i = M_{i+1}$.

8.5. QED Effects in Atomic Calculations

In this review we focus on the calculations of QED effects in atoms with more than three electrons, because very accurate energies of such systems can only be obtained with the use of ECGs. An effective way for calculating atomic QED corrections proportional to α^3 and α^4 was described in the work of Pachucki et al.[198] Let us consider a four-electron atom. The leading QED correction that accounts for the two-photon exchange, the vacuum polarization, and the electron self-energy effects can be expressed as[198]

$$E_{QED} = \sum_{i=1}^{4}\sum_{j>i}^{4}\left\{\left[\frac{164}{15}+\frac{14}{3}\ln\alpha\right]\langle\Psi_{INM}|\delta^3(\mathbf{r}_{ij})|\Psi_{INM}\rangle - \frac{14}{3}\langle\Psi_{INM}|\frac{1}{4\pi}P\left(\frac{1}{r_{ij}^3}\right)|\Psi_{INM}\rangle\right\} + \sum_{i=1}^{4}\left[\frac{19}{30}-2\ln\alpha-\ln(k_0)\right]\frac{4q_0}{3}\langle\Psi_{INM}|\delta^3(\mathbf{r}_i)|\Psi_{INM}\rangle \quad (112)$$

The above expression does not include the recoil contributions, which are usually much smaller than the leading contributions. The last term in eq 112 is the so-called Araki−Sucher distribution.[196,209−211] This contribution is determined as the following limit:

$$\langle\Psi|P\left(\frac{1}{r^3}\right)|\Psi'\rangle = \lim_{a\to 0}\int\Psi^*(\mathbf{r})\,\Psi'(\mathbf{r})\left[\frac{1}{r^3}\Theta(r-a) + 4\pi\delta^3(\mathbf{r})(\gamma+\ln a)\right]d\mathbf{r} \quad (113)$$

where Θ is the step function and γ is the Euler constant. To overcome the usually slow convergence of the highly singular $P(1/r_{ij}^3)$, one can use the so-called expectation value identity approach implemented by Pachucki et al.[212]

The term involving the so-called Bethe logarithm, $\ln(k_0)$, in eq 112 is more difficult to calculate for an atom with more than one electron. The Bethe logarithm can be expressed as

$$\ln(k_0) = -\frac{1}{D}\langle\Psi|\nabla(\hat{H}_{int}-E_{nonrel})\ln[2(\hat{H}_{int}-E_{nonrel})]\nabla|\Psi\rangle \quad (114)$$

where for a four-electron atom

$$\nabla = \sum_{i=1}^{4}\nabla_{\mathbf{r}_i} \quad (115)$$

and

$$D = 2\pi q_0\langle\Psi_{INM}|\sum_{i=1}^{4}\delta^3(\mathbf{r}_i)|\Psi_{INM}\rangle \quad (116)$$

High precision calculations of $\ln(k_0)$ have been done for some one- and two-electron atoms by Drake[213] and Korobov and Korobov,[214] as well as for the three-electron lithium atom by Yan and Drake[197] and Pachucki et al.[198] More recently, values for the Bethe logarithm were also reported for the ground state of Be^+ and Li^- and the ground and the first excited states of the neutral Be atom by Pachucki et al.[27,199] The procedure used to evaluate the Bethe logarithm in those works was based on the integral representation of $\ln(k_0)$ proposed by Schwartz[215] and refined by Pachucki et al.[199]

The α^4 QED correction is smaller than the leading α^3 correction and can be determined approximately. The dominant component of the α^4 correction usually accounting for about 80% of its value can be calculated using the following formula:[199]

$$E_{HQED} \simeq 4\pi q_0^2\left(\frac{139}{128}+\frac{5}{192}-\frac{\ln 2}{2}\right)\langle\Psi_{INM}|\sum_{i=1}^{4}\delta^3(\mathbf{r}_i)|\Psi_{INM}\rangle \quad (117)$$

The remaining α^4 QED contributions are more difficult to calculate because they involve some singular terms.[29,182]

9. RESULTS FOR ATOMS

The spectra of small atoms are measured with very high accuracy. Thus they provide an excellent testing ground for very accurate quantum mechanical methods. Below we will provide a few examples of recent calculations on atomic systems with three, four, five, and six electrons. In this we will particularly emphasize the comparison of the calculated quantities with the experimental values. The goal of the comparison will be also to show how involved the calculations have to be and what effects they need to include to match or even approach the accuracy of the state-of-the-art experiment. We will also comment on the role the calculations can play in refining the spectral energies of small atomic systems.

9.1. Very Accurate Calculations for Three- and Four-Electron Atoms and Atomic Ions

We will show here three examples of recent atomic calculations. They concern the lowest five ^{1}S states of the Be atom,[14] the lowest two ^{1}S states of the C^{2+} ion,[16] and the lowest five ^{2}D states of the Li atom.[138,139] We chose these three examples because they very well represent the interplay between the experiment and theory in studying the atomic spectra.

The calculations of the five lowest ^{1}S states of beryllium were performed for the ^{9}Be isotope.[14] The basis set of 10 000 ECGs was generated independently for each state in a process involving starting with a small randomly chosen set of functions and gradually adding more functions to the set and optimizing them with the variational method employing the analytical energy gradient determined with respect to the nonlinear parameters of the Gaussians. In all other examples presented in this section the basis set was grown in this way. After the final basis sets were generated, the energies of the states were recalculated for an infinite nuclear mass. The difference between the finite- and infinite-nuclear-mass energies for each state gives the mass correction.

dx.doi.org/10.1021/cr200419d | Chem. Rev. 2013, 113, 36−79

Table 4. Transition Energies between Adjacent ^{1}S States of the Be Atom Computed Using Finite- and Infinite-Nuclear-Mass Nonrelativistic Energies and Then Corrected by Accounting for the Leading Relativistic and QED Effects[a]

transition	$2^1S \rightarrow 3^1S$	$3^1S \rightarrow 4^1S$	$4^1S \rightarrow 5^1S$	$5^1S \rightarrow 6^1S$
ΔE_{nonrel} (INM)	54 674.677(2)	10 568.242(3)	4077.009(6)	1998.997(30)
ΔE_{nonrel} (FNM)	54 671.219(2)	10 567.627(3)	4076.765(6)	1998.876(30)
ΔE_{rel}	54 677.907(20)	10 568.090(30)	4076.915(40)	1998.994(70)
ΔE_{QED}	54 677.401(24)	10 568.059(36)	4076.918(50)	1999.016(85)
ΔE_{HQED}	54 677.378(30)	10 568.057(38)	4076.918(50)	1999.015(85)
experiment[216,217]	54 677.26(10)	10 568.07(10)	4076.87(10)	1998.95(10)

[a]The results are taken from ref 14. All values are in cm^{-1}.

Next, the finite-nuclear-mass wave functions were used calculate the leading relativistic correction employing the first-order perturbation theory approach. We also calculated the α^3 and α^4 QED corrections. With the corrections were added to the nonrelativistic energies the transition energies between the adjacent states; i.e., the $2^1S \rightarrow 3^1S$, $3^1S \rightarrow 4^1S$, $4^1S \rightarrow 5^1S$, and $5^1S \rightarrow 6^1S$ transitions, were calculated. The results are shown in Table 4. For each value the numerical uncertainty is shown. They were determined based on the level of the convergence of the particular value with the number of basis functions and on other factors contributing to the numerical noise in the calculations.

In Table 4 we also show the experimental transition energies taken from the review paper of Kramida and Martin,[216] but originally measured by Johansson.[217] The accuracy of the experimental results can be estimated based on Johansson's statement, which can be found in his paper, that the error in his transition energy measurement should be less than $\pm$0.05 cm^{-1}. As each experimental transition included in Table 4 was determined indirectly from two mP $\rightarrow$ nS transitions, it is reasonable to assume the experimental uncertainty is about 0.10 cm^{-1} (or less).

As one can see in Table 4, the energies for the $2^1S \rightarrow 3^1S$, $3^1S \rightarrow 4^1S$, $4^1S \rightarrow 5^1S$, and $5^1S \rightarrow 6^1S$ transitions calculated using the FNM nonrelativistic energies augmented with the relativistic and QED corrections differ from the experimental results by 0.12, 0.01, 0.05, and 0.06 cm^{-1}, respectively. This shows that the accuracy level of the present calculations is very high. This is the first time higher excited states of a four-electron atom have been calculated with such an accuracy. Also, it is clear that including the correction for the finite nuclear mass, and the relativistic and QED corrections, is necessary to achieve this level of agreement between the theory and the experiment.

The next example concerns the lowest two states of the C^{2+} ion. In an ion with a larger positive charge, such as C^{2+}, the relativistic and QED corrections are significantly larger than in neutral atoms with the same number of electrons. For this reason these corrections have a larger effect on of the transition energies. Carbon is also an interesting system because it has three stable isotopes, ^{12}C, ^{13}C, and ^{14}C, and thus the nuclear mass effects on its transition frequencies can be studied. In presenting the results for C^{2+}, we start with showing in Table 5 the convergence of the transition $2^1S_0 \rightarrow 3^1S_0$ energy as a function of the number of basis functions for $^{12}C^{2+}$, $^{13}C^{2+}$, and $^{14}C^{2+}$, as well as $^{\infty}C^{2+}$. As one can see, to achieve the convergence of about 0.01$-$0.02 cm^{-1} of the transition energy, a 10 000 function basis set was needed. This is a typical convergence pattern for a transition energy of a small atom.

In Table 6 we show the convergence of the $2^1S_0 \rightarrow 3^1S_0$ transition energy of the three isotopes of C^{2+} as increasingly higher level of theory is employed in the calculations. As one can see, the inclusion of the finite mass correction changes the transition energy by about 20 cm^{-1}, adding the relativistic correction has a much larger effect of about 300 cm^{-1}, and the QED correction adds about 20 cm^{-1}. When all of the above corrections are accounted for, the calculated transition energy for $^{12}C^{2+}$ becomes 182 519.031(1000) cm^{-1}, which is only less than a wavenumber off the experimental value of 182 519.88 cm^{-1}.[218]

The third example concerns the most recent calculations performed on the five lowest ^{2}D Rydberg states of the lithium atom.[138,139] The results presented in Table 7 concern the energies of the transitions between adjacent states of ^{7}Li. The calculated values are compared with the experimental results.[218] Results obtained for ^{6}Li, which has not yet been measured, as well as the $^{\infty}$Li results, are also shown. For ^{7}Li, the results obtained with different numbers of ECGs are also presented in Table 7 to show the energy convergence pattern and demonstrate that the transition energies obtained with 4000 basis functions are very well converged.

As the relativistic and QED effects can be expected to be very similar for all five ^{2}D states, the energy differences agree very well with the experiment. The $1s^24d \rightarrow 1s^25d$ and $1s^25d \rightarrow 1s^26d$ transitions only differ from the experiment by 0.01 cm^{-1}. However, for $1s^26d \rightarrow 1s^27d$ there is a more noticeable difference mainly caused by a less accurate experimental energy value for the $1s^27d$ state. The results of the calculations allow for a refinement of this energy. This can be done by taking the experimental energy of the $1s^26d$ state of 40 437.31 cm^{-1} and adding to it the very well converged $1s^26d-1s^27d$ energy difference of 809.33 cm^{-1}. Due to a negligible contribution of the relativistic and QED effects, the energy value of 41 246.64 cm^{-1} obtained this way should be quite accurate. This value is slightly different from the experimental value of 41 246.5 cm^{-1}.[218] The same procedure can be applied to determine the energies of the ^{2}D states of ^{6}Li, once the energy of the $1s^23d$ level becomes available from the experiment.

Finally, we should note that performing separate variational calculations for the different isotopes of the same element is not the way these types of calculations are usually performed. Usually, for atoms heavier than hydrogen one first computes the wave function with an infinite nuclear mass and subsequently includes the finite-mass effects by adding the first-order perturbation correction for the mass-polarization operator. There are two reasons for using the finite-mass approach in atomic calculations. First, as mentioned earlier, the basis functions need to be optimized for just one isotope (usually the main one) and in the calculations of other isotopes only the linear expansion coefficients in the wave function are allowed to adjust. The effort involved in such an adjustment (done by solving the secular equation) is similar to the effort

dx.doi.org/10.1021/cr200419d | Chem. Rev. 2013, 113, 36−79

Table 5. Convergence of the $2^1S_0 \rightarrow 3^1S_0$ Nonrelativistic and Relativistic Transition Energies (in cm^{-1}) for Different Isotopes of C^{2+} with the Number of Basis Functions[16] [a]

basis size	$^{12}C^{2+}$, nonrel	$^{12}C^{2+}$, rel	$^{13}C^{2+}$, nonrel	$^{13}C^{2+}$, rel	$^{14}C^{2+}$, nonrel	$^{14}C^{2+}$, rel	$^{\infty}C^{2+}$, nonrel	$^{\infty}C^{2+}$, rel
2000	182 243.038	182 540.527	182 244.792	182 542.281	182 246.291	182 543.780	182 265.773	182 563.260
4000	182 242.341	182 540.013	182 244.095	182 541.767	182 245.594	182 543.266	182 265.076	182 562.746
6000	182 242.254	182 540.038	182 244.008	182 541.792	182 245.507	182 543.291	182 264.989	182 562.771
8000	182 242.222	182 539.986	182 243.977	182 541.741	182 245.475	182 543.239	182 264.957	182 562.719
10000	182 242.208	182 540.150	182 243.963	182 541.905	182 245.461	182 543.403	182 264.944	182 562.883
10000[b]	182 242.205(20)	182 540.245(170)	182 243.959(20)	182 542.000(170)	182 245.458(20)	182 543.498(170)	182 264.940(20)	182 562.978(170)
experiment[218]		182519.88						

[a] The results were calculated using up to 10 000 ECGs. The values in parentheses are estimates of the remaining uncertainty due to finite size of the basis. [b] Several additional optimization cycles were performed.

involved in calculating the first-order perturbation correction accounting for the change of the nuclear mass. However, performing the calculations variationally automatically allows for accounting for higher-order mass effects. Second, the mass-dependent wave function generated in FNM calculation can subsequently be used to calculate relativistic corrections, as well as other expectation values. Thus, these quantities automatically include the mass dependency (for example, the recoil effects in the case of the relativistic corrections), which in the conventional calculation can only be accounted for by a laborious perturbation procedure.

Finally, having compared the results for some ^2D states of lithium with the experiment, we should comment on the accuracy one expects to achieve in variational calculations with explicitly correlated Gaussians in comparison to the best calculations performed with Hylleraas functions. Such a comparison can be made, for example, for the lowest ^2S and ^2P states of Li because high-accuracy results obtained with the Gaussians and Hylleraas functions exist for these states. The comparison is shown in Table 8. As one can see, the Hylleraas results are noticeably more accurate due to larger number of basis functions used. However, the data in Table 8 also demonstrate that when the nonlinear parameters of the Gaussians are thoroughly optimized one can achieve very high accuracy that is good enough for most applications that require high precision. In fact, the convergence in terms of the number of basis functions can be even better in the case of Gaussians than in the case of the Hylleraas functions if sufficient effort is invested in the optimization of the nonlinear parameters of the Gaussians.

9.2. Calculations for Atomic Systems with Five Electrons

Precise calculations on five and more electron systems are of particular importance as no calculations of spectroscopic accuracy for such systems exist at the present time. Due to increased complexity and much larger computational demands, most methods exhibit a huge deterioration of the accuracy for such relatively large systems. At the same time, these larger systems are of great significance since they serve as an important test for developing and tuning less accurate quantum-chemical approaches.

As an example of the high level of accuracy achievable for a five-electron atomic system with ECGs, we can consider the results obtained for the ground and low-lying P and S states of the boron atom.[130] This example aims to demonstrate that, if sufficient computational resources are used in the calculations, ECGs are capable of producing results for the ground state and some lower lying excited states which almost match the accuracy achieved before for four-electron systems.

In Table 9 we present the results of the ECG calculations for the two lowest $L = 0$ states and two lowest $L = 1$ states of the boron atom.[130] The convergence of the total nonrelativistic energies of all four states is shown. A quick look at the convergence patterns suggests that the uncertainty of the total nonrelativistic energies does not exceed 2−3 μhartrees. In Table 10 the ground state energy obtained with ECGs is compared with some of the best literature data. As can be seen, the ECG variational upper bound of −24.653 866 08 hartree for the ground state energy lies noticeably lower than the best recent upper bound of −24.653 837 33 hartree obtained in a state-of-the-art CI calculation[220] with the following very extended basis set of atomic orbitals:

dx.doi.org/10.1021/cr200419d | Chem. Rev. 2013, 113, 36−79

Table 6. Convergence of the $2^1S_0 \rightarrow 3^1S_0$ Transition Energies (in cm^{-1}) for $^{12}C^{2+}$, $^{13}C^{2+}$, and $^{14}C^{2+}$ Including Increasingly Higher Level Corrections (Finite-Mass, Relativistic, and QED) to the Energies of the Two States[a]

contribution included	ΔE ($^{12}C^{2+}$)	ΔE ($^{13}C^{2+}$)	ΔE ($^{14}C^{2+}$)
E_{nonrel} (INM)	182 264.940(20)	182 264.940(20)	182 264.940(20)
E_{nonrel} (FNM)	182 242.205(20)	182 243.959(20)	182 245.458(20)
$\alpha^2 E_{rel}$	182 540.245(170)	182 542.000(170)	182 543.498(170)
$\alpha^3 E_{QED}$	182 520.583(170)	182 522.338(170)	182 523.836(170)
$\alpha^4 E_{HQED}$	182 519.031(1000)	182 520.785(1000)	182 522.283(1000)
experiment[218]	182 519.88		

[a]The values in parentheses indicate the remaining uncertainty due to finite size of the basis. In the case of α^4 correction the uncertainty is due to an approximate treatment of that correction. The results are taken from ref 16.

Table 7. Energy Differences (in cm^{-1}) between Adjacent ^2D States of ^7Li, ^6Li, and $^\infty Li$[a]

basis	$1s^23d-1s^24d$	$1s^24d-1s^25d$	$1s^25d-1s^26d$	$1s^26d-1s^27d$
^7Li				
1500	5340.25	2471.52	1342.44	809.56
2000	5340.27	2471.54	1342.40	809.39
2500	5340.27	2471.54	1342.39	809.35
3000	5340.27	2471.54	1342.39	809.34
3500	5340.27	2471.54	1342.39	809.33
4000	5340.27	2471.54	1342.39	809.33
expt[218]	5340.30	2471.55	1342.38	809.2
^6Li				
4000	5340.20	2471.50	1342.37	809.32
$^\infty Li$				
4000	5340.69	2471.73	1342.49	809.39

[a]For ^7Li, the convergence of the differences with the basis set size is shown. For ^6Li and $^\infty Li$ only the results obtained with 4000 Gaussians are shown. For ^7Li, the results of the calculations are compared with the experimental values. The results are taken from ref 139.

24s23p22d21f20g19h18i17k16l15m14n13o12q11r10t9u8v7w6x5y4z.

Another illustrative example of the calculations of a five-electron system with ECGs is the singly ionized carbon atom. The results of the recent ECG calculations for this system[131] are shown in Table 11. Similar to the boron atom calculations, the accuracy currently achievable with the variational method employing ECGs is significantly higher than that of the best-to-date literature values obtained with other methods. It is interesting to note that the estimated accuracy for the excited ^2S state of C^+ is roughly twice lower than that for the ground ^2P state. In contrast, calculations on the B atom yielded the energy of the first excited ^2S state that was approximately 5 times more tightly converged than the energy of the ground state. Such an order of magnitude difference in the accuracy of the first excited ^2S states of C^+ and B does not result from a lower quality of the C^+ calculations, however. The main reason for a somewhat worse convergence of the energy in the case of C^+ is the fact that the wave function of the lowest excited ^2S state of this system is dominated by the $1s^22s2p^2$ configuration. This

Table 8. Comparison of the Nonrelativistic Variational Energies of the $1s^22s(^2S)$, $1s^23s(^2S)$, and $1s^22p(^2P)$ States of $^\infty Li$ Obtained in ECG Calculations with the Best Literature Values Obtained in Calculations That Used the Hylleraas Basis[a]

state	source	method	basis size	energy
$1s^22s(^2S)$	Puchalski et al.[113]	Hylleraas	4172	−7.478 060 323 845 785
	Puchalski et al.[113]	Hylleraas	13 944	−7.478 060 323 909 560
	Puchalski et al.[113]	Hylleraas	∞	−7.478 060 323 910 10(32)
	Wang et al.[192]	Hylleraas	3910	−7.478 060 323 880 889 238
	Wang et al.[192]	Hylleraas	26 520	−7.478 060 323 910 134 843
	Wang et al.[192]	Hylleraas	∞	−7.478 060 323 910 143 7(45)
	Stanke et al.[13]	ECG	10 000	−7.478 060 323 81
	Bubin[219]	ECG	3600	−7.478 060 323 884 4
$1s^23s(^2S)$	Puchalski et al.[193]	Hylleraas	4172	−7.354 098 421 004 0
	Puchalski et al.[193]	Hylleraas	9576	−7.354 098 421 379 9
	Puchalski et al.[193]	Hylleraas	∞	−7.354 098 421 426(19)
	Wang et al.[192]	Hylleraas	3910	−7.354 098 421 345 692 670
	Wang et al.[192]	Hylleraas	26 520	−7.354 098 421 444 310 034
	Wang et al.[192]	Hylleraas	∞	−7.354 098 421 444 316 4(32)
	Stanke et al.[13]	ECG	10 000	−7.354 098 421 13
	Bubin[21]	ECG	3600	−7.354 098 421 382 4
$1s^22p(^2P)$	Puchalski et al.[193]	Hylleraas	4172	−7.410 156 532 150 2
	Puchalski et al.[193]	Hylleraas	9576	−7.410 156 532 628 6
	Puchalski et al.[193]	Hylleraas	∞	−7.410 156 532 665(14)
	Wang et al.[192]	Hylleraas	4824	−7.410 156 532 310 89
	Wang et al.[192]	Hylleraas	30 224	−7.410 156 532 650 66
	Wang et al.[192]	Hylleraas	∞	−7.410 156 532 651 6(5)
	Bubin[219]	ECG	3600	−7.410 156 532 553 2

[a]Infinite basis size stands for an extrapolated value.

dx.doi.org/10.1021/cr200419d | Chem. Rev. 2013, 113, 36−79

Table 9. Convergence of the Total Nonrelativistic Energies (in hartrees) for the Main Isotope of Boron Atom, ^{11}B[a]

isotope	basis	$^2P^o$ ($1s^22s^22p$)	^2S ($1s^22s^23s$)	$^2P^o$ ($1s^22s^23p$)	^2S ($1s^22s^24s$)
^{11}B	1000	−24.652 494 17	−24.470 106 32	−24.430 979 54	−24.401 841 39
	2000	−24.652 598 09	−24.470 136 27	−24.431 073 08	−24.401 923 14
	3000	−24.652 615 70	−24.470 140 92	−24.431 088 39	−24.401 936 14
	4000	−24.652 621 14	−24.470 142 33	−24.431 093 26	−24.401 939 96
	5000	−24.652 623 43	−24.470 142 90	−24.431 095 31	−24.401 941 47
	5100[b]	−24.652 623 87(250)	−24.470 143 16(50)	−24.431 095 74(250)	−24.401 941 83(150)
^{10}B	5100[b]	−24.652 500 24(250)	−24.470 018 76(50)	−24.430 971 75(250)	−24.401 817 83(150)
$^{\infty}B$	5100[b]	−24.653 866 08(250)	−24.471 393 06(50)	−24.432 341 44(250)	−24.403 187 67(150)

[a]Energies obtained for ^{10}B and $^{\infty}B$ with the largest basis set of 5100 functions are also shown. The values in parentheses are estimates of the remaining uncertainty due to finite basis size used in the calculations. The results are taken from ref 130. [b]Basis set was generated with a more extensive optimization of the nonlinear parameters.

Table 10. Comparison of the Available Literature Results for the Ground State Energy (in hartrees) of $^{\infty}B$ Atom

energy	method (year)
−24.653 93	configuration interaction + experimental data (1991)[221]
−24.653 91	configuration interaction + experimental data (1993)[222]
−24.653 62(3)	diffusion quantum Monte Carlo (2007)[223]
−24.653 79(3)	diffusion quantum Monte Carlo (2011)[224]
−24.653 840	ECG, 2000 basis functions (2009)[225]
−24.653 837 33	selected configuration interaction (2010)[220]
−24.653 866 08	ECG, 5100 basis functions (2011)[130]
−24.653 868 5	estimate of the exact nonrelativistic energy[130]

configuration is different from the dominant configuration ($1s^22s^23s$) in the wave function of the lowest ^2S state of B. The latter configuration is easier and more effectively described with the basis functions (32) than the $1s^22s2p^2$ configuration which results from a coupling of two p electrons to an S state. The convergence in the calculations of the states dominated by the $1s^22s2p^2$ configuration can probably be improved if prefactors in the form of dot products $\mathbf{r}_i'\cdot\mathbf{r}_j$ are included in some basis functions.

9.3. Calculations for Atomic Systems with Six Electrons

The carbon atom (^{12}C) has been the largest system considered so far in calculations performed with all-electron correlated Gaussians.[135,136] The calculations focused on the ground and first excited ^3P states of this six-electron system. As six-electron basis functions are used in these calculations, there are 21 exponential parameters in each function to be optimized. Also, each Hamiltonian or overlap matrix element involves integration over 18 Cartesian coordinates. Even with the aid of the analytic gradient in the variational optimization, such calculations represent a daunting task. As only 32 processors were used in the calculations, after investing a considerable amount of computer time, a basis set of only 1000 Gaussians was generated for each of the two states. Even though the lowest ever variational energies have been obtained for both states with that many functions, their number is clearly not enough to determine the transition energy between the two states with an accuracy even close to what we achieved for smaller atoms. It would take a dedicated computer system with hundreds of processors to reach high accuracy in the carbon calculations.

However, even with up to 1000 basis functions in the basis set, it is interesting to examine the convergence of the total energies of the two states, as well as the convergence of the transition energy. The data for such an analysis are shown in Table 12. As one can see, only at best four digits in the total energies are converged. The transition energy shows the right convergence trend, but it is still off from the experimental value in the third digit after the decimal point.

10. RESULTS FOR DIATOMIC MOLECULES OBTAINED WITHOUT THE BORN–OPPENHEIMER APPROXIMATION

The non-BO approach utilizing ECGs has been so far implemented only for rotationless states (i.e., vibrational states) of diatomic molecules. In this review we present examples of those applications that best illustrate the accuracy level that the approach can deliver.

Table 11. Total Nonrelativistic Energies (in hartrees) for the Lowest S and P States of C^+ Ion[a]

isotope	basis	$^2P^o(1s^22s^22p)$	$^2S(1s^22s2p^2)$	$^2P^o(1s^22s^23p)$
^{12}C	1000	−37.429 043 99	−36.989 923 74	−36.828 842 62
	2000	−37.429 146 64	−36.990 141 16	−36.828 982 35
	3000	−37.429 162 43	−36.990 176 48	−36.829 004 48
	4000	−37.429 167 20	−36.990 187 14	−36.829 011 34
	4500	−37.429 168 35	−36.990 189 85	−36.829 013 05
	5100[b]	−37.429 169 55(250)	−36.990 192 98(500)	−36.829 014 78(350)
^{13}C	5100[b]	−37.429 301 59	−36.99032209	−36.82914677
^{14}C	5100[b]	−37.429 414 35	−36.990 432 34	−36.829 259 49
$^{\infty}C$	5100[b]	−37.430 880 49	−36.991 865 91	−36.830 725 08
	DMC,[c]	−37.43 073(4)		

[a]The ECG results are taken from ref 131. [b]Basis set was generated with a more extensive optimization of the nonlinear parameters. [c]Diffusion Monte Carlo, ref 224.

dx.doi.org/10.1021/cr200419d | Chem. Rev. 2013, 113, 36–79

Table 12. Convergence of the Total Nonrelativistic Energies of the Ground and First Excited ^{3}P States ($2s^22p^2$ and $2s^22p3p$) of ^{12}C and the Corresponding Transition Energy with the Number of Basis Functions[a]

	basis size	$2s^22p^2\ ^3P$	$2s^22p3p\ ^3P$	transition energy
^{12}C				
	100	−37.810 501	−37.471 762	74 344.61
	200	−37.828 749	−37.499 146	72 339.61
	300	−37.834 300	−37.506 665	71 907.57
	400	−37.837 008	−37.509 750	71 824.83
	500	−37.838 416	−37.511 548	71 739.20
	600	−37.839 692	−37.513 040	71 691.82
	700	−37.840 423	−37.513 989	71 644.03
	800	−37.840 982	−37.514 684	71 614.21
	900	−37.841 364	−37.515 233	71 577.38
	1000	−37.841 621	−37.515 565	71 561.08
	experiment[218]			71 352.51
$^{\infty}$C				
	1000	−37.843 333	−37.517 279	71 560.65
	DMC[b 224]	−37.844 46(6)		
	estimated exact[222]	−37.845 0		

[a]Total energies of ^{12}C and $^{\infty}$C are in hartrees and transition energies are in cm^{-1}. The results are taken from ref 136. [b]Diffusion Monte Carlo.

10.1. Diatomics with One and Two Electrons: Charge Asymmetry Induced by Isotopic Substitution

Two examples will be shown here. The first concerns the calculations of the complete spectrum of vibrational states of the HD^+ molecule.[143] As the calculations were performed without invoking the BO approximation and the nuclei in them possessed finite masses, it is interesting to analyze what effect this has on the wave function and, in particular, on the probability that the electron is on average closer to one end of the molecule than to the other. The second example concerns the HD molecule and its pure vibrational spectrum.

The HD^+ pure vibrational spectrum has been studied by many researchers, and very accurate, virtually exact calculated nonrelativistic energies have been published in the literature.[226,227] This includes the energy for the highest vibrational v = 22 state, which is only about 0.4309 cm^{-1} below the D + H^+ dissociation limit. In Table 13 we compare the ECG variational energies for all 23 states[143] with the values of Hilico et al.[227] As one can see, the values agree very well. The agreement is consistently very good for all the states calculated.

The wave functions for all 23 states were used to calculate the average internuclear distances and the average distances between the nuclei and the electron. Also, averages of the squares of the distances were calculated. The results are shown in Table 13. As can be expected, the average internuclear distance increases with the rising level of excitation. This increase becomes more prominent at the vibrational levels near the dissociation threshold. For example, in going from v = 21 to v = 22 the average internuclear distance increases more than 2-fold from 12.95 to 28.62 au. In the v = 22 state the HD^+ ion is almost dissociated. However, the most striking feature that becomes apparent upon examining the results is a sudden increase of the asymmetry between the deuteron−electron and proton−electron average distances above the v = 20 excitation level. In levels up to v = 20 there is some asymmetry of the electron distribution with the p−e distance being slightly longer than the d−e distance. For example, in the v = 20 state the d−e

Table 13. Total Energies, Expectation Values of the Deuteron−Proton Distance, r_{d-p}, the Deuteron−Electron Distance, r_{d-e}, and the Proton−Electron Distance, r_{p-e}, and Their Squares for the Vibrational Levels of HD^+ at the Rotational Ground State[a]

v	E, Bubin et al.[143]	E, ref 227.	$\langle r_{d-p}\rangle$	$\langle r_{d-e}\rangle$	$\langle r_{p-e}\rangle$	$\langle r_{d-p}^2\rangle$	$\langle r_{d-p}^2\rangle$	$\langle r_{p-e}^2\rangle$
0	−0.597 897 968 5	−0.597 897 968 6	2.055	1.688	1.688	4.268	3.534	3.537
1	−0.589 181 829 1	−0.589 181 829 6	2.171	1.750	1.750	4.855	3.839	3.843
2	−0.580 903 700 1	−0.580 903 700 3	2.292	1.813	1.814	5.492	4.169	4.173
3	−0.573 050 546 4	−0.573 050 546 8	2.417	1.880	1.881	6.185	4.526	4.531
4	−0.565 611 041 8	−0.565 611 042 3	2.547	1.948	1.950	6.942	4.915	4.921
5	−0.558 575 520 0	−0.558 575 521 1	2.683	2.020	2.022	7.771	5.339	5.346
6	−0.551 935 948 2	−0.551 935 949 3	2.825	2.095	2.097	8.682	5.804	5.813
7	−0.545 685 913 7	−0.545 685 915 6	2.975	2.175	2.177	9.689	6.318	6.329
8	−0.539 820 639 4	−0.539 820 641 9	3.135	2.259	2.261	10.81	6.888	6.902
9	−0.534 337 011 0	−0.534 337 013 9	3.305	2.348	2.351	12.06	7.527	7.545
10	−0.529 233 631 7	−0.529 233 635 9	3.489	2.445	2.448	13.48	8.250	8.272
11	−0.524 510 905 9	−0.524 510 910 6	3.689	2.549	2.554	15.09	9.074	9.105
12	−0.520 171 137 4	−0.520 171 148 2	3.909	2.664	2.670	16.96	10.03	10.07
13	−0.516 218 698 8	−0.516 218 710 3	4.154	2.791	2.799	19.16	11.15	11.21
14	−0.512 660 176 7	−0.512 660 192 6	4.432	2.934	2.946	21.79	12.49	12.57
15	−0.509 504 627 0	−0.509 504 651 7	4.754	3.099	3.116	25.01	14.13	14.26
16	−0.506 763 834 4	−0.506 763 878 1	5.138	3.292	3.319	29.11	16.20	16.41
17	−0.504 452 646 6	−0.504 452 699 1	5.611	3.527	3.572	34.55	18.92	19.30
18	−0.502 589 181 5	−0.502 589 234 0	6.227	3.821	3.910	42.25	22.66	23.47
19	−0.501 194 732 3	−0.501 194 799 3	7.099	4.198	4.421	54.35	28.13	30.38
20	−0.500 292 401 7	−0.500 292 454 3	8.550	4.569	5.516	77.74	35.66	46.64
21	−0.499 910 333 9	−0.499 910 361 5	12.95	2.306	12.19	176.0	12.94	168.2
22	−0.499 865 777 5	−0.499 865 778 5	28.62	1.600	28.55	910.0	4.266	911.4
D atom[b]	−0.499 863 815 2			1.500			3.002	

[a]All quantities are in atomic units. [b]D atom in the ground state.

dx.doi.org/10.1021/cr200419d | Chem. Rev. 2013, 113, 36−79

Table 14. Comparison of All Pure Vibrational Transition Energies (in cm^{-1}) of HD Calculated with the ECG Non-BO Approach and with (rel) and without (nonrel) Including the α^2 Relativistic Corrections with the Transitions Reported by Pachucki and Komasa (PK)[20] [a]

transition	$E^{v+1}_{nonrel} - E^{v}_{nonrel}$		$E^{v+1}_{rel} - E^{v}_{rel}$		$E^{v+1} - E^{v}$
$v \rightarrow v+1$	Bubin et al.	PK	Bubin et al.	PK	experiment
0 → 1	3632.1586(4)	3632.1583	3632.1802(4)	3632.1792	3632.1595(17)[229]
1 → 2	3454.7187(5)	3454.7173	3454.7368(5)	3454.7341	3454.735(50)[230]
2 → 3	3280.7571(5)	3280.7573	3280.7690(5)	3280.7700	3280.721(49)[230]
3 → 4	3109.2661(5)	3109.2657	3109.2742(5)	3109.2740	3100.264(16)[230]
4 → 5	2939.1564(10)	2939.1548	2939.1604(10)	2939.1586	2948.149(17)[230]
5 → 6	2769.2297(10)	2769.2282	2769.2288(10)	2769.2272	2769.199(36)[230]
6 → 7	2598.1395(20)	2598.1399	2598.1324(20)	2598.1337	
7 → 8	2424.3442(20)	2424.3411	2424.3333(20)	2424.3292	
8 → 9	2246.0106(30)	2246.0103	2245.9915(30)	2245.9920	
9 → 10	2060.9653(30)	2060.9616	2060.9417(30)	2060.9362	
10 → 11	1866.5168(50)	1866.5167	1866.4822(50)	1866.4832	
11 → 12	1659.3318(50)	1659.3302	1659.2894(50)	1659.2872	
12 → 13	1435.1376(50)	1435.1373	1435.0828(50)	1435.0832	
13 → 14	1188.3926(70)	1188.3918	1188.3246(70)	1188.3241	
14 → 15	911.7483(70)	911.7379	911.6628(70)	911.6536	
15 → 16	595.4111(70)	595.4216	595.3069(70)	595.3165	
16 → 17	231.5728(70)	231.5815	231.4462(70)	231.4559	

[a] The values in parentheses indicate the estimated remaining uncertainty due to finite basis size used. The ECG non-BO results are derived from the work of Bubin et al.[149] The last column lists several transition frequencies derived from experimental data.

average distance is 4.569 au and the p−e distance is 5.516 au. The situation becomes completely different for the $v = 21$ state. Here the p−e distance for this state of 12.19 au is almost equal to the average value of the internuclear distance, but the d−e distance becomes much smaller and equals only 2.306 au. It is apparent that in this state the electron is essentially localized at the deuteron and the ion becomes highly polarized. An analogous situation also occurs for the $v = 22$ state. Here, again, the p−e average distance is very close to the internuclear distance while the d−e distance is close to what it is in an isolated D atom. One can say that in the low vibrational state the HD^+ ion is covalently bound, but in the highest two states it becomes ionic.

The second example concerns the non-BO calculations of all 17 rotationless vibrational energies of the HD molecule.[228] For each state 10 000 ECGs were used in those calculations. The total energies were used to calculate the $v \rightarrow v + 1$ transition energies, which are presented in Table 14. In Table 14 the ECG transition energies obtained with and without the relativistic corrections of the order of α^2 are compared with the transitions determined using the results of Pachucki and Komasa (PK).[20] They performed their calculations using the standard approach where the potential energy curve was calculated first and, after being corrected for the adiabatic and nonadiabatic effects, as well as relativistic effects, it was used to calculate the vibrational frequencies. The comparison shown in Table 14 includes vibrational frequencies calculated by the two methods with and without the relativistic corrections.

First let us focus on the nonrelativistic transitions in Table 14. As one can see, the ECG non-BO results agree very well with the PK values. The difference for the transitions between low-lying states, as well as for the states in the middle of the spectrum, is consistently less than 0.005 cm^{-1}. As one can see from the comparison with the experimentally derived transitions, the difference between the ECG non-BO results and those of PK is much smaller than the expected contribution due the α^3 QED and higher order corrections. For the three top transitions the difference increases to about 0.01 cm^{-1}. While the exact reason for this discrepancy is not immediately clear, it is possible that it arises as a result of the perturbation approach used by PK and not accounting for the finite-nucleus-mass effects for those two states as accurately as it is done in the direct variational non-BO approach.

10.2. Diatomics with Three Electrons

As stated, the application of the non-BO ECG approach for diatomic molecules is currently limited because of the form of the basis set to pure vibrational states and to molecules with σ electrons. However, it is not limited with respect to the number of the electrons the molecule has. Hence, this is the first accurate non-BO method available that allows performing calculations of molecules with more than two electrons.

An example of non-BO ECG calculations performed for a molecule with more than two electrons is the work on all five pure vibrational transitions of the $^7LiH^+$ ion.[153] Up to 10 000 ECGs for each state were used in the calculations. Table 15 shows the convergence of the transition frequencies calculated with and without the relativistic corrections with the number of the basis functions. One can see that the third digit after the decimal point for all transitions expressed in wavenumbers is essentially converged. The significance of these calculations lies in the fact that the pure vibrational spectrum of the $^7LiH^+$ ion has not been measured yet, and the very accurate predictions of the vibrational transitions generated in the calculations can guide the future experiment where such a measurement is attempted.

10.3. Diatomics with More than Three Electrons

The major bottleneck in the non-BO calculations with all-particle ECGs is their $n!$ scaling with the number of identical particles (electrons). As mentioned before, $n!$ is the number of permutations in the symmetry operator that needs to be applied to each basis function to enforce the right permutational symmetry of the wave function. For example, in the

dx.doi.org/10.1021/cr200419d | Chem. Rev. 2013, 113, 36−79

Table 15. Convergence of the Pure Vibrational Transition Energies of $^7LiH^+$ Ion Determined with and without the Inclusion of the Leading Relativistic Corrections[a]

$v' \rightarrow v''$	basis size	$E^{v''}_{NR} - E^{v'}_{NR}$	$E^{v''}_{REL} - E^{v'}_{REL}$
1 → 0	8000	355.051	355.072
	9000	355.031	355.053
	10000	355.015	355.037
	10000[b]	355.011	355.034
2 → 1	8000	261.748	261.774
	9000	261.757	261.778
	10000	261.766	261.787
	10000[b]	261.765	261.786
3 → 2	8000	169.991	170.000
	9000	169.986	170.000
	10000	169.981	169.998
	10000[b]	169.980	169.997
4 → 3	8000	89.825	89.837
	9000	89.821	89.821
	10000	89.820	89.819
	10000[b]	89.819	89.818
5 → 4	8000	35.260	35.265
	9000	35.258	35.271
	10000	35.258	35.260
	10000[b]	35.259	35.260

[a]All values are in cm^{-1}. The results are taken from ref 153. [b]Results obtained by performing several additional cyclic optimizations of the nonlinear parameters.

calculations of the BH molecule there are 720 such permutations.

The BH molecule is the largest system ever calculated with the non-BO ECG approach.[225] The aim of the calculations was to determine the dissociation energy of this system. The results are shown in Table 16 with the ECG FNM results obtained for the boron atom also included. As can be expected, the energy for the B atom converges significantly faster than for BH. With 2000 basis functions the nonrelativistic non-BO energy of B is essentially converged within five significant figures while the BH energy is converged within four figures. The better convergence for the B atom than for BH assures that the BH dissociation energy calculated as the difference between the total energy of BH and the sum of the energies of the B and H atoms is a lower bound to the true dissociation energy of this system. We should add that, even with only 2000 basis functions, the non-BO energies of the B atom and the BH molecule shown in Table 16 are the best variational upper bounds ever calculated for these systems. However, 2000 basis functions is only enough to ensure convergence of two significant figures in the dissociation energy. Our best result for this energy is $D_0 = 28\,083$ cm^{-1} ($28\,074$ cm^{-1} after adding the relativistic corrections). An approximate extrapolation to an infinite number of basis functions increases the dissociation energy to $D_0 = 28\,400 \pm 150$ cm^{-1}. This result agrees with the experimental value recommended by Bauschlicher et al.[231] of $28\,535 \pm 210$ cm^{-1}. However, it is clear that in order to match the experimental accuracy with the calculations the energies of both B and BH will have to be computed with higher accuracy and much larger ECG basis sets approaching or even exceeding 10 000 functions.

11. HIGHLY ACCURATE BO MOLECULAR CALCULATIONS

11.1. Hydrogen Clusters

In this section we show that it is possible to reduce the computational time needed for an ECG BO PES calculation by avoiding costly optimization of the ECG nonlinear parameters at every PES point and still maintain high accuracy of the results throughout the whole PES. The approach developed for this purpose will be described and illustrated through its application in the calculations of the potential energy curve (PEC) of the $(H_2)_2$ dimer in the linear geometrical configuration keeping the monomer at the frozen internuclear separation of 1.4 bohr.

An essential part of a very accurate ECG calculation is growing the basis set from a small number of functions to a large one that assures the desired accuracy of the results. In the process of building the basis set is usually initiated with a set of ECGs generated using contraction of basis sets of the monomers.[124] For $(H_2)_2$ this is

$$\phi_{k,(H_2)_2} = \varphi_{i,H_2} \cdot \varphi_{j,H_2} \tag{118}$$

where φ_{i,H_2} and φ_{j,H_2} are ECGs obtained for a hydrogen molecule. As mentioned, the Gaussian centers of φ_{i,H_2} and φ_{j,H_2} are placed at the same monomer or different monomers to produce the so-called ionic or covalent basis function. Next, the basis set is enlarged by adding subsets of ECGs followed by their partial or global optimization depending which of these two procedures is more computationally efficient in the particular case. As shown in Table 17,[95] at $R_{H_2-H_2} = 6$ bohr 99.6% of the binding energy is recovered with the 5000 ECG basis set.

In the calculations reported in ref 95 the procedure was used to generate 5000 ECGs for $(H_2)_2$ for varying intermonomer distances. With that, when moving to the next PEC point, only the linear expansion parameters had to be recalculated. However, as PEC points got further separated from the point where the full basis set optimization was performed (at the equilibrium), the procedure became increasingly less accurate. To remedy this and to reduce the error, 2000 additional ECGs were generated at each PES point with the FICI method and added to the basis set. In this way a 7000 ECG basis set was obtained for each PEC point. To verify if the FICI-optimized

Table 16. Nonrelativistic and Relativistic ($E^{rel} = E^{nonrel} + \alpha^2\langle H_{MV}\rangle + \alpha^2\langle H_D\rangle$) Energies of B and BH in au[a]

basis size	E^{nonrel}(B)	E^{rel}(B)	E^{nonrel}(BH)	E^{rel}(BH)	D_0^{nonrel}	D_0^{rel}
500	−24.652 069	−24.659 230	−25.270 646	−25.277 747	26 084	26 070
1000	−24.652 494	−24.659 659	−25.277 313	−25.284 438	27 454	27 444
1500	−24.652 573	−24.659 733	−25.279 332	−25.286 461	27 880	27 872
2000	−24.652 598	−24.659 758	−25.280 280	−25.287 408	28 083	28 074

[a]Values for D_0 are the corresponding dissociation energies expressed in cm^{-1}. The results are taken from ref 225 with the exception of the last column, D_0^{rel}, which contains corrected data (ref 225 has an error in this quantity).

dx.doi.org/10.1021/cr200419d | Chem. Rev. 2013, 113, 36–79

Table 17. Convergence of the $(H_2)_2$ Interaction Energy, in kelvin[a]

basis size	interaction energy
600	41.7197
700	39.6936
800	38.9714
900	38.6994
1000	38.4557
1500	37.2085
2000	36.3622
2500	35.6462
3000	35.3227
4000	35.0380
5000	34.9311
exact	34.785[b]

[a]The interaction energy is determined with respect to the exact energy of two isolated H_2 molecules each with the internuclear distance equal to R_{H_2} = 1.448 736 bohr ($2E_{H_2}$ = −2.348 155 753 48 hartree[75]). The calculations are performed at the intermonomer separation of 6 bohr.[95]. [b]Best literature value obtained using the monomer contraction method with a 360 000 ECG basis set augmented with additional 2400 ECGs and extrapolated to the complete basis set limit.[232] The estimated standard deviation of the energy value is σ = 0.030 K.

additional set is capable of efficiently correcting the error, full optimization of the 5000 ECG basis set was performed at some selected PEC points. A comparison of the results obtained in those optimizations[95] with the energies obtained with the 7000 function basis sets is shown in Table 18.

Table 18. Comparison of the Total and Interaction Energies of $(H_2)_2$ Obtained with 7000 ECGs (5000 ECGs Generated with the Shifting Procedure and 2000 Generated with the FICI Method) with the Energies Obtained with Fully Optimized 5000 ECGs[a]

$R_{H_2-H_2}$ (bohr)	E_{7000}^{FICI}	E_{5000}^{FO}	ΔE	E_{5000}^{FO}
6.0	−2.348 045 14	−2.348 045 13	0.002	34.826
7.1	−2.348 202 03	−2.348 202 42	0.123	−14.841
8.0	−2.348 185 31	−2.348 185 89	0.182	−9.622
9.0	−2.348 167 82	−2.348 168 41	0.187	−4.101
10.0	−2.348 159 69	−2.348 160 24	0.174	−1.522
14.75	−2.348 154 53	−2.348 155 08	0.175	0.108
100.0	−2.348 154 87	−2.348 155 42	0.175	0.000

[a]Calculations have been performed at six selected PEC points including the $R_{H_2-H_2}$ = 6 bohr point. Total energies, E_{7000}^{FICI} and E_{5000}^{FO}, are in hartrees, and the total energy differences, ΔE, interaction energies, and ΔE_{5000}^{FO}, are in kelvin.[95].

Although the energies calculated with the full optimization procedure are lower than the energies obtained without reoptimizing the ECG nonlinear parameters, the energy difference is nearly constant (about ∼0.19 K) as the intermonomer distance increases beyond 8 bohr. Therefore, one can conclude that the absolute error of the FICI-optimized PEC is just under 0.15 K at $R_{H_2-H_2}$ = 6 bohr and sub-0.3 K for larger intermonomer distances. This validates the approach used in the $(H_2)_2$ calculations and shows that the floating ECGs are capable of representing the ground state wave function of this four-electron four-center molecule with high accuracy.

11.2. Molecules with One Atom Other Than Hydrogen

In this section we describe high-accuracy, state-of-the-art PEC ECG calculations of the LiH molecule.[180] The PEC includes finite-mass adiabatic corrections added to the BO energy. The PEC accuracy is better than 0.3 cm^{-1}, showing once again that the variational method with ECGs complemented with the use of the analytic gradient is a very high accuracy approach for generating PEC/PESs for small molecules.

The ECG calculation of the LiH BO PEC of Tung et al.[180] started with the 2400 ECG basis set (see Table 3) built using the full optimization approach at the equilibrium internuclear distance (R_{Li-H} = 3.015 bohr). Using this basis set, the basis sets for the adjacent PEC points were generated by applying the Gaussian center shifting procedure. After shifting, the basis sets were fully reoptimized using the full optimization approach. This procedure was repeated until the target internuclear distance of R_{Li-H} = 40 bohr was reached. Similarly to the $(H_2)_2$ ECG calculations, a concern one may have is related to possible accumulation of error which may arise at each PEC point due to its initial basis set not being generated from "scratch", but being extrapolated from the previous PEC point. Such an accumulation would likely produce the largest error for the longest internuclear distance (in the calculations it was R_{Li-H} = 40 bohr). In Table 19 the magnitude of this error is

Table 19. Comparison of the Estimated and Calculated LiH BO Energies at R_{Li-H} = 3.015 and R_{Li-H} = ∞[180]

	E, estimated[81]	E, calculated[180]
R_{Li-H} = ∞	−7.978 060	−7.978 059 1[a]
R_{Li-H} = 3.015	−8.070 548	−8.070 547 3

[a]Calculated at R_{Li-H} = 40 bohr.

examined by comparing the energy obtained at 40 bohr with the estimated accurate energy obtained as a sum of the atomic energies (the BO energy in Table 19 at R_{Li-H} = ∞ is the sum of the BO energies of the Li and H atoms). As one can see, the error is only about 10^{-6} hartree. Thus, no significant accumulation of error had occurred.

As mentioned, the BO PEC generated in the calculations of Tung et al.[180] was corrected for the adiabatic effects to partially overcome the deficiency of the BO approximation. At the equilibrium distance the adiabatic correction lowers the depth of the PEC well by 10.7 cm^{-1}. Because the correction varies with the internuclear distance, the shape of the corrected PEC differs slightly from the PEC without the correction. This in turn affects the energies of the vibrational levels, as can be seen in Table 20. In the calculations of Tung et al.[180] these levels were obtained using Le Roy's Level 8.0 program.[233] In Table 20 we also compare the results from ref 180 with recent orbital-based calculations of Holka et al.[234] The first observation one can make upon examining the results of Holka et al. shown in Table 20 is that they were unable to obtain converged values for the two highest transitions and had to resort to extrapolation to determine them. Second, the root-mean-square deviation (from experiment) for the best set of transitions obtained by Tung et al., which were generated with the BO ECG PEC corrected for the adiabatic effects, is half those by Holka et al. It should be noted that the values by Holka et al. also included scalar relativistic corrections. Nonetheless, the comparison between the two sets is valid because those corrections have a negligible effect on the calculated transitions.

dx.doi.org/10.1021/cr200419d | Chem. Rev. 2013, 113, 36−79

Table 20. Comparison of Calculated and Experimental Transition Energies of ^{7}LiH[a]

	Holka et al.[234]		Tung et al.[180]	
$v' \rightarrow v''$	ΔE_1[b,h]	ΔE_2[c,h]	ΔE_{BO}[d,h]	ΔE_3[e,h]
1 → 0	0.88	0.59	0.53	0.06
2 → 1	0.64	0.37	0.47	0.01
3 → 2	0.53	0.28	0.51	0.08
4 → 3	0.39	0.16	0.51	0.09
5 → 4	0.22	0.01	0.48	0.07
6 → 5	0.07	−0.13	0.41	0.03
7 → 6	−0.06	−0.22	0.40	0.02
8 → 7	−0.13	−0.28	0.41	0.05
9 → 8	−0.20	−0.32	0.41	0.07
10 → 9	−0.23	−0.32	0.44	0.12
11 → 10	−0.26	−0.32	0.40	0.11
12 → 11	−0.30	−0.32	0.36	0.08
13 → 12	−0.31	−0.30	0.35	0.09
14 → 13	−0.32	−0.25	0.31	0.07
15 → 14	−0.27	−0.17	0.30	0.09
16 → 15	−0.19	−0.04	0.37	0.15
17 → 16	−0.09	0.09	0.37	0.11
18 → 17	0.03	0.24	0.17	−0.17
19 → 18	0.16	0.40	0.25	−0.22
20 → 19	0.38	0.62	1.21	0.58
21 → 20	(0.89)[f]	(1.13)[f]	0.12	−0.79
22 → 21	(2.43)[f]	(2.70)[f]	1.61	0.60
rms[g]	0.35	0.31	0.48	0.16

[a]The calculated transitions include those obtained with and without the adiabatic correction and are given in cm^{-1}. ΔE is the difference between the experimental and the calculated transitions. [b]The BO PEC includes DBOC, MVD (mass-velocity and Darwin), and nonadiabatic contributions.[234] [c]The BO PEC includes DBOC and MVD contributions.[234] [d]The BO PEC.[180] [e]The BO PEC includes DBOC contributions.[180] [f]Values in parentheses are extrapolated vibrational levels.[234] [g]The root-mean-square calculations include the vibrational transition up to $v' = 20 \rightarrow v'' = 19$. [h]Calculated transitions are compared with the empirical values derived by Coxon and Dickson.[235] The uncertainty is smaller than 0.0001 cm^{-1} for $v = 0$−5, smaller than 0.001 cm^{-1} for $v = 6$, and smaller than 0.01 cm^{-1} for $v \geq 7$.

Let us now examine how well Holka et al.'s[234] and Tung et al.'s[180] calculations reproduce the experimental dissociation energy. In Holka et al.'s calculations, the energy at each PEC point includes three components, i.e., the BO energy, the diagonal adiabatic correction (DBOC), and the relativistic (mass-velocity and Darwin) correction. The contributions of the BO energy, the DBOC, and the relativistic correction to the BO dissociation energy are 20 305.4, −12.0, and ∼−0.5 cm^{-1}, respectively. Compared with the results of Tung et al., Table 21 shows that Holka et al.'s results overestimate the BO contribution by about 6.6 cm^{-1} and the adiabatic correction by about 1.3 cm^{-1}. Even though these two errors have opposite signs and partially cancel each other, there is still a significant difference of about 5.3 cm^{-1} between Holka et al.'s and Tung et al.'s results and the experimental value. This error can be averaged in the calculation of vibrational levels. The differences of energies from the orbital calculation are competitive with the ECG values. It should be noted that the result of Tung et al. is virtually identical to the experimental value, which has an estimated root-mean-square deviation of 0.16 cm^{-1} and a maximum deviation of −0.79 cm^{-1}.

Table 21. Comparison of the BO Potential Depth and the Contribution of the DBOC Calculated by Holka et al. and Tung et al.[a]

	D_e (BO)	ΔDBOC
Holka et al.	20 305.4	−12.0
Tung et al.	20 298.8	−10.7
ΔE	6.6	−1.3

[a]The ΔE is the difference of two calculations.

As the dissociation energy is usually a good indicator of the accuracy of the calculations, we compare the values of this energy obtained with different methods with the experimental energy in Table 22. The comparison shows that the ECG value obtained by Tung et al.[180] best matches the experiment.

Table 22. Comparison of Values of the LiH Dissociation Energy Calculated with Different Methods with the Experimental Energy

authors	D_e (eV)	method
Li and Paldus[240]	∼2.5006	CCSD-[4R]/cc-pVQZ
Lundsgaard and Rudolph[241]	2.492	full CI/all-electron
Gadéa and Leininger[242]	2.512	CCSD(T)/all-electron
Bande et al.[179]	2.521	FC LSE
Holka et al.[234]	2.5159[a]	MR-CISD + Q_p/cc-pwCVXZ (X = Q, 5, 6)
Tung et al.[180]	2.51540[b]	ECG
Stwalley and Zemke[243]	2.51535[c]	experiment (±0.000 04 eV)

[a]^{7}LiH. This value includes BO, DBOC, and MVD (mass-velocity and Darwin) contributions. [b]^{7}LiH. This value includes BO and DBOC contributions. [c]Experimental value for ^{7}LiH.

Another good test of the quality of the calculations is to examine the results obtained at the equilibrium internuclear distance for the system. A large-scale CI [9s8p6d1f] performed for LiH by Bendazzoli et al.[236] gave the energy of −8.069 336 hartree, while the GFMC calculation of Chen et al.[237] yielded −8.070 21(5) hartree. CCSD[T]-R12 coupled-cluster method with linear r_{12} terms[254] gave E = −8.070 491 hartree. This energy is close to the energy of −8.070 516 hartree obtained with the iterative-complement-interaction method by Nakatsuji.[238] The first ECG calculations performed with 200 ECGs by Cencek et al.[239] gave the energy of −8.069 221 hartree. This result, as well as other results obtained with larger ECG basis sets by Cencek et al.[81] were used to make an extrapolation to the infinite basis set limit, which yielded −8.070 553(5) hartree. This energy is consistent with and close to the result of −8.070 547 3 hartree obtained by Tung et al.[180] with a basis of 2400 ECGs. When the ECG results are compared with the MR-CISD calculations of Holka et al.,[234] one becomes puzzled at a discrepancy. Holka et al.'s energy obtained at R = 3.000 bohr of −8.070 792 hartree is 239 μhartrees below the best ECG value obtained at R = 3.015 bohr and about 50 times outside its estimated uncertainty. The reason for this discrepancy is unclear at the moment. It is possible that it is due to an overestimated value of the size-consistency correction and (or) flaws in the extrapolation procedure used in Holka et al.'s calculations. In conclusion, currently only ECG-based approaches can provide reliable data and at the same time achieve microhartree-level accuracy in the LiH calculations.

dx.doi.org/10.1021/cr200419d | Chem. Rev. 2013, 113, 36−79

The relativistic correction to the dissociation energy of 0.5 cm^{-1} (or 0.000 06 eV) calculated by Holka et al.[234] indicates that the accuracy of the calculations of the vibrational transitions cannot be further improved by only including the relativistic (and nonadiabatic) corrections to the BO PEC corrected for the adiabatic effects. It will also need to involve improving the quality of the PEC BO energies. One should be able to achieve the accuracy of at least $\times 10^{-7}$ hartree in calculating these BO energies in order for the relativistic effects to start to matter. Such an increase of the accuracy is certainly within the reach of ECG calculations.

11.3. Diagonal Adiabatic Corrections to the BO Energy for Molecules Containing up to Three Nuclei

In this section we will not discuss specific calculations, but rather describe how to perform calculations of the diagonal adiabatic corrections (DBOC) when employing floating ECGs. Including effects beyond the BO approximation in the calculations involves the calculation of the gradient of the wave function with respect to the nuclear coordinates. Unfortunately, floating ECGs do not explicitly depend on the nuclear coordinates, and therefore indirect methods to retrieve that dependency need to be devised. In this section an approach which is capable of approximately accounting for the implicit dependency of the floating ECG basis functions on the nuclear coordinates in calculating the DBOC is described in mathematical terms. The method was first introduced by Cencek et al.[159] and it is based on the Gaussian product theorem (GPT). The GPT states that the product of two Gaussians is a Gaussian. In addition, it is possible to relate the nonlinear parameters of the two Gaussians in the product to the ones of the Gaussian being the product of the two. Unfortunately, to our knowledge, there is no GPT equivalent for floating ECGs and some approximations need to be made to represent a floating ECG as a product of other floating ECGs. Application of the GPT to diatomics is straightforward and involves minimal approximation. As a testament of this, there are above-reviewed calculations of the LiH molecule by Tung et al.[180] and calculations on other diatomics by Cencek et al.,[159] which have proven a high accuracy of the GTP-based procedure.

More problematic is the extension of the GPT algorithm to triatomics and, more specifically, their linear configurations. In this section, we describe a general derivation of a GPT-based approach to calculate the DBOC. The approach reduces to the procedure of Cencek et al. for the diatomic case, but it also allows for the calculation of the DBOC for triatomics even in their linear configurations.

The calculation of the adiabatic corrections is performed by using the Born−Handy formula:

$$E_{\mathrm{ad}} = \langle\Psi| - \frac{1}{2}\sum_{\alpha=1}^{K}\frac{1}{M_\alpha}\sum_{i_\alpha=1}^{3}\frac{\partial^2}{\partial Q_{i_\alpha}{}^2}|\Psi\rangle \tag{119}$$

where K is the total number of nuclei in the molecule, M_α are the nuclear masses, and i_α denote the Cartesian directions of the nuclear coordinate displacements. In the above approach, the partial second derivative with respect to nuclear coordinate Q_{i_α} is evaluated numerically by calculating the ground state BO wave function at two nuclear configurations, where Q_{i_α} is displaced backward and forward by a small distance, $Q_{i_\alpha}^{+}$ and $Q_{i_\alpha}^{-}$, according to the following formula:[159]

$$\langle\Psi|\frac{\partial^2}{\partial Q_{i_\alpha}{}^2}|\Psi\rangle = -\frac{2}{\Delta Q^2}(1 - S) \tag{120}$$

where $\Delta Q = Q_{i_\alpha}^{+} - Q_{i_\alpha}^{-}$, and $S = \langle\Psi(Q_{i_\alpha}^{+})|\Psi(Q_{i_\alpha}^{-})\rangle$. Let us now describe how the nonlinear parameters of the wave function at the shifted nuclear configuration can be approximated. As an example let us consider H_3^+. Let us first introduce three 3-dimensional vectors, $\mathbf{Q}_1$, $\mathbf{Q}_2$, and $\mathbf{Q}_3$, containing the coordinates of the three nuclei of H_3^+. Next, we introduce three two-electron "ionic" functions, ϕ_{I}, ϕ_{II}, and ϕ_{III}, that have the following shifts of the Gaussian centers:

$$\mathbf{s}_i = \begin{pmatrix}\mathbf{Q}_i \\ \mathbf{Q}_i\end{pmatrix} \tag{121}$$

where i is equal to either 1, 2, or 3.

In this derivation the subscript i denotes the nonlinear parameters of the newly introduced, atom-centered functions ϕ_{I}, ϕ_{II}, and ϕ_{III}, while the subscript k denotes the nonlinear parameters of the function we are shifting.

The ϕ_{I}, ϕ_{II}, and ϕ_{III} functions are called ionic because in eq 121 both Gaussian centers coincide with the position of a nucleus. With that, we can approximate any floating ECG basis function (ϕ_k) by a product of the three ionic functions introduced above as

$$\phi_k = \phi_{\mathrm{I}}\phi_{\mathrm{II}}\phi_{\mathrm{III}} = \exp[\sum_{i=1}^{3}(-\mathbf{r}'\mathbf{A}_i\mathbf{r} + 2\mathbf{r}'\mathbf{A}_i\mathbf{s}_i - \mathbf{s}_i'\mathbf{A}_i\mathbf{s}_i)] \tag{122}$$

where $\mathbf{A}_i$ is $\mathrm{A}_i \otimes \mathrm{I}_3$. By equating like terms in eq 122, one gets

$$\sum_{i=1}^{3}\mathbf{A}_i = \mathbf{A}_k \tag{123}$$

$$\sum_{i=1}^{3}\mathbf{A}_i\mathbf{s}_i = \mathbf{A}_k\mathbf{s}_k \tag{124}$$

$$\mathbf{s}_k'\mathbf{A}_k\mathbf{s}_k = \sum_{i=1}^{3}\mathbf{s}_i'\mathbf{A}_i\mathbf{s}_i \tag{125}$$

where $\mathbf{s}_k$ is the $3n$-dimensional (six-dimensional for H_3^+) Gaussian shift vector. By assuming that $\mathbf{A}_i = a_i\mathbf{A}_k$, eqs 123 and 124 become

$$\sum_{i=1}^{3}a_i = 1 \tag{126}$$

$$\sum_{i=1}^{3}a_i\mathbf{s}_i = \mathbf{s}_k \tag{127}$$

Notice that eq 127 is actually composed of two independent equations, one for the x coordinates and one for the y coordinates. For nonlinear geometries of H_3^+ eqs 126 and 127 are sufficient to predict the floating-ECG shift vectors for the new geometrical configuration of the nuclei. The procedure involves the following steps.

1. For each floating ECG, the three auxiliary functions, ϕ_{I}−ϕ_{III}, are constructed by using the H_3^+ nuclear coordinates as the shift vectors as shown in eq 121.

2. Three independent equations in eqs 126 and 127 are solved to obtain the values of the a_1, a_2, and a_3 parameters.

dx.doi.org/10.1021/cr200419d | Chem. Rev. 2013, 113, 36−79

3. The new Gaussian shift vector $\mathbf{s}_k$ is computed directly from eq 127 for the new, changed H_3^+ geometry, i.e., $\mathbf{Q}_i \pm (1/2)\Delta\mathbf{Q}_i$.

However, eqs 126 and 127 are not independent when the H_3^+ geometry becomes linear. The linear case is dealt with by making use of only those equations in eqs 127 and 125 which do not zero out in this situation. In addition, eq 125 needs to be simplified (approximated) by "decoupling" the terms corresponding to different electrons in order to make eqs 123−125 specific to each Gaussian center. In the "decoupling" we assume that the off-diagonal terms in $\mathbf{A}_k$ are small compared to the diagonal terms. This turns eq 125 into an equation that constrains the squares of the x-coordinates of the Gaussian centers to the square of the corresponding x-coordinate of the α nucleus:

$$a_1 + a_2 + a_3 = 1 \tag{128}$$

$$a_1x_1 + a_2x_2 + a_3x_3 = x_\alpha \tag{129}$$

$$a_1{x_1}^2 + a_2{x_2}^2 + a_3{x_3}^2 = {x_\alpha}^2 \tag{130}$$

where it is assumed that the linear H_3^+ lies on the x-axis. With that, even for a linear H_3^+ configuration, the system of equations, eqs 123−125, is nonsingular and can be solved. We should point out that, strictly speaking, eq 125 (and in turn also eq 130) is an ad hoc condition as it formally enforces the product of the three nuclear-centered ECGs to have the same norm as the original Gaussian.

12. CALCULATING MOLECULAR PROPERTIES WITH ECGS: THE BO CASE

In addition to the total energy, some molecular properties calculated with ECGs have also been a focus of recent studies. Important properties, such as the quadrupole moment,[244] dipole and quadrupole polarizabilities,[245] one-electron density,[92] electric field gradient at the nuclei,[246] and post-BO corrections to the total energy[26,103,212] have been successfully calculated with the ECG basis set even though ECGs are not capable of satisfying the Kato cusp condition[115] (see section 2.6). The ECGs decaying faster at large interparticle distances than expected by the asymptotic conditions for the exact solutions of the SE usually have small effects on the energy, but may more strongly affect the calculations of some properties. BO calculations performed with ECGs may need to involve thousands of basis functions (from about 1000 for two-electron systems[176] to over 5000 for systems having more than four particles[95,180]), if convergence of 10 significant digits in the energy is targeted. In this review we limit ourselves to describing only one example of property calculations. The example concerns the electric field gradient (EFG) at the nuclear positions in the H_2 molecule, as well as its isotopologues involving deuterium.

12.1. EFG at the Nuclei and the Deuterium Quadrupole Constant

The EFG is an important quantity for many spectroscopies: molecular beam resonance, nuclear magnetic resonance,[247] nuclear quadrupole resonance,[248] Mössbauer spectroscopy,[249] and electron paramagnetic resonance,[250] just to mention a few. These techniques exploit specific nuclear characteristics (i.e., distinct isotopes, decay of excited nuclear states, nuclear spin transitions, etc.), which may involve the coupling between the quadrupole moment of a nucleus with the gradient of the electric field due to the electron and nuclear charges at the position of that nucleus.

The coupling constant of the nuclear quadrupole/EFG interaction is defined by first-order perturbation theory as $\gamma = (2e^2Q\langle q\rangle)/(4\pi\varepsilon_0 h)$, where $\langle q\rangle$ is the vibrationally averaged anisotropic part of the EFG evaluated at the nucleus whose quadrupole moment is Q, e and h are the electron charge and the Planck constant, respectively, and $4\pi\varepsilon_0$ is the usual constant that appears in Coulomb's law. γ in HD and D_2 has been obtained with four to five digit accuracy by Ramsey and coworkers from molecular-beam magnetic resonance measurements.[251,252]

The fundamental constant Q can be estimated by combining the measured γ with a calculated value of $\langle q\rangle$. It is important to stress that the accuracy of the calculations of $\langle q\rangle$ determines the accuracy of the determination of the hyperfine quadrupole interaction. The ECG calculation of $\langle q\rangle$ does not come without complications, as EFG matrix elements over basis functions of the type shown in eq 48 contain the second derivative of the error function.[246]

In Figure 1 a plot of the difference between the EFG calculated at the nuclei of the H_2 molecule obtained by

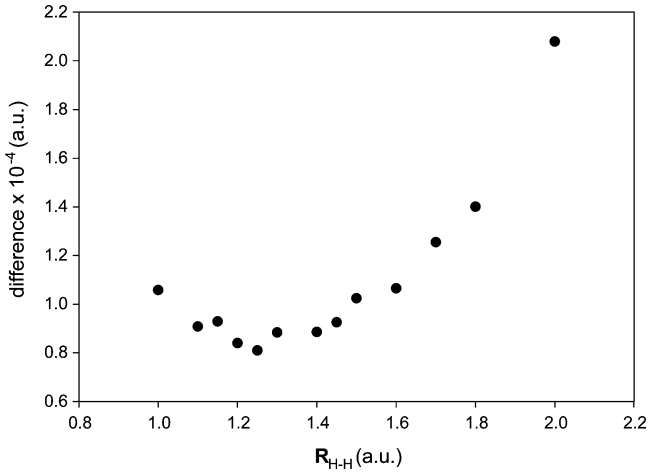

Figure 1. Difference between the field gradient calculated with ECGs in ref 246 and the one calculated with the Kołos−Wolniewicz basis functions in ref 253.

Pavanello et al.[246] and the previously best literature results[253] for q as a function of the H−H internuclear distance is shown. There are two important observations to be made about Figure 1. The first one is that the U-shaped trend of the curve seems to suggest that the Kołos−Wolniewicz-type basis set used by Reid et al. is likely not large enough. In addition, the curve shows that the values calculated by Reid et al. are subject to some numerical instability. Namely, there are some q values which seem too high and some which seem too low.

In Table 23 the values of the deuteron quadrupole constant Q are derived from the vibrationally averaged $\langle q\rangle$ value and the experimentally measured quadrupole splitting. The value of Q of 0.285 783(30) fm^2 derived in ref 246 is so far the most accurate to date. The uncertainty in this value is almost entirely due to the experimental uncertainty of the quadrupole interaction constant, γ (and perhaps also to the nonadiabatic effects).

dx.doi.org/10.1021/cr200419d | Chem. Rev. 2013, 113, 36−79

Table 23. Calculated Deuteron's Quadrupole (in fm^2) from D_2 and HD in the State $v = 0$ and $J = 1, 2$[a]

J	ECG[246]	Bishop–Cheung[76]	Kołos–Wolniewicz[253]
D_2			
1	0.285 783(30)	0.2862(15)	0.2860(15)
2	0.285 759(230)	0.2861(17)[b]	0.2860(17)[b]
HD			
1	0.285 814(140)		0.2875(16)[b]

[a]All values are calculated using the experimental value eqQ/h = 225.037 and 223.380 kHz for $J = 1$ and $J = 2$, respectively, for D_2 and 224.540 kHz for HD in the $J = 1$ state.[251,253] Maximum uncertainties (in parentheses) are estimated based on the experimental standard deviations. [b]Uncertainties corrected by adding the contribution from experimental random error.

13. SUMMARY

In this work we have attempted to review the current state of efforts to use ECGs in calculations of small atomic and molecular systems with very high accuracy. Such high accuracy can be achieved either by performing very precise BO calculations and correcting the results for adiabatic and nonadiabatic effects or by treating the nuclei (nucleus for an atom) and electrons on equal footing and explicitly including their motions in the Hamiltonian and in the wave function. For high accuracy, the results have to be also corrected for the relativistic and QED effects. It is shown that by using large basis sets of ECGs and by variationally optimizing their nonlinear parameters with a method based on the analytical energy gradient it is possible to determine the energies of ground and excited states of these systems with an accuracy approaching the accuracy of the most precise experimental measurements. The ECGs seem to be capable of very well describing the oscillatory nature of the wave function at any excitation level.

In moving forward with the development of ECG techniques for very accurate BO and non-BO atomic and molecular calculations, several directions need to be considered. Future work needs to include extending the non-BO approach presented in this review to diatomic states with rotational quantum numbers higher than zero. It will also need to include extending the non-BO approach to molecules with more than two nuclei. Furthermore, the work, which is currently already in progress, needs to concern the development of BO and non-BO tools to calculate the leading QED effects in ground and excited molecular states. With that, it is hoped that the remaining differences between the results of the theoretical calculations and the data acquired in experiments will be further narrowed.

AUTHOR INFORMATION

Corresponding Author

*E-mail: sergiy.bubin@vanderbilt.edu (S.B.); m.pavanello@rutgers.edu (M.P.); ludwik@u.arizona.edu (L.A).

Notes

The authors declare no competing financial interest.

Biographies

Sergiy Bubin received his B.S. and M.S. degrees in physics from Taras Shevchenko National University of Kyiv, Ukraine. He was awarded his Ph.D. in physics at the University of Arizona in 2006, carrying out research under the supervision of Ludwik Adamowicz. After spending two years as a postdoc at Arizona and one year at Quantum Chemistry Research Institute (Kyoto, Japan), he then went to Vanderbilt University to work with Prof. Kalman Varga. His research interests include explicitly correlated methods for highly accurate treatment of various few-body systems, non-Born–Oppenheimer quantum chemistry, quantum dynamics in molecules and nanostructures, and the interaction of strong laser fields with matter.

Michele Pavanello obtained the Laurea degree in 2004 at the University of Pisa in the PCM group working on NMR properties of solutes in liquid crystals under the supervision of Benedetta Mennucci. From 2004 to 2010 he was a graduate student at the University of Arizona in the group of Ludwik Adamowicz. There he came in contact with explicitly correlated methods in quantum chemistry. A Marie Curie fellowship took him to the Neugebauer group in Leiden (Netherlands) from 2010 to 2012, exploring density partitioning techniques and charge transfer phenomena. Since September 2012, he has been an assistant professor at Rutgers University, Newark.

dx.doi.org/10.1021/cr200419d | Chem. Rev. 2013, 113, 36–79

Wei-Cheng Tung received his B.S. degree in chemistry from National Taiwan University in 2002. He is currently a graduate student under the direction of Prof. Ludwik Adamowicz at the University of Arizona. His research interests focus on very accurate variational Born–Oppenheimer quantum-mechanical calculation of molecules using explicitly correlated Gaussian basis function with floating centers.

Keeper Layne Sharkey, current doctoral candidate at the University of Arizona, graduated from the University of Arizona in 2009 with an undergraduate degree in chemistry and mathematics. She is a member of the Adamowicz group and has participated in a number of academic publications within the group. Her doctoral studies center on chemical physics. She is the receipient of an NSF graduate research fellowship (2012). Her work includes non-Born–Oppenheimer calculations of atoms and molecules.

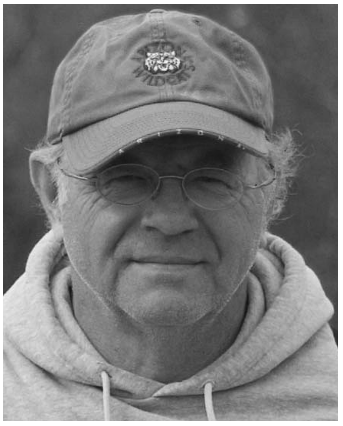

For Ludwik Adamowicz it all started in 1973 with a M.S. degree in Quantum Chemistry from Warsaw University (UW) obtained under the supervision of Profs. Kolos and Piela followed by a year as an assistant researcher under the supervision of Prof. Joanna Sadlej. After several months of unemployment and three failed attempts to be admitted to a Ph.D. program at UW and the Institute of the Organic Chemistry of the Polish Academy of Sciences (PAN), he finally made gainful employment in the Calorimetry Department of the Institute of Physical Chemistry (PAN) as a research assistant. In his free time at PAN, he worked on his PhD in Quantum Chemistry under supervision of Prof. Andrzej Sadlej (1977). In 1980 he joined the group of Prof. Ed McCullough at Utah State University as a postdoctoral fellow working on the numerical-orbital MCSCF method for diatomics. In 1983 he moved to the University of Florida as a postdoctoral fellow with Prof. Rod Bartlett, where he worked on the analytical gradients for the CC method, on the CC method with numerical orbitals, and on the optimal virtual orbital space (OVOS) method. In 1987 we was appointed an assistant professor in the Chemistry Department at the University of Arizona (UA). He is currently a professor in the Department of Chemistry and Biochemistry and in the Department of Physics at UA. He has published over 500 papers which encompass his current research interests of the development of very accurate methods for atomic and molecular quantum-mechanical calculations with and without assuming the Born–Oppenheimer approximation using explicitly correlated methods and multireference coupled cluster methods. He also develops methods for electron and energy transport in biomolecules. Application studies performed in his lab include works on anions, fullerenes, and nanotubes, molecular complexes involving nucleic acid bases, etc. Most of the application works have been performed in collaboration with experimental groups across the globe.

ACKNOWLEDGMENTS

The authors thank the National Science Foundation for partial support of this work. M.P. acknowledges support from the start-up funding by the Department of Chemistry and the office of the Dean of FASN of Rutgers University, Newark. The work of S.B. was supported in part by NSF Grant CMMI-0927345.

REFERENCES

(1) Hylleraas, E. A. *Z. Phys.* **1929**, *54*, 347.
(2) Boys, S. F. *Proc. R. Soc. London, Ser. A: Math. Phys. Sci.* **1960**, *258*, 402.
(3) Singer, K. *Proc. R. Soc. London, Ser. A: Math. Phys. Sci.* **1960**, *258*, 412.
(4) Rychlewski, J. Explicitly Correlated Functions in Molecular Quantum Chemistry. In *Advances in Quantum Chemistry*; Sabin, J. R., Zerner, M. C., Brändas, E., Wilson, S., Maruani, J., Smeyers, Y., Grout, P., McWeeny, R., Eds.; Elsevier: New York, 1998; Vol. *31*, p 173.
(5) Suzuki, Y.; Varga, K. *Stochastic Variational Approach to Quantum-Mechanical Few-Body Problems*; Lecture Notes in Physics; Springer: Berlin, 1998.
(6) Rychlewski, J. *Explicitly Correlated Wave Functions in Chemistry and Physics: Theory and Applications*; Progress in Theoretical Chemistry and Physics; Kluwer: Dordrecht, The Netherlands, 2003.
(7) Bubin, S.; Cafiero, M.; Adamowicz, L. *Adv. Chem. Phys.* **2005**, *131*, 377.
(8) Stanke, M.; Kędziera, D.; Molski, M.; Bubin, S.; Barysz, M.; Adamowicz, L. *Phys. Rev. Lett.* **2006**, *96*, 233002.
(9) Stanke, M.; Kędziera, D.; Bubin, S.; Adamowicz, L. *Phys. Rev. A* **2007**, *75*, 052510.
(10) Stanke, M.; Kędziera, D.; Bubin, S.; Adamowicz, L. *Phys. Rev. Lett.* **2007**, *99*, 043001.
(11) Stanke, M.; Kędziera, D.; Bubin, S.; Adamowicz, L. *J. Chem. Phys.* **2007**, *127*, 134107.
(12) Stanke, M.; Komasa, J.; Kędziera, D.; Bubin, S.; Adamowicz, L. *Phys. Rev. A* **2008**, *77*, 062509.
(13) Stanke, M.; Komasa, J.; Kędziera, D.; Bubin, S.; Adamowicz, L. *Phys. Rev. A* **2008**, *78*, 052507.

(14) Stanke, M.; Komasa, J.; Bubin, S.; Adamowicz, L. *Phys. Rev. A* **2009**, *80*, 022514.
(15) Bubin, S.; Komasa, J.; Stanke, M.; Adamowicz, L. *J. Chem. Phys.* **2009**, *131*, 234112.
(16) Bubin, S.; Komasa, J.; Stanke, M.; Adamowicz, L. *Phys. Rev. A* **2010**, *81*, 052504.
(17) Bubin, S.; Komasa, J.; Stanke, M.; Adamowicz, L. *J. Chem. Phys.* **2010**, *132*, 114109.
(18) Stanke, M.; Bubin, S.; Adamowicz, L. *Phys. Rev. A* **2009**, *79*, 060501.
(19) Piszczatowski, K.; Łach, G.; Przybytek, M.; Komasa, J.; Pachucki, K.; Jeziorski, B. *J. Chem. Theory Comput.* **2009**, *5*, 3039.
(20) Pachucki, K.; Komasa, J. *Phys. Chem. Chem. Phys.* **2010**, *12*, 9188.
(21) Bubin, S.; Stanke, M.; Adamowicz, L. *Chem. Phys. Lett.* **2010**, *500*, 229.
(22) Bushaw, B. A.; Nörtershäuser, W.; Drake, G. W. F.; Kluge, H.-J. *Phys. Rev. A* **2007**, *75*, 052503.
(23) Morton, D. C.; Wu, Q. X.; Drake, G. W. F. *Can. J. Phys.* **2006**, *84*, 83.
(24) Morton, D. C.; Wu, Q.; Drake, G. W. F. *Phys. Rev. A* **2006**, *73*, 034502.
(25) Korobov, V. I. *Phys. Rev. A* **2004**, *69*, 054501.
(26) Pachucki, K. *Phys. Rev. A* **2006**, *74*, 062510.
(27) Pachucki, K.; Komasa, J. *J. Chem. Phys.* **2006**, *125*, 204304.
(28) Puchalski, M.; Moro, A. M.; Pachucki, K. *Phys. Rev. Lett.* **2006**, *97*, 133001.
(29) Pachucki, K. *Phys. Rev. A* **2006**, *74*, 022512.
(30) Pachucki, K. *Phys. Rev. Lett.* **2006**, *97*, 013002.
(31) Yan, Z.-C.; Nörtershäuser, W.; Drake, G. W. F. *Phys. Rev. Lett.* **2008**, *100*, 243002.
(32) Puchalski, M.; Kędziera, D.; Pachucki, K. *Phys. Rev. A* **2010**, *82*, 062509.
(33) Karr, J. P.; Bielsa, F.; Valenzuela, T.; Douillet, A.; Hilico, L.; Korobov, V. I. *Can. J. Phys.* **2007**, *85*, 497.
(34) Drake, G.; Yan, Z.-C. *Hyperfine Interact.* **2006**, *172*, 141.
(35) Drake, G. W. F.; Yan, Z.-C. *Nucl. Phys. A* **2007**, *790*, 151c.
(36) Pachucki, K.; Moro, A. M. *Phys. Rev. A* **2007**, *75*, 032521.
(37) Kutzelnigg, W. *Theor. Chem. Acc.* **1985**, *68*, 445.
(38) Klopper, W.; Kutzelnigg, W.; Müller, H.; Noga, J.; Vogtner, S. Extremal Electron Pairs—Application to Electron Correlation, Especially the R12 Method. In *Correlation and Localization*; Surján, P., et al., Eds.; Springer: Berlin, 1999; Vol. *203*, p 215.
(39) Noga, J.; Valiron, P.; Klopper, W. *J. Chem. Phys.* **2001**, *115*, 2022.
(40) Klopper, W.; Manby, F. R.; Ten-No, S.; Valeev, E. F. *Int. Rev. Phys. Chem.* **2006**, *25*, 427.
(41) Shiozaki, T.; Kamiya, M.; Hirata, S.; Valeev, E. F. *J. Chem. Phys.* **2009**, *130*, 054101.
(42) Newbury, N. R.; Swann, W. C. *J. Opt. Soc. Am. B* **2007**, *24*, 1756.
(43) Oka, T. *Proc. Natl. Acad. Sci. U.S.A.* **2006**, *103*, 12235.
(44) Oka, T. *Faraday Discuss.* **2011**, *150*, 9–22.
(45) Nakai, H.; Hoshino, M.; Miyamoto, K.; Hyodo, S. *J. Chem. Phys.* **2005**, *122*, 164101.
(46) Nakai, H. *Int. J. Quantum Chem.* **2002**, *86*, 511.
(47) Ishimoto, T.; Tachikawa, M.; Nagashima, U. *J. Chem. Phys.* **2006**, *125*, 144103.
(48) Bochevarov, A. D.; Valeev, E. F.; Sherrill, C. D. *Mol. Phys.* **2004**, *102*, 111.
(49) Pak, M. V.; Chakraborty, A.; Hammes-Schiffer, S. *J. Phys. Chem. A* **2007**, *111*, 4522.
(50) Swalina, C.; Pak, M. V.; Chakraborty, A.; Hammes-Schiffer, S. *J. Phys. Chem. A* **2006**, *110*, 9983.
(51) Webb, S. P.; Iordanov, T.; Hammes-Schiffer, S. *J. Chem. Phys.* **2002**, *117*, 4106.
(52) Kołos, W.; Wolniewicz, L. *J. Mol. Spectrosc.* **1975**, *54*, 303.
(53) Lester, W. A., Jr.; Krauss, M. *J. Chem. Phys.* **1964**, *41*, 1407.
(54) Adamowicz, L.; Sadlej, A. J. *Chem. Phys. Lett.* **1977**, *48*, 305.
(55) Adamowicz, L.; Sadlej, A. J. *J. Chem. Phys.* **1977**, *67*, 4298.
(56) Adamowicz, L. *Acta Phys. Pol.* **1978**, *53*, 471.
(57) Adamowicz, L. *Int. J. Quantum Chem.* **1978**, *13*, 265.
(58) Adamowicz, L.; Sadlej, A. J. *Acta Phys. Pol.* **1978**, *54*, 73.
(59) Adamowicz, L.; Sadlej, A. J. *J. Chem. Phys.* **1978**, *69*, 3992.
(60) Szalewicz, K.; Adamowicz, L.; Sadlej, A. J. *Chem. Phys. Lett.* **1979**, *61*, 548.
(61) Jeziorski, B.; Szalewicz, K. *Phys. Rev. A* **1979**, *19*, 2360.
(62) Szalewicz, K.; Jeziorski, B. *Mol. Phys.* **1979**, *38*, 191.
(63) Bartlett, R. J.; Purvis, G. D. *Int. J. Quantum Chem.* **1978**, *14*, 561.
(64) Bartlett, R. J.; Purvis, G. D. *Phys. Scr.* **1980**, *21*, 255.
(65) Szalewicz, K.; Zabolitzky, J. G.; Jeziorski, B.; Monkhorst, H. J. *J. Chem. Phys.* **1984**, *81*, 2723.
(66) Jeziorski, B.; Monkhorst, H. J.; Szalewicz, K.; Zabolitzky, J. G. *J. Chem. Phys.* **1984**, *81*, 368.
(67) Szalewicz, K.; Jeziorski, B.; Monkhorst, H. J.; Zabolitzky, J. G. *J. Chem. Phys.* **1983**, *79*, 5543.
(68) Szalewicz, K.; Jeziorski, B.; Monkhorst, H. J.; Zabolitzky, J. G. *J. Chem. Phys.* **1983**, *78*, 1420.
(69) Klopper, W.; Kutzelnigg, W. *Chem. Phys. Lett.* **1987**, *134*, 17.
(70) Kutzelnigg, W.; Klopper, W. *J. Chem. Phys.* **1991**, *94*, 1985.
(71) Noga, J.; Kutzelnigg, W.; Klopper, W. *Chem. Phys. Lett.* **1992**, *199*, 497.
(72) Shiozaki, T.; Knizia, G.; Werner, H.-J. *J. Chem. Phys.* **2011**, *134*, 034113.
(73) Hättig, C.; Tew, D. P.; Köhn, A. *J. Chem. Phys.* **2010**, *132*, 231102.
(74) Cencek, W.; Rychlewski, J. *J. Chem. Phys.* **1995**, *102*, 2533.
(75) Cencek, W.; Szalewicz, K. *Int. J. Quantum Chem.* **2008**, *108*, 2191.
(76) Bishop, D. M.; Cheung, L. M. *Phys. Rev. A* **1979**, *20*, 381.
(77) Bishop, D. M.; Cheung, L. M. *Phys. Rev. A* **1977**, *16*, 640.
(78) Bishop, D. M.; Cheung, L. M. *J. Chem. Phys.* **1983**, *78*, 7265.
(79) Bishop, D. M.; Cheung, L. M. *Chem. Phys. Lett.* **1981**, *79*, 130.
(80) Pachucki, K. *Phys. Rev. A* **2010**, *82*, 032509.
(81) Cencek, W.; Rychlewski, J. *Chem. Phys. Lett.* **2000**, *320*, 549.
(82) Komasa, J.; Cencek, W.; Rychlewski, J. *Chem. Phys. Lett.* **1999**, *304*, 293.
(83) Cencek, W.; Rychlewski, J.; Jaquet, R.; Kutzelnigg, W. *J. Chem. Phys.* **1998**, *108*, 2831.
(84) Jaquet, R.; Cencek, W.; Kutzelnigg, W.; Rychlewski, J. *J. Chem. Phys.* **1998**, *108*, 2837.
(85) Komasa, J.; Rychlewski, J. *Mol. Phys.* **1997**, *91*, 909.
(86) Komasa, J.; Rychlewski, J. *Chem. Phys. Lett.* **1996**, *249*, 253.
(87) Cencek, W.; Komasa, J.; Rychlewski, J. *Chem. Phys. Lett.* **1995**, *246*, 417.
(88) Kozlowski, P. M.; Adamowicz, L. *J. Chem. Phys.* **1992**, *96*, 9013.
(89) Gilmore, D. W.; Kozlowski, P. M.; Kinghorn, D. B.; Adamowicz, L. *Int. J. Quantum Chem.* **1997**, *63*, 991.
(90) Cafiero, M.; Adamowicz, L. *Chem. Phys. Lett.* **2001**, *335*, 404.
(91) Cafiero, M.; Adamowicz, L. *Int. J. Quantum Chem.* **2001**, *82*, 151.
(92) Pavanello, M.; Cafiero, M.; Bubin, S.; Adamowicz, L. *Int. J. Quantum Chem.* **2008**, *108*, 2291.
(93) Rychlewski, J.; Cencek, W.; Komasa, J. *Chem. Phys. Lett.* **1994**, *229*, 657.
(94) Pavanello, M.; Tung, W.-C.; Leonarski, F.; Adamowicz, L. *J. Chem. Phys.* **2009**, *130*, 074105.
(95) Tung, W.-C.; Pavanello, M.; Adamowicz, L. *J. Chem. Phys.* **2010**, *133*, 124106.
(96) Komasa, J. *Phys. Chem. Chem. Phys.* **2008**, *10*, 3383.
(97) Heitler, W. H.; London, F. W. *Z. Phys.* **1927**, *44*, 455.
(98) Born, M.; Oppenheimer, R. *Ann. Phys. (Leipzig)* **1927**, *84*, 457.
(99) Handy, N. C.; Lee, A. M. *Chem. Phys. Lett.* **1996**, *252*, 425.
(100) Kutzelnigg, W. *Mol. Phys.* **1997**, *90*, 909.
(101) Sutcliffe, B. *Theor. Chem. Acc.* **2010**, *127*, 121.
(102) Wolniewicz, L.; Dressler, K. *J. Chem. Phys.* **1992**, *96*, 6053.
(103) Pachucki, K.; Komasa, J. *J. Chem. Phys.* **2008**, *129*, 034102.
(104) Pachucki, K.; Komasa, J. *J. Chem. Phys.* **2009**, *130*, 164113.

(105) Pelzl, P. J.; Smethells, G. J.; King, F. W. *Phys. Rev. E* **2002**, *65*, 036707.
(106) Feldmann, D. M.; Pelzl, P. J.; King, F. W. *J. Math. Phys.* **1998**, *39*, 6262.
(107) Yan, Z.-C.; Drake, G. W. F. *Phys. Rev. A* **1995**, *52*, 3711.
(108) Yan, Z.-C.; Tambasco, M.; Drake, G. W. F. *Phys. Rev. A* **1998**, *57*, 1652.
(109) Puchalski, M.; Pachucki, K. *Phys. Rev. A* **2006**, *73*, 022503.
(110) Fromm, D. M.; Hill, R. N. *Phys. Rev. A* **1987**, *36*, 1013.
(111) Harris, F. E. *Phys. Rev. A* **1997**, *55*, 1820.
(112) Zotev, V. S.; Rebane, T. K. *Phys. Rev. A* **2002**, *65*, 062501.
(113) Puchalski, M.; Kędziera, D.; Pachucki, K. *Phys. Rev. A* **2009**, *80*, 032521.
(114) Rebane, T. K.; Zotev, V. S.; Yusupov, O. N. *Zh. Eksp. Teor. Fiz.* **1996**, *110*, 55−62; *J. Exp. Theor. Phys.* **1996**, *83*, 28.
(115) Kato, T. *Commun. Pure Appl. Math.* **1957**, *10*, 151.
(116) James, H. M.; Coolidge, A. S. *J. Chem. Phys.* **1933**, *1*, 825.
(117) Kołos, W. *J. Chem. Phys.* **1994**, *101*, 1330.
(118) Kołos, W.; Wolniewicz, L. *J. Chem. Phys.* **1966**, *45*, 509.
(119) Wolniewicz, L. *Can. J. Phys.* **1976**, *54*, 672.
(120) Wolniewicz, L. *J. Chem. Phys.* **1995**, *103*, 1792.
(121) Kołos, W.; Wolniewicz, L. *J. Chem. Phys.* **1965**, *43*, 2429.
(122) Nakatsuji, H.; Nakashima, H.; Kurokawa, Y.; Ishikawa, A. *Phys. Rev. Lett.* **2007**, *99*, 240402.
(123) Sims, J. S.; Hagstrom, S. A. *J. Chem. Phys.* **2006**, *124*, 094101.
(124) Cencek, W.; Komasa, J.; Pachucki, K.; Szalewicz, K. *Phys. Rev. Lett.* **2005**, *95*, 233004.
(125) King, H. F. *J. Chem. Phys.* **1967**, *46*, 705.
(126) Jeziorski, B.; Bukowski, R.; Szalewicz, K. *Int. J. Quantum Chem.* **1997**, *61*, 769.
(127) Hill, R. N. *Int. J. Quantum Chem.* **1998**, *68*, 357.
(128) Bubin, S.; Adamowicz, L. *J. Chem. Phys.* **2008**, *128*, 114107.
(129) Bubin, S.; Adamowicz, L. *Phys. Rev. A* **2009**, *79*, 022501.
(130) Bubin, S.; Adamowicz, L. *Phys. Rev. A* **2011**, *83*, 022505.
(131) Bubin, S.; Adamowicz, L. *J. Chem. Phys.* **2011**, *135*, 214104.
(132) Sharkey, K. L.; Adamowicz, L. *J. Chem. Phys.* **2011**, *134*, 094104.
(133) Rebane, T. K.; Vitushinskii, P. V. *Opt. Spectrosc.* **2002**, *92*, 17.
(134) Bubin, S.; Adamowicz, L. *J. Chem. Phys.* **2006**, *124*, 224317.
(135) Sharkey, K. L.; Pavanello, M.; Bubin, S.; Adamowicz, L. *Phys. Rev. A* **2009**, *80*, 062510.
(136) Sharkey, K. L.; Bubin, S.; Adamowicz, L. *J. Chem. Phys.* **2010**, *132*, 184106.
(137) Sharkey, K. L.; Bubin, S.; Adamowicz, L. *J. Chem. Phys.* **2011**, *134*, 044120.
(138) Sharkey, K. L.; Bubin, S.; Adamowicz, L. *J. Chem. Phys.* **2011**, *134*, 194114.
(139) Sharkey, K. L.; Bubin, S.; Adamowicz, L. *Phys. Rev. A* **2011**, *83*, 012506.
(140) Cafiero, M.; Bubin, S.; Adamowicz, L. *Phys. Chem. Chem. Phys.* **2003**, *5*, 1491.
(141) Bubin, S.; Cafiero, M.; Adamowicz, L. Quantum mechanical calculations on molecules containing positrons. In *Fundamental World of Quantum Chemistry*; Brändas, E. J., Kryachko, E. S., Eds.; Kluwer: Dordrecht, The Netherlands, 2004; Vol. 3, p 521.
(142) Bednarz, E.; Bubin, S.; Adamowicz, L. *J. Chem. Phys.* **2005**, *122*, 164302.
(143) Bubin, S.; Bednarz, E.; Adamowicz, L. *J. Chem. Phys.* **2005**, *122*, 041102.
(144) Kędziera, D.; Stanke, M.; Bubin, S.; Barysz, M.; Adamowicz, L. *J. Chem. Phys.* **2006**, *125*, 084303.
(145) Bubin, S.; Adamowicz, L. *J. Chem. Phys.* **2003**, *118*, 3079.
(146) Kędziera, D.; Stanke, M.; Bubin, S.; Barysz, M.; Adamowicz, L. *J. Chem. Phys.* **2006**, *125*, 014318.
(147) Stanke, M.; Kędziera, D.; Bubin, S.; Molski, M.; Adamowicz, L. *J. Chem. Phys.* **2008**, *128*, 114313.
(148) Bubin, S.; Leonarski, F.; Stanke, M.; Adamowicz, L. *Chem. Phys. Lett.* **2009**, *477*, 12.
(149) Bubin, S.; Stanke, M.; Adamowicz, L. *Phys. Rev. A* **2011**, *83*, 042520.
(150) Pavanello, M.; Bubin, S.; Molski, M.; Adamowicz, L. *J. Chem. Phys.* **2005**, *123*, 104306.
(151) Stanke, M.; Kędziera, D.; Bubin, S.; Adamowicz, L. *Phys. Rev. A* **2008**, *77*, 022506.
(152) Bubin, S.; Adamowicz, L. *J. Chem. Phys.* **2006**, *125*, 064309.
(153) Bubin, S.; Stanke, M.; Adamowicz, L. *J. Chem. Phys.* **2011**, *134*, 024103.
(154) Bednarz, E.; Bubin, S.; Adamowicz, L. *Mol. Phys.* **2005**, *103*, 1169.
(155) Cafiero, M.; Adamowicz, L. *Phys. Rev. Lett.* **2002**, *88*, 033002.
(156) Cafiero, M.; Adamowicz, L. *Phys. Rev. Lett.* **2002**, *89*, 073001.
(157) Fernández, F. M. *J. Chem. Phys.* **2009**, *130*, 166101.
(158) Komasa, J. *Mol. Phys.* **2006**, *104*, 2193.
(159) Cencek, W.; Kutzelnigg, W. *Chem. Phys. Lett.* **1997**, *266*, 383.
(160) Hamermesh, M. *Group Theory and Its Application to Physical Problems*; Addison-Wesley: Reading, MA, 1962.
(161) Pauncz, R. *Spin Eigenfunctions*; Plenum: New York, 1979.
(162) Varshalovich, D. A.; Moskalev, A. N.; Khersonskii, V. K. *Quantum Theory of Angular Momentum*; World Scientific: Reading, MA, 1988.
(163) Varga, K.; Suzuki, Y.; Usukura, J. *Few-Body Syst.* **1998**, *24*, 81.
(164) Magnus, J. R.; Neudecker, H. *Matrix-Differential Calculus with Applications in Statistics and Econometrics*; Wiley: Chichester, U.K., 1988.
(165) Kinghorn, D. B. *Int. J. Quantum Chem.* **1996**, *57*, 141.
(166) Kinghorn, D. B.; Adamowicz, L. *J. Chem. Phys.* **1999**, *110*, 7166.
(167) Kinghorn, D. B.; Adamowicz, L. *J. Chem. Phys.* **2000**, *113*, 4203.
(168) Cafiero, M.; Adamowicz, L. *Int. J. Quantum Chem.* **2007**, *107*, 2679.
(169) Varga, K.; Suzuki, Y. *Phys. Rev. C* **1995**, *52*, 2885.
(170) Parlett, B. N. *The Symmetric Eigenvalue Problem*; SIAM: Philadelphia, 1998.
(171) Kukulin, V. I.; Krasnopol'sky, V. M. *J. Phys. G* **1977**, *3*, 795.
(172) Varga, K.; Suzuki, Y. *Phys. Rev. A* **1996**, *53*, 1907.
(173) Alexander, S. A.; Monkhorst, H. J.; Szalewicz, K. *J. Chem. Phys.* **1986**, *85*, 5821.
(174) Alexander, S. A.; Monkhorst, H. J.; Szalewicz, K. *J. Chem. Phys.* **1987**, *87*, 3976.
(175) Pavanello, M.; Tung, W.-C.; Adamowicz, L. *J. Chem. Phys.* **2009**, *131*, 184106.
(176) Pavanello, M.; Adamowicz, L. *J. Chem. Phys.* **2009**, *130*, 034104.
(177) Nakatsuji, H. *Phys. Rev. Lett.* **2004**, *93*, 030403.
(178) Nakatsuji, H. *Phys. Rev. A* **2005**, *72*, 062110.
(179) Bande, A.; Nakashima, H.; Nakatsuji, H. *Chem. Phys. Lett.* **2010**, *496*, 347.
(180) Tung, W.-C.; Pavanello, M.; Adamowicz, L. *J. Chem. Phys.* **2011**, *134*, 064117.
(181) Nash, S. G. *SIAM J. Numer. Anal.* **1984**, *21*, 770.
(182) Korobov, V.; Yelkhovsky, A. *Phys. Rev. Lett.* **2001**, *87*, 193003.
(183) Korobov, V. I. *Phys. Rev. A* **2002**, *66*, 024501.
(184) Pachucki, K. *Phys. Rev. Lett.* **2000**, *84*, 4561.
(185) Kołos, W.; Wolniewicz, L. *Rev. Mod. Phys.* **1963**, *35*, 473.
(186) Kołos, W.; Wolniewicz, L. *J. Chem. Phys.* **1967**, *46*, 1426.
(187) Kolos, W.; Wolniewicz, L. *Phys. Lett.* **1962**, *2*, 222.
(188) Yelkhovsky, A. *Phys. Rev. A* **2001**, *64*, 062104.
(189) Drake, G. W. F.; Martin, W. C. *Can. J. Phys.* **1998**, *76*, 679.
(190) Shiner, D.; Dixson, R.; Vedantham, V. *Phys. Rev. Lett.* **1995**, *74*, 3553.
(191) Drake, G. W. F.; Nörtershäuser, W.; Yan, Z.-C. *Can. J. Phys.* **2005**, *83*, 311.
(192) Wang, L. M.; Yan, Z.-C.; Qiao, H. X.; Drake, G. W. F. *Phys. Rev. A* **2011**, *83*, 034503.
(193) Puchalski, M.; Pachucki, K. *Phys. Rev. A* **2008**, *78*, 052511.
(194) Pachucki, K. *Phys. Rev. A* **2002**, *66*, 062501.

(195) King, F. W. *Phys. Rev. A* **2007**, *76*, 042512.
(196) Yan, Z.-C.; Drake, G. W. F. *Phys. Rev. Lett.* **1998**, *81*, 774.
(197) Yan, Z.-C.; Drake, G. W. F. *Phys. Rev. Lett.* **2003**, *91*, 113004.
(198) Pachucki, K.; Komasa, J. *Phys. Rev. A* **2003**, *68*, 042507.
(199) Pachucki, K.; Komasa, J. *Phys. Rev. Lett.* **2004**, *92*, 213001.
(200) Pachucki, K.; Komasa, J. *Phys. Rev. A* **2006**, *73*, 052502.
(201) Caswell, W. E.; Lepage, G. P. *Phys. Lett. B* **1986**, *167*, 437.
(202) Kinoshita, T.; Nio, M. *Phys. Rev. D* **1996**, *53*, 4909.
(203) Bethe, H. A.; Salpeter, E. E. *Quantum Mechanics of One- and Two-Electron Atoms*; Plenum: New York, 1977.
(204) Stanke, M.; Kędziera, D.; Bubin, S.; Molski, M.; Adamowicz, L. *Phys. Rev. A* **2007**, *76*, 052506.
(205) Salpeter, E. E.; Bethe, H. A. *Phys. Rev.* **1951**, *84*, 1232.
(206) Greiner, W.; Reinhardt, J. *Quantum Electrodynamics*; Springer: Berlin, 2003.
(207) Datta, S. N.; Misra, A. *J. Chem. Phys.* **2006**, *125*, 084111.
(208) Bjorken, J. D.; Drell, S. D. *Relativistic Quantum Fields*; McGraw-Hill: New York, 1965.
(209) Araki, H. *Prog. Theor. Phys.* **1957**, *17*, 619.
(210) Sucher, J. *Phys. Rev.* **1958**, *109*, 1010.
(211) Pachucki, K. *J. Phys. B* **1998**, *31*, 5123.
(212) Pachucki, K.; Cencek, W.; Komasa, J. *J. Chem. Phys.* **2005**, *122*, 184101.
(213) Drake, G. W. F. In *High Precision Calculations for the Rydberg States of Helium*; Levine, F. S., Micha, D. A., Eds.; Plenum Press: New York, 1993; p 107.
(214) Korobov, V. I.; Korobov, S. V. *Phys. Rev. A* **1999**, *59*, 3394.
(215) Schwartz, C. *Phys. Rev.* **1961**, *123*, 1700.
(216) Kramida, A.; Martin, W. C. *J. Phys. Chem. Ref. Data* **1997**, *26*, 1185.
(217) Johansson, L. *Ark. Fys.* **1963**, *23*, 119.
(218) Ralchenko, Yu.; Kramida, A.; Reader, J.; NIST ASD Team. *NIST Atomic Spectra Database, version 4.0* [Online], 2010. Available at http://physics.nist.gov/asd.
(219) Bubin, S. Unpublished results.
(220) Almora-Díaz, C. X.; Bunge, C. F. *Int. J. Quantum Chem.* **2010**, *110*, 2982.
(221) Davidson, E. R.; Hagstrom, S. A.; Chakravorty, S. J.; Umar, V. M.; Fischer, C. F. *Phys. Rev. A* **1991**, *44*, 7071.
(222) Chakravorty, S. J.; Gwaltney, S. R.; Davidson, E. R.; Parpia, F. A.; Fischer, C. F. *Phys. Rev. A* **1993**, *47*, 3649.
(223) Brown, M. D.; Trail, J. R.; Ríos, P. L.; Needs, R. J. *J. Chem. Phys.* **2007**, *126*, 224110.
(224) Seth, P.; Ríos, P. L.; Needs, R. J. *J. Chem. Phys.* **2011**, *134*, 084105.
(225) Bubin, S.; Stanke, M.; Adamowicz, L. *J. Chem. Phys.* **2009**, *131*, 044128.
(226) Moss, R. E. *Mol. Phys.* **1993**, *78*, 371.
(227) Hilico, L.; Billy, N.; Grémaud, B.; Delande, D. *Eur. Phys. J. D* **2000**, *12*, 449.
(228) Bubin, S.; Leonarski, F.; Stanke, M.; Adamowicz, L. *J. Chem. Phys.* **2009**, *130*, 124120.
(229) Stanke, M.; Bubin, S.; Molski, M.; Adamowicz, L. *Phys. Rev. A* **2009**, *79*, 032507.
(230) Chuang, M.-C.; Zare, R. N. *J. Mol. Spectrosc.* **1987**, *121*, 380.
(231) Bauschlicher, C. W., Jr.; Langhoff, S. R.; Taylor, P. R. *J. Chem. Phys.* **1990**, *93*, 502.
(232) Patkowski, K.; Cencek, W.; Jankowski, P.; Szalewicz, K.; Mehl, J. B.; Garberoglio, G.; Harvey, A. H. *J. Chem. Phys.* **2008**, *129*, 094304.
(233) Le Roy, R. J. *A Computer Program for Solving the Radial Schrödinger Equation for Bound and Quasibound Levels*; 2007.
(234) Holka, F.; Szalay, P. G.; Fremont, J.; Rey, M.; Peterson, K. A.; Tyuterev, V. G. *J. Chem. Phys.* **2011**, *134*, 094306.
(235) Coxon, J. A.; Dickinson, C. S. *J. Chem. Phys.* **2004**, *121*, 9378.
(236) Bendazzoli, G. L.; Monari, A. *Chem. Phys.* **2004**, *306*, 153.
(237) Chen, B.; Anderson, J. B. *J. Chem. Phys.* **1995**, *102*, 4491.
(238) Nakatsuji, H.; Nakashima, H.; Kurokawa, Y.; Ishikawa, A. *Phys. Rev. Lett.* **2007**, *99*, 240402.
(239) Cencek, W.; Rychlewski, J. *J. Chem. Phys.* **1993**, *98*, 1252.
(240) Li, X.; Paldus, J. *J. Chem. Phys.* **2003**, *118*, 2470.
(241) Lundsgaard, M. F. V.; Rudolph, H. *J. Chem. Phys.* **1999**, *111*, 6724.
(242) Gadéa, F. X.; Leininger, T. *Theor. Chem. Acc.* **2006**, *116*, 566.
(243) Stwalley, W. C.; Zemke, W. T. *J. Phys. Chem. Ref. Data* **1993**, *22*, 87.
(244) Komasa, J. *J. Chem. Phys.* **2000**, *112*, 7075.
(245) Komasa, J. *Phys. Rev. A* **2002**, *65*, 012506.
(246) Pavanello, M.; Tung, W.-C.; Adamowicz, L. *Phys. Rev. A* **2010**, *81*, 042526.
(247) Slichter, C. P. *Principles of Magnetic Resonance*, 3rd ed.; Springer-Verlag: Berlin, 1990.
(248) Semin, G. K.; Babushkina, T. A.; Iakobson, G. G. *Nuclear Quadrupole Resonance in Chemistry*; Wiley: New York, 1975.
(249) Gosner, U.; Fujita, F. E. *Mössbauer Spectroscopy*; Springer-Verlag: Berlin, 1975.
(250) Weil, J. A.; Bolton, J. R. In *The Interpretation of EPR Parameters*; Wiley: New York, 2006; p 253.
(251) Code, R. F.; Ramsey, N. F. *Phys. Rev. A* **1971**, *4*, 1945.
(252) Quinn, W. E.; Baker, J. M.; LaTourrette, J. T.; Ramsey, N. F. *Phys. Rev.* **1958**, *112*, 1929.
(253) Reid, R. V.; Vaida, M. L. *Phys. Rev. A* **1973**, *7*, 1841.
(254) Noga, J.; Tunega, D.; Klopper, W.; Kutzelnigg, W. *J. Chem. Phys.* **1995**, *103*, 309.